RELIABILITY OF TRANSPORTATION LIFELINE SYSTEMS SUBJECTED TO EARTHQUAKE LOADS

A THESIS SUBMITTED TO
THE GRADUATE SCHOOL OF NATURAL AND APPLIED SCIENCES
OF
MIDDLE EAST TECHNICAL UNIVERSITY

BY

NAZ TOPKARA ÖZCAN

IN PARTIAL FULFILLMENT OF THE REQUIREMENTS
FOR
THE DEGREE OF MASTER OF SCIENCE
IN
CIVIL ENGINEERING

FEBRUARY 2016

Approval of the thesis:

RELIABILITY OF TRANSPORTATION LIFELINE SYSTEMS SUBJECTED TO EARTHQUAKE LOADS

submitted by **NAZ TOPKARA ÖZCAN** in partial fulfillment of the requirements for the degree of **Master of Science in Civil Engineering Department, Middle East Technical University** by,

Prof. Dr. Gülbin Dural Ünver
Dean, Graduate School of **Natural and Applied Sciences** _____

Prof. Dr. İsmail Özgür Yaman
Head of Department, **Civil Engineering** _____

Prof. Dr. M. Semih Yücemen
Supervisor, **Civil Engineering Dept., METU** _____

Examining Committee Members:

Assoc. Prof. Dr. Alp Caner
Civil Engineering Dept., METU _____

Prof. Dr. M. Semih Yücemen
Civil Engineering Dept., METU _____

Assoc. Prof. Dr. Ayşegül Askan Gündoğan
Civil Engineering Dept., METU _____

Assoc. Prof. Dr. Sevtap Kestel
Institute of Applied Mathematics, METU _____

Asst. Prof. Dr. Fatih Kürşat Fırat
Civil Engineering Dept., Aksaray University _____

Date: 05.02.2016

I hereby declare that all information in this document has been obtained and presented in accordance with academic rules and ethical conduct. I also declare that, as required by these rules and conduct, I have fully cited and referenced all material and results that are not original to this work.

Name, Surname: Naz Topkara Özcan

Signature:

ABSTRACT

RELIABILITY OF TRANSPORTATION LIFELINE SYSTEMS SUBJECTED TO EARTHQUAKE LOADS

Topkara Özcan, Naz

M.S., Department of Civil Engineering

Supervisor: Prof. Dr. M. Semih Yücemen

February 2016, 157 pages

Lifelines, such as highway, gas, water and power distribution systems, are networks which extend spatially over large geographical regions. The assessment of the reliability of a lifeline under seismic loads requires particular attention, since the proper functioning of these systems during or after a destructive earthquake is very important. The main objective of this study is to investigate the system reliability of lifeline networks subjected to earthquake loads by concentrating on highway systems consisting of viaducts, bridges, roads and highways. System reliability analysis basically evaluates the performance of a system in terms of the reliability of its components. Reliability of a structural component which is subjected to earthquake forces is determined based on the seismic capacity of the structure and earthquake loads on the structure. In this study, determination of the future earthquake threat on the components is calculated by performing a probabilistic seismic hazard analysis.

Failure reasons of bridges and asphalt roads are explained and behaviors of these components under earthquake loads are discussed to determine the seismic capacity of them. In this respect, the system reliability concepts are utilized and bounds on the seismic reliability of a system are established. A case study based on real life data is also presented in order to illustrate the implementation of the method.

Keywords: Lifelines, Highway Systems, Earthquake, Probabilistic Seismic Hazard, System Reliability.

ÖZ

DEPREM YÜKLERİNE MARUZ ULAŞIM CANDAMARI SİSTEMLERİNİN GÜVENİRLİĞİ

Topkara Özcan, Naz

Yüksek Lisans, İnşaat Mühendisliği Bölümü

Tez Yöneticisi: Prof. Dr. Mehmet Semih Yücemen

Şubat 2016, 157 sayfa

Candamarı şebekeleri olarak adlandırılan iletişim, gaz, su, enerji dağıtım ve ulaşım şebekeleri geniş coğrafi alanlara yayılmış enterkonekte sistemlerdir. Sismik yükler altındaki bir candamarı şebekesinin güvenirliğinin hesaplanması, bu tür sistemlerin hasar yaratıcı bir deprem esnasında ya da sonrasında işlevlerini yerine getirebilmelerinin önemi nedeni ile gereklidir. Bu çalışmanın temel amacı, köprüler ve anayollardan oluşan karayolu sistemlerinin üzerine yoğunlaşarak deprem yüklerine maruz kalmış candamarı şebeklerinin sismik güvenirliğini incelemektir. Sistemlerin güvenirlik analizi, şebekeyi oluşturan elemanların güvenirliğine bağlı olarak değerlendirilmiştir. Deprem yüklerine maruz kalan elemanların güvenirliği, elemanın kapasitesine ve üzerine gelen deprem yüküne bağlı olarak belirlenir. Bu çalışmada, elemanın maruz kalabileceği deprem yükünün belirlenmesinde olasılıksal sismik tehlike analizi kullanılmıştır. Elemanların kapasitelerini belirlemek için öncelikle köprülerin ve asfalt yolların çökme nedenleri tartışılmış ve bu yapıların

deprem yükleri altında nasıl davrandığı açıklanmıştır. Bu bağlamda sistem güvenirlik prensipleri uygulanarak, ulaşım candamarı şebekesinin sismik güvenirliği için alt ve üst güvenirlik sınırları belirlenmiştir. Önerilen yöntemin uygulaması gerçek verilere dayanan bir örnek çalışma ile gösterilmiştir.

Anahtar Kelimeler: Candamarı Şebekeleri, Karayolları Sistemleri, Deprem, Olasılıksal Sismik Tehlike, Sistem Güvenirliği.

To my big and beautiful family

ACKNOWLEDGEMENTS

I would like to express my sincere gratitude to my supervisor Prof. Dr. M. Semih Yücemen who has been supported me since the beginning of my study. He always trusted in me and encouraged me to do better. This thesis would not have been possible without his patience and guidance.

Besides my advisor, I would like to thank my thesis committee, Assoc. Prof. Dr. Alp Caner, Assoc. Prof. Dr. Ayşegül Askan Gündoğan, Assoc. Prof. Dr. Sevtap Kestel and Asst. Prof. Dr. Fatih Kürşat Fırat for their valuable comments and suggestions. Also I would like to thank Dr. Nazan Yılmaz Kılıç for her help and contributions.

It is a pleasure for me to acknowledge Prof. Dr. Uğurhan Akyüz, Prof. Dr. Ahmet Yakut and once again Assoc. Prof. Dr. Alp Caner for their support. They provided me an opportunity to work on my thesis project going along with my job. I am honored to be a part of their team.

I am also thankful to my associates Seda Özdemir, Ezgi Karakaya and Tuba Mumcu for their moral supports. They cheered me up and motivated me during my study. I would also like to thank my colleagues and friends Alper Aldemir, Ozan Demirel, Erhan Budak, Feyza Soysal Albostan, Görkem Deniz Köksoy and Özlem Temel Yalçın for the good memories that we shared.

I am grateful to my friends Berk Bora Çakır, Cihat Çağın Yakar, Müge Özgenoğlu and Gizem Mestav Sarıca for their contributions to this thesis. They made a way for me to enter the bridge world.

I want to thank my sister Demet Topkara Okur and my brother Levent Topkara for inspiring me and enlightening the way of my life. I would never survive without your support.

I would like to thank my dearest friend Pelin Ergen for being with me whatever happens. We shared a lot; smiled, cried and got angry all the time together. Her place cannot be replaced.

My greatest gratitude goes to Arzu İpek Yılmaz and Ceren Usalan for giving a meaning to awesome memories in METU from beginning to end. Half of my academic success belongs to you. Thank you for being with me in my good and bad days. True friends stay forever, beyond words.

My deepest thanks belong to my beloved husband Murat Özcan for making my life wonderful. Thanks for supporting me to achieve my goals and always being with me with your unconditional love. I cannot think how life would be without you.

Finally, I would like to thank my family wholeheartedly, my parents Nevin Topkara and Mustafa Topkara and my brother Barış Topkara. No words can truly express my indebtedness to them. With their unconditional love and support, and their never-ending faith in me, they have been the greatest source of motivation. I am so lucky to have you.

TABLE OF CONTENTS

LIST OF TABLES

TABLES

LIST OF FIGURES

FIGURES

LIST OF SYMBOLS

a	Empirically determined coefficient
b	Empirically determined coefficient
e_i	Factor transforming load to the load effect in the i^{th} member in the weakest mode
$f_m(M)$	Probability density function of magnitude
$f_M(m)$	Probability density function of safety margin
$f_R(r)$	Probability density function of distance from seismic source to the site
$f_s(s)$	Probability density function of load
$f_t(t)$	Probability density function of inter event time
$f_x(\tilde{X})$	Joint probability density function of random variables $\tilde{X}$
$g(\tilde{X})$	Limit state function, failure function, performance function
$h(t)$	Hazard function
n	Number of earthquakes
p	Annual probability of occurrence
r_{cl}	Closest horizontal distance from the source to the site of interest

r_{jb}	Joyner Boore distance
t	Time interval
A	Area of fault rupture
D	Average displacement over the rupture surface
D_F	Failure domain (failure region)
D_S	Safe domain (survival region)
E_i	Failure event of i^{th} failure mode
$\bar{E}_i$	Survival event of the i^{th} failure mode
F	Fault type parameters
$F_t(t)$	Cumulative distribution function of inter event time
HW	Hanging wall parameters
L	Rupture length
M	Earthquake magnitude
M	Safety Margin
M_b	Body wave magnitude
M_{char}	Characteristic earthquake magnitude
M_d	Duration magnitude
M_L	Local magnitude

M_{min}	Minimum magnitude
M_{max}	Maximum magnitude
M_S	Surface wave magnitude
M_w	Moment magnitude
M_0	Seismic moment of the earthquake
M_0'	Seismic moment rate
P_T	Probability that an event occur at least once within a T year time period
P_{D_S}	Probability of damage to the system
P_F	Probability of failure
P_{F_S}	Probability of system failure
$P_{F_{S_i}}$	Probability of system failure through the i^{th} path
P_S	Survival probability of a structural element
P_{S_i}	Survival probability in the i^{th} failure mode
P_{S_S}	Survival probability of the system
P_S'	Survival probability of the system in the case of perfectly correlated system components
R	Distance to the site from the source
R	Resistance or strength capacity

R_i'	Capacity of ith member in the weakest mode
S	Load or demand
S	Average slip rate along the fault
S'	Site parameters
$\tilde{X}$	Vector of basic variables
V_s	Average shear-wave velocity
Y	Ground motion parameter
Z_i	Reduced (transformed) ith basic variable
$\bar{\alpha}$	Unit vector
β_c	Reliability index of Cornell
β_e	Reliability index of a single element
β_{HL}	Reliability index of Hasofer and Lind
$\Phi( )$	Cumulative standard normal probability distribution function
μ	Shear modulus of the crust
μ_i	Mean of the ith random variable
μ_M	Mean value of safety margin
μ_R	Mean value of resistance
μ_S	Mean value of load

ν	Mean rate of earthquake occurrence with magnitude equal or greater than M_{min}
ν_i	Annual rate of earthquake occurrence due to the i^{th} seismic source
ν_M	Activity rate at which earthquakes with magnitudes greater than or equal to M occur on a source
ρ	Correlation coefficient among member failures
ρ_{ij}	Correlation coefficient between random variables X_i and X_j
$\bar{\rho}$	Average correlation coefficient
σ_i	Standard deviation of the i^{th} random variable
σ_M	Standard deviation of safety margin
σ_R	Standard deviation of resistance
σ_S	Standard deviation of load
∂g	Failure surface in the z coordinate system
$\cap$	Intersection of events
$\cup$	Union of events

CHAPTER 1

INTRODUCTION

1.1 General

Lifelines are geographically dispersed over broad areas, and are exposed to a wide range of seismic and geotechnical hazards, community uses, and interactions with other sectors of the built environment (O'Rourke, 2000). Lifelines are vital networks, and it is important that these networks are still functional after major natural disasters such as earthquakes (Kestel et al., 2012). These systems share three common characteristics: geographical dispersion, interconnectivity, and diversity (O'Rourke, 1998).

The lifeline systems include:

- Water supply systems: potable water and industrial water supply.
- Energy supply systems: electric power supply, gas and oil supply, etc.
- Disposal systems: sewer, garbage and waste treatment, etc.
- Transportation systems: road and highway traffic, railway, etc.
- Telecommunication systems: telephone, facsimile, digital data communication.

In this thesis, transportation lifeline systems, which are comprised of viaducts, bridges, roads and highways are focused on and, reliability of highway components and systems are analyzed.

Highway transportation systems are essential components of society. They act as the key links between population centers and provide access to other modes of

transportation. They also provide access to manufacturing plants, agricultural facilities, offices, hospitals, residential areas etc.

After an earthquake, lifeline transportation systems are necessary to maintain their functions since emergency situations may arise at different locations. In that case, access to each disaster region has a vital importance. Especially, transportation between disaster regions and hospitals should be available at all times. For this reason, reliability of those highway systems, which reflects the probability of survival of the system, should be examined under earthquake loads.

In order to make a study of the reliability of highway systems due to the earthquakes, probabilistic and stochastic approaches are utilized. As the first step, reliability of each component of the lifeline transportation system is evaluated. To calculate the reliability of a component, capacity of the component and earthquake load on the component should be determined. Earthquake load is obtained by performing a probabilistic seismic hazard analysis, whereas capacity is generally determined from empirical ways or by conducting structural analysis. System reliability is calculated based on the reliability of components by considering the connection of alternative paths whether they are connected in series or parallel.

Among all the components of the highway systems, bridges have been shown to be the most vulnerable to earthquake damage. About 70 percent of the approximately 600,000 highway bridges in the U.S. were constructed prior to 1971, with little or no consideration given to seismic resistance. The devastating damage and loss of life resulting from recent damaging earthquakes, including the 1989 Loma Prieta, 1994 Northridge, 1995 Kobe (Japan), 1999 Chi-Chi (Taiwan), and the 1999 Kocaeli (Turkey) earthquakes, demonstrate the need to provide new and improved procedures and specifications for designing and constructing earthquake-resistant bridges and highways (MCEER 094, 2000). The target damage levels for design of bridges have been studied by many researchers. In Turkey, similar studies have been conducted by Yilmaz and Caner (2012).

Roads and highways are more resistant to the earthquake load since asphalt is more ductile than concrete. Therefore, fault cracks or embankment failures control the damage of asphalt roads (SYNER-G Project 244061, 2011).

1.2 Aim and Scope of the Study

The main objective of this study is to investigate the system reliability of lifelines subjected to earthquake loads by concentrating on highway systems consisting of viaducts, bridges, roads and highways. A general flow chart of the study is shown in Figure 1.1 to explain the steps to be followed.

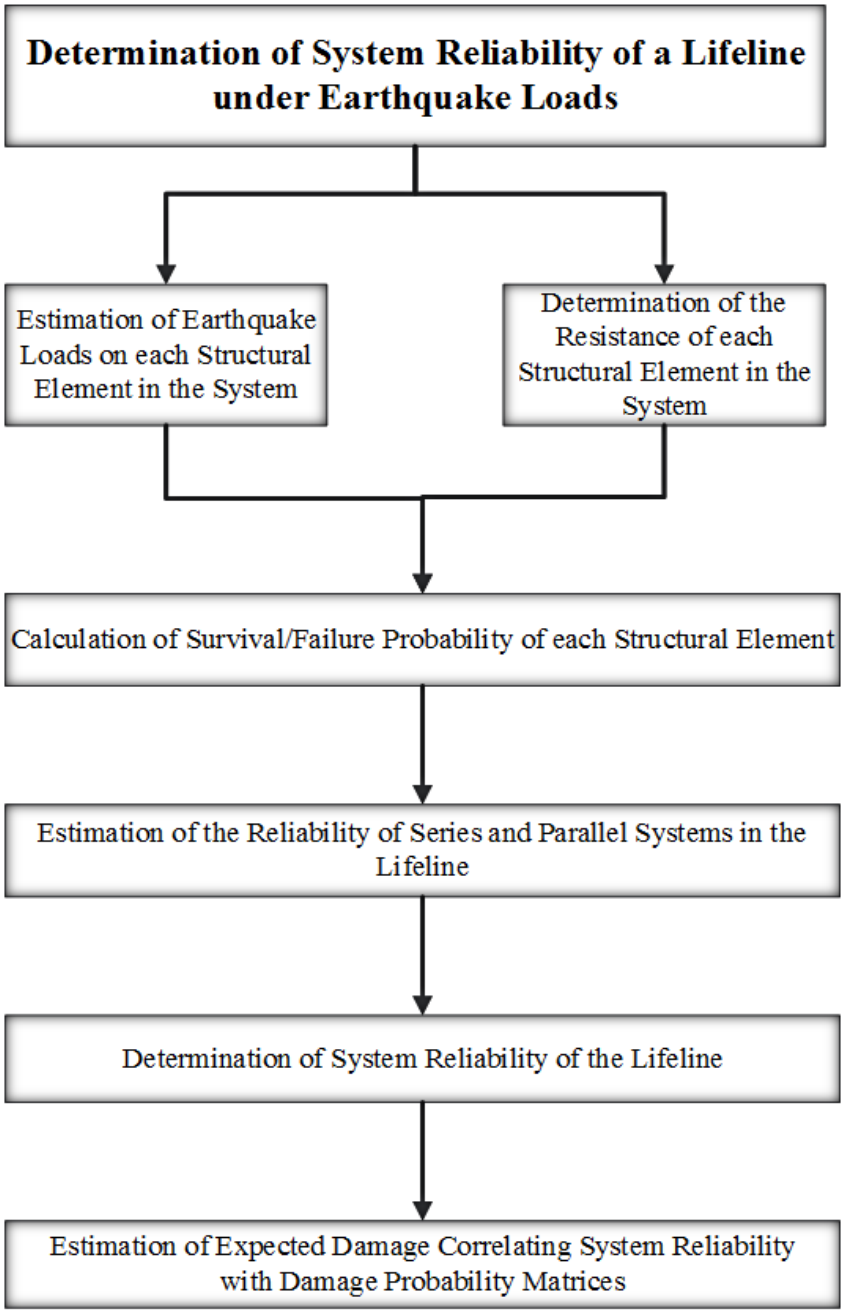

Figure 1.1 Flow Chart of the Study

After this introductory chapter, in the following chapter of the thesis, deterministic and probabilistic hazard calculations which are the two alternative approaches to estimate earthquake hazard level in a specified region are explained. Procedures for both deterministic seismic hazard analysis (DSHA) and probabilistic seismic hazard analysis (PSHA) are summarized. Steps for PSHA, which are characterization of seismic sources, determination of seismicity of seismic sources, earthquake occurrence, hazard calculations and uncertainties are explained in detail.

In Chapter 3, effects of earthquake loads on lifelines are explained with particular emphasis on highway systems. Failure reasons of these systems are discussed with respect to viaducts, bridges, roads and highways. Correspondingly, capacity determination methods of these components are presented.

In Chapter 4, safety concept is described based on structural reliability methods. First, reliability assessment of a single member of the system is presented, which corresponds to the survival probability of the component. Then, reliability of series and parallel systems are discussed and as a part of this, upper and lower bounds on system reliability are discussed.

In Chapter 5, a case study is carried out for a district located in the city center of Bursa. This region is selected as a pilot area by considering the fault locations and the highway network between hospitals and the industrial zone, where human population is concentrated, and an earthquake scenario is established. On that ground, reliability of each component of the system is calculated and later on system reliability is computed. Reliability results are compared with damage probability matrices proposed by various researches in order to check the consistency of the results of the study.

In the last chapter, a summary of the study is presented and results are discussed. Additionally, recommendations for future studies are stated.

In Appendix A, fault parameters for the Bursa Region and in Appendix B, probabilistic spectra results computed for bridges corresponding to different return periods are given.

CHAPTER 2

PROBABILISTIC SEISMIC HAZARD ANALYSIS

2.1 Introduction

Earthquakes are random events both in time and space. However, it is possible to have an idea about the occurrence probability of future earthquakes in a specified geographic region within a time period with the help of statistical methods by considering past earthquake data.

Seismic hazard analysis involves the estimation of the likelihood of a future earthquake in a specified geographic area within a time period. In other words, seismic hazard analysis helps to determine the expected intensity of ground motion at a site corresponding to a specified probability. It is also an essential tool to estimate seismic risk, which reflects the overall damage and losses due to earthquakes on a system i.e. lifelines, structures or other entities.

To perform a seismic hazard analysis, generally five steps are required:

- Identification of seismic sources that may affect the site
- Determination of distances of seismic sources to the site
- Determination of the magnitude distribution for each source from past earthquake data
- Determination of a stochastic model to describe the occurrence of earthquakes in the time domain based on earthquake events

- Selection of a ground motion prediction equation (GMPE) in order to calculate the value of a ground motion parameter for a given magnitude and distance from the site of a particular earthquake

There are two approaches to conduct seismic hazard analysis, which are deterministic and probabilistic. Deterministic approach considers the most critical earthquake scenario although probabilistic approach takes into consideration all possible earthquake scenarios. One of these two approaches or preferably both could be chosen depending on the problem type.

In this chapter, a general overview and basic methodologies of seismic hazard analysis are presented. Deterministic and probabilistic methods are explained by putting emphasis on the probabilistic one. Furthermore, steps of probabilistic approach are explained in detail.

2.2 Deterministic Seismic Hazard Analysis

Deterministic seismic hazard analysis (DSHA) considers the worst case scenario to obtain the ground motion at the site which means closest distance to the site and maximum magnitudes are selected in evaluating the seismic hazard. Basic DSHA steps are as follows:

- Identification of active seismic sources around the site
- Determination of maximum earthquake magnitude that will occur at the closest distance to the site
- Calculation of seismic hazard at the site by using a suitable GMPE.

Generally to conduct a DSHA, less data is required. Therefore, if limited data is available for a site, this approach could give an idea to the analyst. On the other hand, it is not a rational engineering practice to choose the worst-case scenario. Deterministic approach is simple compared to the probabilistic one, but uncertainties are not taken into consideration directly.

2.3 Probabilistic Seismic Hazard Analysis

Due to the randomness involved in the occurrences of earthquakes, statistical and probabilistic methods are preferable in estimating seismic hazard. Probabilistic seismic hazard analysis (PSHA) was first developed by Cornell (1968). This approach considers all possible earthquake scenarios with respect to all magnitude and distance to the site combinations. Additionally, probabilistic approach accounts for uncertainties in each step.

Main steps of the probabilistic seismic hazard analysis, which is also shown in Figure 2.1, are given below.

- Identification of all seismic sources which are capable of producing earthquakes of engineering interest at the selected site
- Determination of earthquake magnitude distribution and recurrence relationships
- Modelling of earthquake occurrence in the time domain
- Estimation of ground motion at the site.

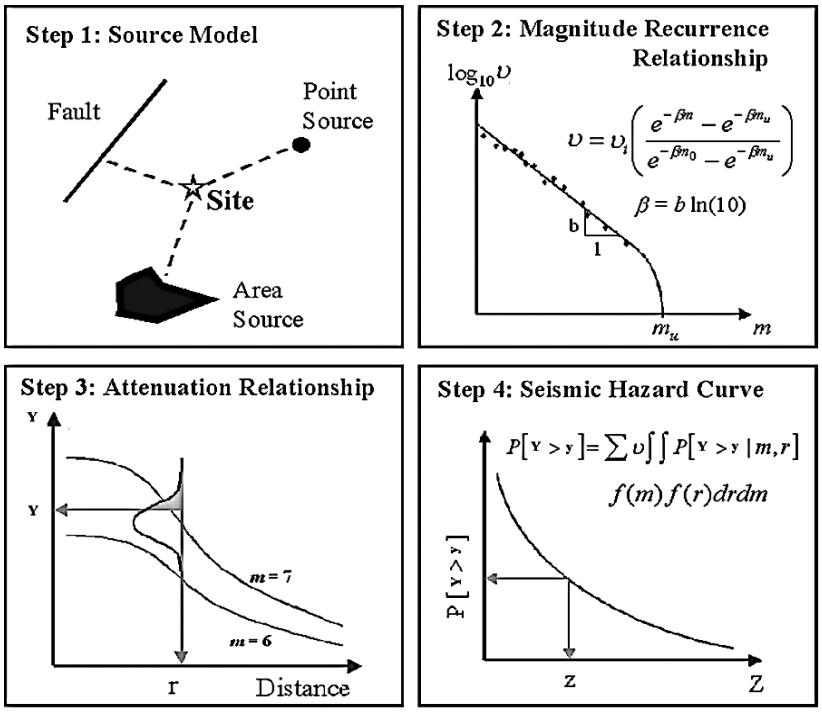

Figure 2.1 Steps Involved in the Conventional Probabilistic Seismic Hazard Assessment (PSHA) (after Reiter, 1991).

In this approach, the probability distribution of ground motion in a given time period is obtained.

If two methods are compared, less data is necessary to carry out a deterministic analysis. Accordingly, computational time is not as long as that required for the PSHA. On the other hand, deterministic approach does not consider uncertainties in each step as the probabilistic approach.

2.4 Seismic Source Characterization

The first step of PSHA is to define the potential seismic sources around the site which means the characterization of seismic sources. Characterization of seismic sources involves identification of source type, determination of source dimensions, and determination of earthquake magnitude distribution, estimation of rupture dimensions throughout the seismic source for each earthquake magnitude and calculation of earthquake occurrence rate.

2.4.1 Source Types

Seismic sources can be modelled as point, line and area sources.

2.4.1.1 Point Sources

A point seismic source is the basic form of seismic sources. If epicenters of past earthquakes are concentrated on a region or the distance to the site is relatively far, the source could be defined as a point source. For a point source, the distance to site is fixed (Yücemen, 1982).

2.4.1.2 Line (Fault) Sources

In case adequate geological data is available, faults are modelled as line sources. For fault sources, earthquake ruptures are spread over the fault plane. Usually, the

ruptures are uniformly distributed along the fault strike, but may have a non-uniform distribution along the strike (Abrahamson, 2006).

2.4.1.3 Area Sources

If sufficient geological data is not available, seismic sources are modelled as area sources. Area sources are assumed to have the same properties all over the source in time and space and they represent the spatial distribution of seismicity in that region. Area source model is also useful to define a seismic source in the regions where past seismic activity may not correlate with any one of the active geologic structure or the available data are not adequate to recognize a particular fault system (Yücemen, 1982).

2.5 Seismicity of Seismic Sources

2.5.1 Magnitude Scales

After the determination of geometric properties of seismic sources, distribution of possible earthquakes that may occur within the seismic sources should be investigated. Since earthquake data is obtained from various earthquake catalogs, which use different instruments, magnitude of an earthquake may be expressed according to different magnitude scales. The most widely used scales are local magnitude (M_L), body wave magnitude (M_b), surface wave magnitude (M_S), duration magnitude (M_d) and moment magnitude (M_w). Here, except the moment magnitude scale, all scales are related with the seismic wave amplitudes which are directly related with the ground shaking. Therefore, for large size earthquakes, saturation of the scale comes into question, which means that the magnitude scale becomes less sensitive. Abrahamson (2006) stated that M_b and M_L saturate around magnitude 7.0 and M_S saturates around magnitude 8.0.

It is important to obtain a single scale earthquake database to conduct PSHA consistently. There are several empirical conversion equations available in the

literature to convert these scales into each other. Conversion relationships used in this thesis are based on the ones derived by Deniz and Yücemen (2010) which utilized the orthogonal regression and an earthquake database consisting of a series of earthquake occurred in the last century in Turkey. These conversion equations are shown below by the equation group (2.1).

$$\left.\begin{aligned} M_w &= 2.25\, M_b - 6.14 \\ M_w &= 1.57\, M_L - 2.66 \\ M_w &= 1.27\, M_d - 1.12 \\ M_w &= 0.54\, M_S + 2.81 \end{aligned}\right\} \quad (2.1)$$

2.5.1.1 Moment Magnitude

Moment magnitude ($M_{w)}$ is a frequently used earthquake scale which reflects the total amount of released energy during an earthquake. Moment magnitude was developed by Hanks and Kanamori (1979) which is based on the seismic moment of the earthquake (M_0), as shown below:

$$M_w = \frac{2}{3} log_{10}(M_0) - 10.7 \quad (2.2)$$

Seismic moment is the product of the rigidity of the Earth, average amount of slip on the fault and the size of the slipped area (Aki, 1966) as given in equation (2.3).

$$\mathrm{M_0} = \mu\, \mathrm{A}\, \mathrm{D} \quad (2.3)$$

where,

μ = shear modulus of the crust (3 x 10^{11} dyne/cm^2)

A = area of fault rupture (cm^2)

D = average displacement over the rupture surface (cm)

By substituting equation (2.3) into equation (2.2), moment magnitude is directly obtained in terms of the physical properties of the seismic source as in equation (2.4).

$$M_w = \frac{2}{3}\log(\mu) + \frac{2}{3}\log(A) + \frac{2}{3}\log(D) - 10.7 \quad (2.4)$$

2.5.2 Magnitude Recurrence Relationships

After the determination of seismic source type and selection of the magnitude scale, seismicity of the source should be described. Seismicity of a source is expressed by the magnitude recurrence relationships. Magnitude recurrence relationships are related with the magnitude distribution function and activity rate of seismic sources.

General form of the magnitude recurrence relationship of a seismic source is given by equation (2.5).

$$\nu_M = \nu_{M_{min}} \int_{M}^{M_{max}} f_m(M)dM \quad (2.5)$$

where,

ν_M = activity rate at which earthquakes with magnitudes greater than or equal to M occur on a source

ν_{Mmin} = activity rate for earthquakes greater or equal to minimum magnitude, M_{min}

$f_m(M)$ = probability density function of magnitude

M_{max} = maximum magnitude

M = earthquake magnitude

2.5.2.1 Minimum and Maximum Magnitudes for Seismic Sources

Magnitude distribution functions are generally limited with minimum and maximum earthquake magnitudes that seismic sources can produce. Minimum magnitude, also called as the lower bound magnitude, is the smallest magnitude that can cause damage on the structures. According to Abrahamson (2006), minimum magnitude should be taken as 5.0, because no damage is observed for well-engineered structures in earthquakes less than 5.0. However, depending on the PSHA, it is common to use 4.0 or 4.5 as lower bound magnitudes.

Estimation of maximum earthquake magnitude depends on the source type. For area sources, largest historical earthquake is used as the basis and half magnitude unit is added to this value. If past earthquake data is not available for the region, the largest value for another region which has the same seismic properties could be used. For fault sources, rupture dimensions are used to estimate the maximum magnitude. In literature, there are several equations which relate the magnitude with rupture dimensions. The general form of the equation is shown in equation (2.6).

$$M = a + b \log_{10} L \tag{2.6}$$

where,

M = earthquake magnitude

a, b = empirically determined coefficients

L = rupture length

In fault segmentation approach, it is accepted that rupture dimensions are controlled by the fault segmentations. Maximum dimension of the rupture is defined by the

segmentation points. The magnitude due to the rupture of a segment is called the characteristic magnitude for the segment (Abrahamson, 2006).

2.5.3 Magnitude Distribution

A seismic source produces earthquake of varying magnitudes randomly. This randomness in the earthquake occurrence is described by a magnitude probability density function, $f_m(M)$. Magnitude probability density function reflects the likelihood of small, moderate and large magnitude earthquakes that can be created by a seismic source.

In the literature, there are two main models to describe magnitude distribution of earthquakes, namely exponential and characteristic models. Exponential model is appropriate for large areas where hazard is not controlled by a particular seismic source and it is commonly used for the distribution of small to moderate magnitude earthquakes. For particular seismic sources, especially for major fault sources, it is better to use the characteristic model. Additionally, for large magnitude earthquakes characteristic model works better.

2.5.3.1 Truncated Exponential Model

Truncated exponential model is derived based on the empirical Gutenberg-Richter (1944) magnitude recurrence relationship which is stated as

$$log\nu_M = a - bM \tag{2.7}$$

here,

a, b = constants depending on the seismic characteristic of the region

M = Richter magnitude

The rewritten form of the equation is given in the following:

$$\nu_M = \nu_0 . \exp(-\beta M) \quad (2.8)$$

where,

$\nu_0 = 10^a$

$\beta = b \ln(10) \approx 2.3b$

Truncated exponential model is applicable for all magnitudes, but usually bounds are constructed for minimum and maximum magnitudes. The magnitude probability density function, $f_m(M)$ given in equation (2.9), which is doubly truncated at the minimum magnitude, M_{min} and at the maximum magnitude, M_{max}.

$$f_m(M) = \frac{\beta \, . \, e^{-\beta(M-M_{min})}}{1 - e^{-\beta(M_{max}-M_{\min})}} \quad (2.9)$$

2.5.3.2 Characteristic Earthquake Model

Schwartz and Coppersmith (1984) specified that the truncated exponential model determines the earthquake magnitudes pretty good for large regions, but underestimate the recurrence rate of large earthquakes on fault segments. Thus, Schwartz and Coppersmith (1984) proposed the characteristic earthquake model. Magnitude probability density function for characteristic earthquake model is derived by Youngs and Coppersmith (1985) which is shown in Figure 2.2. The reason behind the philosophy is that: When a fault starts to rupture by producing a large magnitude earthquake, then entire fault segment is prone to rupture correspondingly. In this regard, an earthquake with a characteristic magnitude occurs on the fault depending on the dimension of the fault segment.

Characteristic earthquake model considers that during the characteristic earthquakes, all energy is discharged. Thus, characteristic earthquake is associated with large magnitude earthquakes which means small to moderate magnitude earthquakes are not taken into consideration.

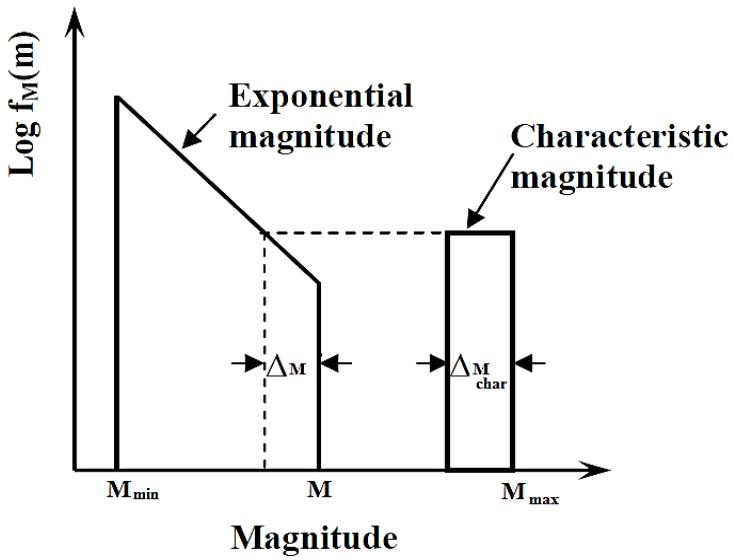

Figure 2.2 Characteristic Earthquake Model Proposed by Youngs and Coppersmith (1985)

In this model, Youngs and Coppersmith (1985) assumed a ΔM_{char} which is equal to the 0.5 magnitude unit, $M = M_{max} - \Delta M_{char}$ and frequency of the characteristic part equals to frequency exponential part at $M_{max} - 1.0$.

The probability density function corresponding to the characteristic earthquake model can be described by the truncated normal distribution which permits a constricted range of magnitudes for the characteristic earthquake. The magnitude probability density function for the truncated normal model is given in the following equation group (Youngs and Coppersmith , 1985).

$$f_m(M) = \begin{cases} \frac{1}{1+c_2}\frac{\beta\, e^{-\beta(M_{char}-M_{min}-1.25)}}{1-e^{-\beta(M_{char}-M_{min}-0.25)}} & M_{min} \le M \le M_{max} - 0.5 \\ \frac{1}{1+c_2}\frac{\beta\, e^{-\beta(M_{char}-M_{min}-1.25)}}{1-e^{-\beta(M_{char}-M_{min}-0.25)}} & M_{max} - 0.5 \le M \le M_{max} \end{cases} \quad (2.10)$$

where,

M_{char} = characteristic earthquake magnitude

$$c_2 = \frac{0.5\beta e^{-\beta(M_{char}-M_{min}-1.25)}}{1-e^{-\beta(M_{char}-M_{min}-0.25)}}$$

2.5.4 Earthquake Activity Rates

Magnitude distribution functions explained in the previous section express the relative rate for various earthquake magnitudes for a seismic source. For obtaining the activity rate of a seismic source, either past earthquake data or seismological information is used.

To determine the activity rate from the past recorded earthquake data, an earthquake catalog is compiled. Then the truncated exponential model is fitted to the data in the earthquake catalog.

While compiling the earthquake catalogs, some important points should be kept in mind as stated in the following. Firstly, different magnitude scales should be converted into a common scale. Preferably, all magnitude scales in the database be converted into the moment magnitude. Secondly, an alternative earthquake catalog should be prepared where foreshocks, aftershocks and other dependent events to the main shock are removed from the catalog since the Poisson model is based on the assumption that earthquake occurrences are independent events. Lastly, completeness of the catalog should be evaluated carefully. Some events, especially small magnitude earthquakes, may not be reported in the earlier periods. After the earthquake catalog corrected for the completeness, activity rate and b value are calculated by using either the maximum likelihood method or least square regression.

Calculation of b value by using maximum likelihood method (Weichert, 1980) is given in the following equation.

$$b = \frac{1}{\ln(10)(M - M_{min})} \tag{2.11}$$

Gutenberg and Richter (1954) suggested that b values range from 0.45 to 1.50 for various region of the world.

Although the use of past earthquake data recorded in earthquake catalogs is suitable for estimation of activity rates conforming the truncated exponential model, geological information especially slip rate, is used to calculate activity rates for the characteristic earthquake model.

Activity rate is also determined by using the geographical information. If slip rate for the fault source is available, then activity rate is calculated by using the seismic moment balancing concept.

Considering the definition of seismic moment given in equation (2.3), seismic moment rate, M_0' is calculated by taking the time derivative of the equation (2.3) as follows:

$$M_0' = \mu \, A \frac{dD}{dt} = \mu \, A \, S \tag{2.12}$$

where,

S = average slip rate along the fault

D = average displacement over the rupture surface

The moment magnitude is calculated from equation (2.2) as explained in section 2.5.1.1. Equation (2.2) can be rewritten in the following form:

$$M_0 = 10^{1.5M_w + 16.05} \tag{2.13}$$

Then, the activity rate of earthquakes with magnitude M_w is calculated as follows:

$$\nu_M = \frac{M_0'}{M_0} = \frac{\mu\, A\, S}{10^{1.5M_w+16.05}} \tag{2.14}$$

2.6 Earthquake Occurrence Models

After the calculation of the activity rates of earthquakes for different magnitude levels, probability of the occurrence of a future earthquake can be determined by assuming that earthquake occurrences follow either time dependent or independent models (i.e. models with memory or without memory). At that point, it is significant to comprehend the physical process of the earthquake occurrence in order to evaluate the suitability of each assumption stated above. This condition is stipulated by Reid (1911) via the elastic rebound theory. This theory states that the occurrence of earthquakes is the result of the continuous accumulation and discharge of energy in the rocks which are next to the earthquake faults. Since faults are the boundaries between the plates of Earth, relative movement of these plates causes the accumulation of strain energy and shear stress on faults. Once the shear stress is equal to the shear strength of the adjacent rocks, the rocks fail and the build-up strain energy is released. In the event that rocks are weak or ductile, the accumulated strain energy is discharged gradually. On the other hand, if rocks are strong or brittle, the strain energy is released suddenly.

2.6.1 Time-Independent (Memoryless) Models

Time independent models assume that there is no correlation between the previous earthquake events and the current ones in terms of size, location and time. In other words, the probability of an earthquake which occurs in a given time period is not related with the time elapsed since the previous earthquake.

Classical probabilistic seismic hazard calculation assumes that earthquake occurrences are independent events and so earthquake occurrence is modelled as a Poisson process. In equation (2.15), occurrence probability of "n" number of earthquakes with magnitude equal or greater than M_{min} in time interval "t" is expressed as:

$$\Pr(N = n/\nu\,, t) = \frac{e^{-\nu t}(\nu t)^n}{n!} \tag{2.15}$$

Probability density function of inter event time, $f_t(t)$ for time independent model is defined as in equation (2.16).

$$f_t(t) = \nu e^{-\nu t} \tag{2.16}$$

and cumulative distribution function of inter event time, $F_t(t)$ which represents the probability of at least one earthquake occurrence in the time period, t, is defined as

$$F_t(t) = \int_0^t f_t(t)dt = \int_0^t \nu e^{-\nu t}\, dt = 1 - e^{-\nu t} \tag{2.17}$$

where,

ν = mean rate of earthquake occurrence with magnitude equal or greater than M_{min}

t = time period considered

2.6.2 Time –Dependent (with Memory) Models

Models with memory, which are also called time dependent models, consider the earthquake occurrence with time on the basis of memory of previous events, specifically for large earthquakes. In other words, these models are based on the assumption of a periodicity relation in the occurrence of earthquakes. Since large earthquakes are related with the characteristic earthquakes, occurrence probability of a characteristic earthquake increases with the elapsed time from the previous time (Thenhaus and Campbell, 2003).

The most popular time-dependent models are the renewal models which are applied based on various distributions for the elapsed time since the previous earthquake (Cornell & Winterstein, 1988). Common distributions of earthquake recurrence intervals are Gamma, Weibull, Brownian Passage Time and Lognormal. Two statistical parameters, namely mean and covariance, describe the distribution of the renewal model. The mean shows the average recurrence time and covariance represents the periodicity of the earthquake recurrence intervals.

In renewal models, hazard rate, which is dependent on the probability distribution, is utilized to express the time dependency. Hazard rate is determined from the hazard function, h(t), given in equation (2.18).

$$h(t) = \frac{f_t(t)}{1 - F_t(t)} \tag{2.18}$$

here,

$f_t(t)$ = probability density function of inter event time

$F_t(t)$ = cumulative distribution function of inter event time

2.7 Ground Motion Prediction Equations

Ground motion prediction equations (GMPE's), which are also known as attenuation relationships, are mathematical descriptions to predict the ground motion at a site

which are derived based on empirical data applying different regression methods. The reason they are called as attenuation relationships is the attenuation of the seismic waves while distance to the epicenter increases based on the soil conditions. The main parameters of a GMPE are magnitude, distance to the site from the source. In addition to these, site parameters and seismological parameters are also used in various GMPE's. More than 500 published attenuation models are available around the world.

The general form of a GMPE is shown in equation (2.19) below.

$$Ln\,(Y) = c_0 + c_2 M + c_3 M^{c_4} + c_5 \ln(R) + f(F) + f(HW) + f(S') + \varepsilon \qquad (2.19)$$

where,

Y= ground motion parameter

c_0, c_1, c_2, c_3, c_4, c_5 = constants determined from regression analysis

M = magnitude

R = distance to the site from the source

S' = site parameters

F = fault type parameters

HW = hanging wall parameters

The GMPE's used in this thesis are listed below:

- Boore, Joyner and Fumal (1997)
- Kalkan and Gülkan (2004)
- Abrahamson and Silva (2008)
- Gülerce et al (2015)

Boore, Joyner and Fumal (1997) derived a ground motion prediction equation to estimate horizontal response spectra and peak ground acceleration for shallow earthquakes in western North America. Fault types are reverse, strike-slip and

unknown. For propagation effect, Joyner-Boore distance is used. Pseudo-spectral acceleration is calculated for 5% damping. In this ground motion prediction equation, to represent site effects, V_{S30} value is used.

Ground motion prediction equation derived by Boore, Joyner and Fumal (1997) is as follows:

$$\ln Y = b_1 + b_2(M-6) + b_3(M-6)^2 + b_5\, lnr + b_V\, ln\frac{V_s}{V_A} \qquad (2.20)$$

where,

$$r = \sqrt{r_{jb}^2 + h^2}$$

and

$$b_1 = \begin{cases} b_{1SS} & \text{for strike slip earthquakes} \\ b_{1RS} & \text{for reverse slip earthquakes} \\ b_{1ALL} & \text{if mechanism is not sepcified} \end{cases}$$

here,

Y: peak ground acceleration or pseudo-spectral acceleration (g)

M: moment magnitude

r_{jb}: Joyner Boore distance (km)

V_s: average shear-wave velocity to 30 m (m/sec)

b_{1SS}, b_{1RS}, b_{1ALL}, b_2, b_3, b_5, h, b_v and V_A are the coefficients which shall be determined from Table 2.1.

Table 2.1 Attenuation Coefficients in the Equation Derived by Boore, Joyner and Fumal (1997)

Period (s)	b_{1SS}	b_{1RV}	b_{1ALL}	b_2	b_3	b_5	b_v	V_A (m/s)	σln(y)	h (km)
0.00	-0.313	-0.117	-0.242	0.527	0.000	-0.778	-0.371	1396	0.520	5.57
0.10	1.006	1.087	1.059	0.753	-0.226	-0.934	-0.212	1112	0.479	6.27
0.11	1.072	1.164	1.130	0.732	-0.230	-0.937	-0.211	1291	0.481	6.65
0.12	1.109	1.215	1.174	0.721	-0.233	-0.939	-0.215	1452	0.485	6.91
0.13	1.128	1.246	1.200	0.711	-0.233	-0.939	-0.221	1596	0.486	7.08
0.14	1.135	1.261	1.208	0.707	-0.230	-0.938	-0.228	1718	0.489	7.18
0.15	1.128	1.264	1.204	0.702	-0.228	-0.937	-0.238	1820	0.492	7.23
0.16	1.112	1.257	1.192	0.702	-0.226	-0.935	-0.248	1910	0.495	7.24
0.17	1.090	1.242	1.173	0.702	-0.221	-0.933	-0.258	1977	0.497	7.21
0.18	1.063	1.222	1.151	0.705	-0.216	-0.930	-0.270	2037	0.499	7.16
0.19	1.032	1.198	1.122	0.709	-0.212	-0.927	-0.281	2080	0.501	7.10
0.20	0.999	1.170	1.089	0.711	-0.207	-0.924	-0.292	2118	0.502	7.02
0.22	0.925	1.104	1.019	0.721	-0.198	-0.918	-0.315	2158	0.508	6.83
0.24	0.847	1.033	0.941	0.732	-0.189	-0.912	-0.338	2178	0.511	6.62
0.26	0.764	0.958	0.861	0.744	-0.180	-0.906	-0.360	2173	0.514	6.39
0.28	0.681	0.881	0.780	0.758	-0.168	-0.899	-0.381	2158	0.518	6.17
0.30	0.598	0.803	0.700	0.769	-0.161	-0.893	-0.401	2133	0.522	5.94
0.32	0.518	0.725	0.619	0.783	-0.152	-0.888	-0.420	2104	0.525	5.72
0.34	0.439	0.648	0.540	0.794	-0.143	-0.882	-0.438	2070	0.530	5.50
0.36	0.361	0.570	0.462	0.806	-0.136	-0.877	-0.456	2032	0.532	5.30
0.38	0.286	0.495	0.385	0.820	-0.127	-0.872	-0.472	1995	0.536	5.10
0.40	0.212	0.423	0.311	0.831	-0.120	-0.867	-0.487	1954	0.538	4.91
0.42	0.140	0.352	0.239	0.840	-0.113	-0.862	-0.502	1919	0.542	4.74
0.44	0.073	0.282	0.169	0.852	-0.108	-0.858	-0.516	1884	0.545	4.57
0.46	0.005	0.217	0.102	0.863	-0.101	-0.854	-0.529	1849	0.549	4.41
0.48	-0.058	0.151	0.036	0.873	-0.097	-0.850	-0.541	1816	0.551	4.26
0.50	-0.122	0.087	-0.025	0.884	-0.090	-0.846	-0.553	1782	0.556	4.13
0.55	-0.268	-0.063	-0.176	0.907	-0.078	-0.837	-0.579	1710	0.562	3.82
0.60	-0.401	-0.203	-0.314	0.928	-0.069	-0.830	-0.602	1644	0.569	3.57
0.65	-0.523	-0.331	-0.440	0.946	-0.060	-0.823	-0.622	1592	0.575	3.36
0.70	-0.634	-0.452	-0.555	0.962	-0.053	-0.818	-0.639	1545	0.582	3.20
0.75	-0.737	-0.562	-0.661	0.979	-0.046	-0,813	-0.653	1507	0.587	3.07
0.80	-0.829	-0.666	-0.760	0.992	-0.041	-0.809	-0.666	1476	0.593	2.98
0.85	-0.915	-0.761	-0.851	1.006	-0.037	-0.805	-0.676	1452	0.598	2.92

Table 2.1(cont'd) Attenuation Coefficients in the Equation Derived by Boore, Joyner and Fumal (1997)

Period (s)	b_{1SS}	b_{1RV}	b_{1ALL}	b_2	b_3	b_5	b_v	V_A (m/s)	σln(y)	h (km)
0.90	-0.993	-0.848	-0.933	1.018	-0.035	-0.802	-0.685	1432	0.604	2.89
0.95	-1.066	-0.932	-1.010	1.027	-0.032	-0.800	-0.692	1416	0.609	2.88
1.00	-1.133	-1.009	-1.080	1.036	-0.032	-0.798	-0.698	1406	0.613	2.90
1.10	-1.249	-1.145	-1.208	1.052	-0.030	-0.795	-0.706	1396	0.622	2.99
1.20	-1.345	-1.265	-1.315	1.064	-0.032	-0.794	-0.710	1400	0.629	3.14
1.30	-1.428	-1.370	-1.407	1.073	-0.035	-0.793	-0.711	1416	0.637	3.36
1.40	-1.495	-1.460	-1.483	1.080	-0.039	-0.794	-0.709	1442	0.643	3.62
1.50	-1.552	-1.538	-1.550	1.085	-0.044	-0.796	-0.704	1479	0.649	3.92
1.60	-1.598	-1.608	-1.605	1.087	-0.051	-0.798	-0.697	1524	0.654	4.26
1.70	-1.634	-1.668	-1.652	1.089	-0.058	-0.801	-0.689	1581	0.660	4.62
1.80	-1.663	-1.718	-1.689	1.087	-0.067	-0.804	-0.679	1644	0.664	5.01
1.90	-1.685	-1.763	-1.720	1.087	-0.074	-0.808	-0.667	1714	0.669	5.42
2.00	-1.699	-1.801	-1.743	1.085	-0.085	-0.812	-0.655	1795	0.672	5.85

Kalkan and Gülkan (2004) carried out a study to estimate horizontal peak ground acceleration and pseudo spectral acceleration with 5% damping for shallow crustal earthquakes for Turkey. They used a total of 112 records compiled from 57 events. They derived this equation for normal, strike-slip and reverse faults. To represent ground condition, V_{S30} value is used and source distance is represented with closest horizontal distance. Form of the ground motion prediction equation is similar to the one proposed by Boore, Joyner and Fumal (1997).

Empirical ground motion prediction equation is given as follows:

$$\ln Y = b_1 + b_2(M-6) + b_3(M-6)^2 + b_5\, lnr + b_V\, ln\frac{V_s}{V_A} \qquad (2.21)$$

where,

$$r = \sqrt{r_{cl}^2 + h^2}$$

here,

Y: peak ground acceleration or pseudo-spectral acceleration (g)

M: moment magnitude

r_{cl}: closest horizontal distance from the source to the site of interest (km)

V_S: average shear-wave velocity to 30 m (m/sec)

Coefficients of this ground motion prediction equation are given in Table 2.2

Table 2.2 Attenuation Coefficients in the Equation Derived by Kalkan and Gülkan (2004)

Period (s)	**b_1**	**b_2**	**b_3**	**b_5**	**b_v**	**V_A (m/s)**	**σln(y)**	**h (km)**
PGA	0.393	0.576	-0.107	-0.899	-0.200	1112	0.612	6.91
0.10	1.796	0.441	-0.087	-1.023	-0.054	1112	0.658	10.07
0.11	1.627	0.498	-0.086	-1.030	-0.051	1290	0.643	10.31
0.12	1.109	0.721	-0.233	-0.939	-0.251	1452	0.650	6.91
0.13	1.474	0.500	-0.127	-1.070	-0.300	1953	0.670	10.00
0.14	0.987	0.509	-0.114	-1.026	-0.500	1717	0.620	9.00
0.15	1.530	0.511	-0.127	-1.070	-0.300	1953	0.623	10.00
0.16	1.471	0.517	-0.125	-1.052	-0.298	1954	0.634	9.59
0.17	1.500	0.530	-0.115	-1.060	-0.297	1955	0.651	9.65
0.18	1.496	0.547	-0.115	-1.060	-0.301	1957	0.646	9.40
0.19	1.468	0.575	-0.108	-1.055	-0.302	1958	0.657	9.23
0.20	1.419	0.597	-0.097	-1.050	-0.303	1959	0.671	8.96
0.22	0.989	0.628	-0.118	-0.951	-0.301	1959	0.683	6.04
0.24	0.736	0.654	-0.113	-0.892	-0.302	1960	0.680	5.16
0.26	0.604	0.696	-0.109	-0.860	-0.305	1961	0.682	4.70
0.28	0.727	0.733	-0.127	-0.891	-0.303	1963	0.674	5.74
0.30	0.799	0.751	-0.148	-0.909	-0.297	1964	0.720	6.49
0.32	0.749	0.744	-0.161	-0.897	-0.300	1954	0.714	7.18
0.34	0.798	0.741	-0.154	-0.891	-0.266	1968	0.720	8.10
0.36	0.589	0.752	-0.143	-0.867	-0.300	2100	0.650	7.90
0.38	0.490	0.763	-0.138	-0.852	-0.300	2103	0.779	8.00
0.40	0.530	0.775	-0.147	-0.855	-0.264	2104	0.772	8.32

Table 2.2 (cont'd) Coefficients in the Equation Derived by Kalkan and Gülkan (2004)

Period (s)	b_1	b_2	b_3	b_5	b_v	V_A (m/s)	σln(y)	h (km)
0.42	0.353	0.784	-0.150	-0.816	-0.267	2104	0.812	7.69
0.44	0.053	0.782	-0.132	-0.756	-0.268	2103	0.790	7.00
0.46	0.049	0.780	-0.157	-0.747	-0.290	2059	0.781	7.30
0.48	-0.170	0.796	-0.153	-0.704	-0.275	2060	0.789	6.32
0.50	-0.146	0.828	-0.161	-0.710	-0.274	2064	0.762	6.22
0.70	-0.576	0.914	-0.190	-0.681	-0.301	2102	0.840	5.70
0.75	-0.648	0.933	-0.185	-0.676	-0.300	2104	0.828	5.90
0.80	-0.713	0.968	-0.183	-0.676	-0.301	2090	0.839	5.89
0.85	-0.567	0.986	-0.214	-0.695	-0.333	1432	0.825	6.27
0.90	-0.522	1.019	-0.225	-0.708	-0.313	1431	0.826	6.69
0.95	-0.610	1.050	-0.229	-0.697	-0.303	1431	0.841	6.89
1.00	-0.622	1.070	-0.250	-0.696	-0.305	1405	0.874	6.89
1.10	-1.330	1.089	-0.255	-0.684	-0.500	2103	0.851	7.00
1.20	-1.370	1.120	-0.267	-0.690	-0.498	2103	0.841	6.64
1.30	-1.474	1.155	-0.269	-0.696	-0.496	2103	0.856	6.00
1.40	-1.665	1.170	-0.258	-0.674	-0.500	2104	0.845	5.44
1.50	-1.790	1.183	-0.262	-0.665	-0.501	2104	0.840	5.57
1.60	-1.889	1.189	-0.265	-0.662	-0.503	2102	0.834	5.50
1.70	-1.968	1.200	-0.272	-0.664	-0.502	2101	0.828	5.30
1.80	-2.037	1.210	-0.284	-0.666	-0.505	2098	0.849	5.10
1.90	-1.970	1.210	-0.295	-0.675	-0.501	1713	0.855	5.00
2.00	-2.110	1.200	-0.300	-0.663	-0.499	1794	0.878	4.86

Abrahamson and Silva (2008) developed a next generation attenuation (NGA) relationship within the scope of the NGA project. Ground motion data set is selected from the NGA data base. The site condition is classified using two parameters: the average shear-wave velocity in the top 30 m V_{S30} and the depth to V_S=1.0 km/s . Primary distance measure is the closest distance to the rupture plane, R_{rup}. Format of the equation is taken from Abrahamson and Silva (1997). Basic form of AS08 is given in equation (2.22).

$$f_1(M, R_{rup}) = \begin{cases} a_1 + a_4(M - c_1) + a_8(8.5 - M)^2 + [a_2 + a_3(M - c_1)] \ln R & (M \leq c_1) \\ a_1 + a_5(M - c_1) + a_8(8.5 - M)^2 + [a_2 + a_3(M - c_1)] \ln R & (M > c_1) \end{cases} \quad (2.22)$$

Since complete form of the equations includes many parameters, only basic form of them are given in this thesis.

All coefficients of next generation attenuation relationship derived by Abrahamson and Silva (2008) are given in Tables 2.3 and 2.4.

Table 2.3 Basic Next Generation Attenuation Equation Coefficients Derived by Abrahamson and Silva (2008)

c_1	6.75
c_2	50
c_4	4.5
a_3	0.265
a_4	-0.231
a_5	-0.398
soil_n	1.18
soil_c	1.88

Table 2.4 Next Generation Attenuation Equation Coefficients Derived by Abrahamson and Silva (2008)

T (s)	VLIN	b	a1	a2	a8	a10	a12	a13	a14	a15	a16	a18	s1_est	s2_est	s1_msrd	s2_msrd	s3	s4	rh/t
0.000	865.1	-1.186	0.8040	-0.9679	-0.0372	0.9445	0.0000	-0.0600	1.0800	-0.3500	0.9000	-0.0067	0.590	0.470	0.576	0.453	0.470	0.300	1.000
0.010	865.1	-1.186	0.8110	-0.9679	-0.0372	0.9445	0.0000	-0.0600	1.0800	-0.3500	0.9000	-0.0067	0.590	0.470	0.576	0.453	0.420	0.300	1.000
0.020	865.1	-1.219	0.8550	-0.9774	-0.0372	0.9834	0.0000	-0.0600	1.0800	-0.3500	0.9000	-0.0067	0.590	0.470	0.576	0.453	0.420	0.300	1.000
0.030	907.8	-1.273	0.9620	-1.0024	-0.0372	1.0471	0.0000	-0.0600	1.1331	-0.3500	0.9000	-0.0067	0.605	0.478	0.591	0.461	0.462	0.305	0.991
0.040	994.5	-1.308	1.0370	-1.0289	-0.0315	1.0884	0.0000	-0.0600	1.1708	-0.3500	0.9000	-0.0067	0.615	0.483	0.602	0.466	0.492	0.309	0.982
0.050	1053.5	-1.346	1.1330	-1.0508	-0.0271	1.1333	0.0000	-0.0600	1.2000	-0.3500	0.9000	-0.0076	0.623	0.488	0.610	0.471	0.515	0.312	0.973
0.075	1085.7	-1.471	1.3750	-1.0810	-0.0191	1.2808	0.0000	-0.0600	1.2000	-0.3500	0.9000	-0.0093	0.630	0.495	0.617	0.479	0.550	0.317	0.952
0.100	1032.5	-1.624	1.5630	-1.0833	-0.0166	1.4613	0.0000	-0.0600	1.2000	-0.3500	0.9000	-0.0093	0.630	0.501	0.617	0.485	0.550	0.321	0.929
0.150	877.6	-1.931	1.7160	-1.0357	-0.0254	1.8071	0.0181	-0.0600	1.1683	-0.3500	0.9000	-0.0093	0.630	0.509	0.616	0.491	0.550	0.326	0.896
0.200	748.2	-2.188	1.6870	-0.9700	-0.0396	2.0773	0.0309	-0.0600	1.1274	-0.3500	0.9000	-0.0083	0.630	0.514	0.614	0.495	0.520	0.329	0.874
0.250	654.3	-2.381	1.6460	-0.9202	-0.0539	2.2794	0.0409	-0.0600	1.0956	-0.3500	0.9000	-0.0069	0.630	0.518	0.612	0.497	0.497	0.332	0.856
0.300	587.1	-2.518	1.6010	-0.8974	-0.0656	2.4201	0.0491	-0.0600	1.0697	-0.3500	0.9000	-0.0057	0.630	0.522	0.611	0.499	0.479	0.335	0.841
0.400	503.0	-2.657	1.5110	-0.8677	-0.0807	2.5510	0.0619	-0.0600	1.0288	-0.3500	0.8423	-0.0039	0.630	0.527	0.608	0.501	0.449	0.338	0.818
0.500	456.6	-2.669	1.3970	-0.8475	-0.0924	2.5395	0.0719	-0.0600	0.9971	-0.3191	0.7458	-0.0025	0.630	0.532	0.606	0.504	0.426	0.341	0.783
0.750	410.5	-2.401	1.1370	-0.8206	-0.1137	2.1493	0.0800	-0.0600	0.9395	-0.2629	0.5704	0.0000	0.630	0.539	0.602	0.506	0.385	0.346	0.680
1.000	400.0	-1.955	0.9150	-0.8088	-0.1289	1.5705	0.0800	-0.0600	0.8985	-0.2230	0.4460	0.0000	0.630	0.545	0.594	0.503	0.350	0.350	0.607
1.500	400.0	-1.025	0.5100	-0.7995	-0.1534	0.3991	0.0800	-0.0600	0.8409	-0.1668	0.2707	0.0000	0.615	0.552	0.566	0.497	0.350	0.350	0.504
2.000	400.0	-0.299	0.1920	-0.7960	-0.1708	-0.6072	0.0800	-0.0600	0.8000	-0.1270	0.1463	0.0000	0.604	0.558	0.544	0.491	0.350	0.350	0.431
3.000	400.0	0.000	-0.2800	-0.7960	-0.1954	-0.9600	0.0800	-0.0600	0.4793	-0.0708	-0.0291	0.0000	0.589	0.565	0.527	0.500	0.350	0.350	0.328
4.000	400.0	0.000	-0.6390	-0.7960	-0.2128	-0.9600	0.0800	-0.0600	0.2518	-0.0309	-0.1535	0.0000	0.578	0.570	0.515	0.505	0.350	0.350	0.255

Table 2.4 (cont'd) Next Generation Attenuation Equation Coefficients Derived by Abrahamson and Silva (2008)

T (s)	VLIN	b	a1	a2	a8	a10	a12	a13	a14	a15	a16	a18	s1_est	s2_est	s1_msrd	s2_msrd	s3	s4	rh/t
5.000	400.0	0.000	-0.9360	-0.7960	-0.2263	-0.9208	0.0800	-0.0600	0.0754	0.0000	-0.2500	0.0000	0.570	0.587	0.510	0.529	0.350	0.350	0.200
7.500	400.0	0.000	-1.5270	-0.7960	-0.2509	-0.7700	0.0800	-0.0600	0.0000	0.0000	-0.2500	0.0000	0.611	0.618	0.572	0.579	0.350	0.350	0.200
10.000	400.0	0.000	-1.9930	-0.7960	-0.2683	-0.6630	0.0800	-0.0600	0.0000	0.0000	-0.2500	0.0000	0.640	0.640	0.612	0.612	0.350	0.350	0.200

Gülerce et al. (2015) proposed TR-Adjusted NGA-W1 models as an alternative to NGA-W1 models and regional GMPE developed for Turkey based on Abrahamson and Silva (2008). The form of the equation is same as the equation proposed by Abrahamson and Silva (2008). Coefficients of this ground motion equation are given in Tables 2.5 and 2.6

Table 2.5 Basic Ground Motion Prediction Equation Coefficients Derived by Gülerce et al. (2015)

c1	6.75
c2	50
c4	4.5
a3	0.265
a5	-0.398
soil_n	1.18
soil_c	1.88

Table 2.6 Ground Motion Prediction Equation Coefficients Derived by Gülerce et al. (2015)

T (s)	VLIN	b	a1	a2	a4	a8	a10	a12	a13	a14	a15	a16	a18	s1_est	s2_est	s1_msrd	s2_msrd	s3	s4	rh/t	c3_TA	Vhinge
0.000	865.1	-1.186	0.8040	-0.9679	0.470	-0.0372	0.9445	0.0000	-0.0600	1.0800	-0.3500	0.9000	-0.0040	0.590	0.470	0.576	0.453	0.470	0.300	1.000	-0.1806	450
0.010	865.1	-1.186	0.8110	-0.9679	0.470	-0.0372	0.9445	0.0000	-0.0600	1.0800	-0.3500	0.9000	-0.0040	0.590	0.470	0.576	0.453	0.420	0.300	1.000	-0.1806	450
0.020	865.1	-1.219	0.8550	-0.9774	0.470	-0.0372	0.9834	0.0000	-0.0600	1.0800	-0.3500	0.9000	-0.0040	0.590	0.470	0.576	0.453	0.420	0.300	1.000	-0.1818	450
0.030	907.8	-1.273	0.9620	-1.0024	0.470	-0.0372	1.0471	0.0000	-0.0600	1.1331	-0.3500	0.9000	-0.0040	0.605	0.478	0.591	0.461	0.462	0.305	0.991	-0.1570	450
0.040	994.5	-1.308	1.0370	-1.0289	0.470	-0.0315	1.0884	0.0000	-0.0600	1.1708	-0.3500	0.9000	-0.0040	0.615	0.483	0.602	0.466	0.492	0.309	0.982	-0.1360	450
0.050	1053.5	-1.346	1.1330	-1.0508	0.470	-0.0271	1.1333	0.0000	-0.0600	1.2000	-0.3500	0.9000	-0.0050	0.623	0.488	0.610	0.471	0.515	0.312	0.973	-0.1200	450
0.075	1085.7	-1.471	1.3750	-1.0810	0.470	-0.0191	1.2808	0.0000	-0.0600	1.2000	-0.3500	0.9000	-0.0069	0.630	0.495	0.617	0.479	0.550	0.317	0.952	-0.0939	450
0.100	1032.5	-1.624	1.5630	-1.0833	0.470	-0.0166	1.4613	0.0000	-0.0600	1.2000	-0.3500	0.9000	-0.0075	0.630	0.501	0.617	0.485	0.550	0.321	0.929	-0.0900	450
0.150	877.6	-1.931	1.7160	-1.0357	0.470	-0.0254	1.8071	0.0181	-0.0600	1.1683	-0.3500	0.9000	-0.0075	0.630	0.509	0.616	0.491	0.550	0.326	0.896	-0.1180	450
0.200	748.2	-2.188	1.6870	-0.9700	0.466	-0.0396	2.0773	0.0309	-0.0600	1.1274	-0.3500	0.9000	-0.0067	0.630	0.514	0.614	0.495	0.520	0.329	0.874	-0.1682	450
0.250	654.3	-2.381	1.6460	-0.9202	0.459	-0.0539	2.2794	0.0409	-0.0600	1.0956	-0.3500	0.9000	-0.0051	0.630	0.518	0.612	0.497	0.497	0.332	0.856	-0.2242	450
0.300	587.1	-2.518	1.6010	-0.8974	0.453	-0.0656	2.4201	0.0491	-0.0600	1.0697	-0.3500	0.9000	-0.0037	0.630	0.522	0.611	0.499	0.479	0.335	0.841	-0.2550	450
0.400	503.0	-2.657	1.5110	-0.8677	0.443	-0.0807	2.5510	0.0619	-0.0600	1.0288	-0.3500	0.8423	-0.0016	0.630	0.527	0.608	0.501	0.449	0.338	0.818	-0.2900	450
0.500	456.6	-2.669	1.3970	-0.8475	0.435	-0.0924	2.5395	0.0719	-0.0600	0.9971	-0.3191	0.7458	0.0000	0.630	0.532	0.606	0.504	0.426	0.341	0.783	-0.3100	450
0.750	410.5	-2.401	1.1370	-0.8206	0.422	-0.1137	2.1493	0.0800	-0.0600	0.9395	-0.2629	0.5704	0.0000	0.630	0.539	0.602	0.506	0.385	0.346	0.680	-0.3320	450
1.000	400.0	-1.955	0.9150	-0.8088	0.412	-0.1289	1.5705	0.0800	-0.0600	0.8985	-0.2230	0.4460	0.0000	0.630	0.545	0.594	0.503	0.350	0.350	0.607	-0.3270	450
1.500	400.0	-1.025	0.5100	-0.7995	0.393	-0.1534	0.3991	0.0800	-0.0600	0.8409	-0.1668	0.2707	0.0000	0.615	0.552	0.566	0.497	0.350	0.350	0.504	-0.2830	450
2.000	400.0	-0.299	0.1920	-0.7960	0.380	-0.1708	-0.6072	0.0800	-0.0600	0.8000	-0.1270	0.1463	0.0000	0.604	0.558	0.544	0.491	0.350	0.350	0.431	-0.2200	450
3.000	400.0	0.000	-0.2800	-0.7960	0.340	-0.1954	-0.9600	0.0800	-0.0600	0.4793	-0.0708	-0.0291	0.0000	0.589	0.565	0.527	0.500	0.350	0.350	0.328	-0.1200	450
4.000	400.0	0.000	-0.6390	-0.7960	0.311	-0.2128	-0.9600	0.0800	-0.0600	0.2518	-0.0309	-0.1535	0.0000	0.578	0.570	0.515	0.505	0.350	0.350	0.255	-0.0100	450

Table 2.6 (cont'd) Ground Motion Prediction Equation Coefficients Derived by Gülerce et al. (2015)

T (s)	VLIN	b	a1	a2	a4	a8	a10	a12	a13	a14	a15	a16	a18	s1_est	s2_est	s1_msrd	s2_msrd	s3	s4	rh/t	c3_TA	Vhinge
5.000	400.0	0.000	-0.9360	-0.7960	0.289	-0.2263	-0.9208	0.0800	-0.0600	0.0754	0.0000	-0.2500	0.0000	0.570	0.587	0.510	0.529	0.350	0.350	0.200	0.0000	450
7.500	400.0	0.000	-1.5270	-0.7960	0.249	-0.2509	-0.7700	0.0800	-0.0600	0.0000	0.0000	-0.2500	0.0000	0.611	0.618	0.572	0.579	0.350	0.350	0.200	0.0000	450
10.000	400.0	0.000	-1.9930	-0.7960	0.220	-0.2683	-0.6630	0.0800	-0.0600	0.0000	0.0000	-0.2500	0.0000	0.640	0.640	0.612	0.612	0.350	0.350	0.200	0.0000	450

2.8 Calculation of Seismic Hazard

The final step in PSHA is to determine the exceedance rate of a specified ground motion parameter at a particular site. Seismic hazard can be calculated in terms of many ground motion parameters such as peak ground acceleration, spectral acceleration, displacement etc. Total hazard is calculated by combining the contribution of each single source based on the total probability theorem.

Hazard equation for an individual seismic source is defined by equation (2.23).

$$\nu(Y \geq y) = \sum_i \nu_i \iint \dots \int \Pr\left(Y \geq y \ / \tilde{X}\right) f_x\left(\tilde{X}\right) dx \qquad (2.23)$$

where,

$\nu(Y \geq y)$= annual frequency of the ground motion parameter, Y, exceeding y.

ν_i = annual rate of earthquake occurrence due to the i^{th} seismic source

$\tilde{X}$= vector of random variables that influence Y, such as magnitude (M), distance between seismic source and the site (R) etc.

$f_x(\tilde{X})$ = joint probability density function of random variables $\tilde{X}$

If only M and R are taken into consideration and by assuming that these two random variables are independent, annual frequency of exceedance can be written as:

$$\nu(Y \geq y) = \sum_i \nu_i \int_{r=0}^{\infty} \int_{M_{min}}^{M_{max}} \Pr(Y \geq y/M,R)\, f_M(M) f_R(R) dm dr \qquad (2.24)$$

where,

f_M = probability density function of magnitude

f_R = probability density function of distance between seismic source and the site

Here, total hazard is expressed in terms of annual frequency of exceedance events and also it corresponds approximately to the annual probability of exceedance. When this probability is calculated once, the procedure is repeated for various ground motion levels which results into a series of different ground motion levels and their corresponding probabilities of exceedance, from which the decision maker can select the design levels for the specified parameters.

2.9 Uncertainties in Probabilistic Seismic Hazard Analysis

Describing and dealing with uncertainties are essential parts of a probabilistic seismic hazard analysis. Uncertainties are classified into two main types: Aleatory and epistemic. Inherent randomness is considered as the aleatory uncertainty, whereas epistemic uncertainty is mainly due to lack of sufficient data and information. In probabilistic seismic hazard analysis, aleatory uncertainty arises from the random occurrence of earthquakes and epistemic uncertainty roots in the hazard calculation process involving distribution models, ground motion prediction equations etc. It is essential to comprehend the difference between these two types of uncertainties to understand what are the reasons of these uncertainties and in what way these uncertainties can be handled.

2.9.1 Aleatory Uncertainty

Inherent variability in a process is called as the aleatory uncertainty which is unavoidable and omnipresent. It is described by probability density functions defining parameter distributions in continuous variables, whereas it is described by the probability of occurrence of each possible value in the case of discrete random variables.

Aleatory uncertainty is generally quantified in hazard analysis by using variance, standard deviation or coefficient of variation. Thus, it has direct quantitative impact on the results of seismic hazard analysis (Abrahamson & Bommer, 2005).

2.9.2 Epistemic Uncertainty

Epistemic uncertainty comes into existence due to limited data and knowledge, so it can be diminished as more information and data become available.

Epistemic uncertainty is described by the implementation of alternative probability density functions utilized by using of random parameters which include known and unknown values. Thus, epistemic uncertainty is not directly taken into account in the hazard calculations and instead alternative models are taken into consideration to produce corresponding alternative hazard curves (Abrahamson & Bommer, 2005). The most widely used tool is the logic tree model which is based on the theorem of total probability.

2.9.2.1 Logic Tree

Logic trees are commonly used to deal with epistemic uncertainty. A logic tree comprises of branches and these branches represent alternative models to be used in the steps of PSHA calculations i.e. source characterizations, alternative GMPE's. A probability value is assigned to each alternative model and then these alternative models are combined and a weighted average seismic output is obtained.

CHAPTER 3

BEHAVIOR OF TRANSPORTATION LIFELINE SYSTEM COMPONENTS UNDER EARTHQUAKE LOADS

3.1 Introduction

As stated in Chapter 1, to determine the reliability of a system, firstly reliability of the elements of the system should be determined. To calculate the element reliability, capacity and demand associated with the element should be assessed. Hence, to find the highway system reliability against earthquakes, earthquake loads on each element and the capacity against earthquake should be determined. In Chapter 2, PSHA is explained in detail, which is a method to estimate the parameters which forms the basis to obtain the earthquake load at a given site. Once the earthquake load on a given site is determined, seismic loads on the elements can be determined, too. In this chapter, failure reasons and earthquake response of highway structures are explained and capacity determinations of these structures are presented.

Highway systems are composed of various components, such as viaducts, bridges, roads, highways, tunnels, culverts, retaining walls, trenches and slopes etc. In this thesis, only viaducts, highway bridges and asphalt roads are taken into consideration, since they are the most encountered components on a highway system.

Highway bridges and viaducts are identified in many categories based on their materials, types of decks, number of spans etc. In this thesis, reinforced concrete highway bridges and viaducts are considered. Roads (pavements) are usually classified in three categories (Adlinge and Gupta, 2013) namely, flexible pavements, rigid pavements and unpaved pavements. Flexible pavements consist of many layers

and have ability to bend under the tyre load. Asphalt roads fall into the category of flexible pavements due to the elasticity of the material. Rigid pavements are formed of concrete and they are stiffer than the flexible pavements. Rigid pavements are generally supported with the reinforcements. Unpaved pavements consist of gravels ordinarily.

3.2 Failure Reasons of Highway Systems

Components of highway systems may fail due to many factors. In this section, causes of failure of highway bridges and asphalt roads are discussed.

3.2.1 Failure Reasons of Highway Bridges

Based on the study carried out by Wardhana and Hadipriono (2003) for over 500 failed bridges, main failure reasons of bridges are listed as follows:

- Hydraulic: Flood, scour, debris, drift etc.
- Collision: Car/truck, barge/ship/tanker
- Overloading
- Deterioration: Steel, concrete
- Construction Quality and Design
- Fire
- Ice
- Fatigue
- Storm/Hurricane/Tsunami
- Earthquake

3.2.2 Failure Reasons of Asphalt Roads

Failure reasons of asphalt roads are as follows:

- Improper Construction
- Excessive Loading

- Water: Flood, Poor Drainage, Moisture
- Settlement of Underlying Material
- Ice
- Temperature Change
- Differential Movement of Layers
- Earthquakes

Within the scope of this study, failure modes due to earthquake loads are examined in the following sections.

3.3 Earthquake Effects on Highway Systems

3.3.1 Seismic Behavior of Highway Bridges

Damages on bridges due to the earthquake loads can be divided into three groups as follows (Hsu and Fu, 2004):

- Severe Damage: Traffic is interrupted due to failure of bridge components i.e. failure of bridge piers.
- Moderate Damage: Controlled traffic is maintained in spite of cracking of decks, beams, or piers etc.
- Minor Damage: Normal traffic is continued with slight cracking, minor settlement.

Seismic activity may affect the different components of bridges. Most sensitive bridge components are pier columns, abutments, bearing and foundations (Mohseni, 2012). Seismic load effects on the highway bridge components and failure mechanism are explained in detail in the following (Chang et al., 2000; Hsu and Fu, 2004):

- Pier Column Damage: Bridge pier column failure is a common failure type for the highway bridges (Kawashima and Unjoh, 1997; Hsu and Fu, 2004). Major damages are caused by shear cracks.

- Bearing Damage: Due to the improper connection of bearings, superstructure of the bridges may become in a floating condition which will result in failure of the deck.
- Girder Damage: Because of the weak connection of the deck to girders at the pier, higher stresses occur at the joint during the earthquake.
- Expansion Joint Damage: Differential movements of the spans may cause the pounding of superstructure of the bridge at expansion joints.
- Unseating of Spans: Span failure due to the earthquake is generally caused by unseating of the span. Main reasons are the design of bridges based on insufficient seat width or placement of the bridge directly on a major fault.
- Cap Beam Damage: Cap beams are expected to remain in elastic range during the earthquake. If columns are rigid and cap beams are flexible, plastic hinges occur at cap beams first (Avşar et al., 2008).
- Abutment Damage: Abutment damage is usually caused by the settlement and lateral spreading.

3.3.2 Seismic Behavior of Asphalt Roads and Highways (Flexible Pavements)

The potential seismic damages to asphalt roads are categorized in three groups namely, direct damages, indirect damages and induced damages (SYNER-G Project 244061, 2011).

- Direct damages: Damages due to fault rupture, embankment failures due to soil liquefaction are included in direct damages.
- Indirect damages: Since roads and highways are long elements and in interaction with many components around, they may become dysfunctional due to the indirect effects. For example, due to the collapsed buildings, partial or complete blockage of the roads may come into question. Another example is interruption of traffic due to landslides.
- Induced damages: Induced damages are secondary effects due to the earthquake i.e. closure due to collapse risk of heavily damaged buildings during an aftershock.

3.4 Capacity Determination of Highway System Components Against Earthquake

3.4.1 Determination of Seismic Capacities of Highway Bridges

The structural capacity of a bridge may be determined by examining the structural capacity of entire structure or its individual elements. In bridge design, the second option is preferred since the resisting elements are generally the columns (Monteiro et al., 2015). In terms of earthquake, superstructures have more resistance then other structural components, since they are usually designed based on the elastic theory (Han et al., 2009).

For an elastically designed superstructure with energy emitting devices or designed with adequate spaces between neighboring elements, the displacements due to different expected or unexpected causes may be overcome. Moreover, undesired damages to superstructure elements may be handled by element to element (in the bridge case girder to girder) redistribution, if the structure is statically indeterminate. A similar case is applicable to the foundation systems, if one pier fails, other piers share the loads and generally their residual capacity would be enough since the designs are made with high safety factors. So it can be said that a bridge fails as soon as the first column failure occurs. Thus, if the system behavior is accepted as series, the collapse of a single pier would immediately cause failure of the bridge and consequently complete traffic interruption. In other words, assuming that the deck will show elastic behavior and neglecting possible soil failure at the foundations, the piers are the essential elements that may cause the collapse of a bridge.

The height inequalities of bridge substructure elements, especially in the viaducts constructed on deep and long valleys produces unequal force demands in piers. For instance shear force concentrations in comparatively short piers of the viaducts is responsible of seismic damages. Several studies relate the observed seismic damages of bridges in China, Japan, New Zealand, Chile and other countries to the substructures composed by piers with different heights and consequently different

lateral stiffness (Jara et al., 2015). Thus the capacity of the bridge is highly correlated to the capacity of the piers.

By considering all these factors, in this study, it is assumed that column piers are the first damaged elements during the earthquakes, which cause the failure of highway bridges. Therefore, capacity determination of pier columns due to earthquakes is the main concern here.

Examples of severe column pier damages are shown in Figures 3.1 and 3.2.

Figure 3.1 Concrete Bridge Columns After the 1994 Northridge Earthquake, California (Highway 118/Bull Creek Bridge) (Adopted from NISEE e-Library, 1994)

Figure 3.2 Baihua Bridge After 2008 Wenchuan Earthquake

(Adopted from Han et al., 2009)

Capacities of pier columns are determined by structural modeling and by analysis. It is generally convenient to model the whole bridge, but for long bridges, models can be constructed from expansion joints to expansion joints. According to Monteiro et al. (2015), to find the capacity of pier columns during an earthquake, it is necessary to consider nonlinear behavior. In other words, the deck is assumed to show an elastic behavior and plastic hinges should be assigned to columns. Rigid links are defined between column piers and deck. Abutments are modelled as spring members to represent the soil or piles. Analyses can be performed either by using response spectrum data or ground motion data. Ground motion data should be selected by considering the tectonic regime of the site.

3.4.2 Determination of Seismic Capacities of Asphalt Roads

Studies about the capacity determination of asphalt roads due to earthquakes are very limited since they exhibit elastic behavior and design life of them is approximately 15 years. In this thesis, only direct damages to roads and highways are considered. Therefore, for asphalt roads, two failure mechanisms namely, fault crossings (Figure 3.3) and embankment failures (Figures 3.4 and 3.5) are evaluated.

Figure 3.3 Damage to Highway Caused by Fault Rupture During the 1999 Kocaeli Earthquake, Turkey (Adopted from SYNER-G Project 244061, 2011)

Figure 3.4 Road Embankment Failure Caused by Lateral Slumping During the 1995 Kozani Earthquake, Greece (Adopted from SYNER-G Project 244061, 2011)

Figure 3.5 Road Embankment Damage Caused by Lateral Slumping During the 2008 Iwate Miyagi-Nairiku Earthquake, Japan

(Adopted from SYNER-G Project 244061, 2011)

Embankments are compacted soil fillings constructed on loose soils. Due to an earthquake, bearing capacity of the underlying soil may be exceeded. This condition results in the sliding of embankments and opening of cracks on the road pavement. Crack widths may vary from a few centimeters to many meters. Additionally, embankment failures may occur due to the liquefaction of the soil.

Main parameters that affect the capacity of embankments are geometrical parameters i.e. height, slope angle. Capacity of embankments can be determined based on analyses, but instead it is practical to use available fragility curves derived for the different embankment heights.

General procedure of deriving fragility curves for embankments is given in Figure (3.6).

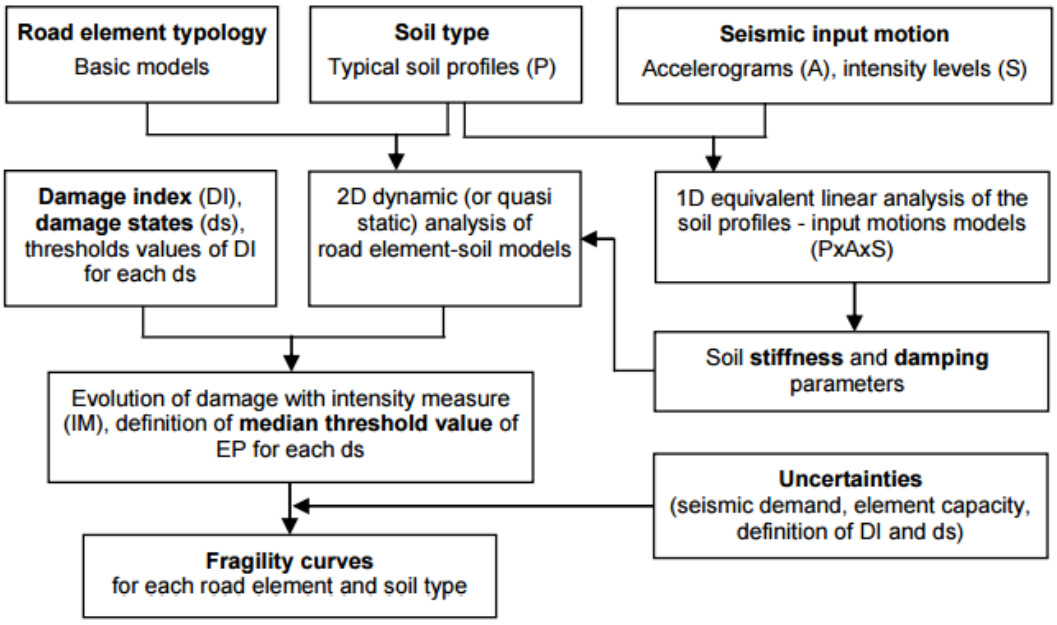

Figure 3.6 General Procedure for Deriving Numerical Fragility Curves for Road Elements (SYNER-G Project 244061, 2011)

CHAPTER 4

RELIABILITY OF STRUCTURAL SYSTEMS

4.1 Introduction

In the previous chapters, methods are explained to determine demand and capacity of structural elements of a highway system which are subjected to earthquake loads. In this chapter, methods to evaluate structural reliability of systems are explained based on capacity and demand of the structural elements. In this study, reliability of highway systems under earthquake loads is examined. Thus, the term "demand" corresponds to earthquake loads on highway elements and "capacity" corresponds to resistances of these elements to earthquake loads.

In reliability approach, safety is evaluated by probability of failure or survival of a structural element. In other words, reliability of a structure requires the probabilistic determination of structural performance.

The basis of reliability approach is the theory of probability and statistics. Since it is not easy to determine capacity and demand in real life due to the uncertainties, the load and resistance are defined as random variables.

There are three different levels to evaluate the reliability of a structure and depending on the available information, one of the methods can be selected. These are:

Level 3 methods: Classical reliability approach

Level 2 methods: First Order Second Moment (FOSM) method, Advanced First Order Second Moment (AFOSM) method

Level 1 methods: Load and Resistance Factor Design (LRFD), Monte Carlo Simulation

4.2 Methods of Structural Reliability Analysis

4.2.1 Classical Reliability Approach

In the classical reliability approach, structural reliability is basically determined based on the assumption that load and resistance are random variables and computations are based on full-distributions. A structural element should have enough capacity to withstand possible loadings in order to maintain its function. In this manner, failure of a structure occurs if resistance is less than the applied load. The relationship between load and capacity is stated by the safety margin, M which is shown in equation (4.1).

$$M = R - S \tag{4.1}$$

here,

R = resistance or strength or capacity

S = load or demand

R and S are taken as random variables.

Failure occurs is safety margin, M is smaller than zero (Figure 4.1). In this case probability of failure, P_F is defined as in equation (4.2).

$$P_F = P(M \leq 0) = P(R \leq S) \tag{4.2}$$

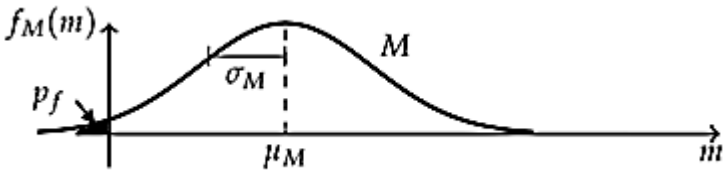

Figure 4.1 Definition of Failure in Terms of Safety Margin, M

Assuming load and resistance are statically independent and normally distributed random variables as shown in Figure 4.2, probability of failure is rewritten as follows:

$$P_F = 1 - \Phi\left(\frac{\mu_M}{\sigma_M}\right) = 1 - \Phi\left(\frac{\mu_R - \mu_S}{\sqrt{\sigma_R^2 + \sigma_S^2}}\right) \tag{4.3}$$

where,

$\Phi(\ )$ = cumulative standard normal probability distribution function

μ_M = mean value of safety margin

σ_M = standard deviation of safety margin

$f_M(m)$ = probability density function of safety margin

μ_R = mean value of resistance

μ_S = mean value of load

σ_R = standard deviation of resistance

σ_S = standard deviation of load

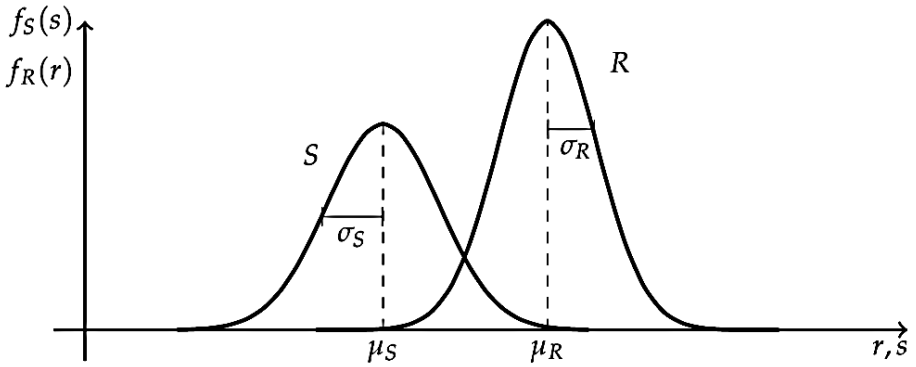

Figure 4.2 Distributions of Load and Resistance in Classical Reliability Approach

In Figure 4.2, $f_S(s)$ is probability density function for load and $f_R(r)$ is probability density function for resistance.

In a similar way, reliability of a structure, which equals to the probability of survival, P_S is expressed by equation (4.4).

$$P_S = 1 - P_F = \Phi\left(\frac{\mu_M}{\sigma_M}\right) = \Phi\left(\frac{\mu_R - \mu_S}{\sqrt{\sigma_R^2 + \sigma_S^2}}\right) \tag{4.4}$$

Classical reliability method has the following shortcomings:

- In structural engineering, the acceptable risk levels are quite small. Therefore, designs are quite sensitive to the distributions of R and S. On the other hand, lack of the data makes the accurate determination of these distributions almost impossible (tail sensitivity).
- R and S depend on many other parameters, such as material properties, dimensions, load parameters etc.

4.2.2 First Order Second Moment Method

First Order Second Moment (FOSM) method is a way to compute reliability by considering limit state functions. Limit state is the state where a structure or a part of

it can no longer fulfill the functions or satisfies the conditions for which it is designed for i.e. ultimate or serviceability limit states.

Limit state is defined by a function, $g(\tilde{X})$ in such a way that the following conditions are satisfied:

- $g(\tilde{X}) > 0$ when $\tilde{X} \in D_S$
- $g(\tilde{X}) < 0$ when $\tilde{X} \in D_F$
- $g(\tilde{X}) = 0$ (limit state surface)

where,

$g(\tilde{X})$ = limit state function, failure function, performance function

$\tilde{X}$ = vector of basic variables

D_S = safe domain (survival region)

D_F = failure domain (failure region)

Since the basic variables are random, the output of $g(\tilde{X})$ will also be a random variable shown by the random safety margin. In equation (4.5), failure surface is defined in terms of the safety margin.

$$M = g(\tilde{X}) = g\ (X_1, \dots X_n) = 0 \tag{4.5}$$

where,

n = number of random variables

Cornell (1969) proposed a reliability index as stated in equation (4.6) for linear failure functions assuming random variable, X_i has a normal distribution.

$$\beta_C = \frac{\mu_M}{\sigma_M} = \frac{\mu_R - \mu_S}{\sqrt{\sigma_R^2 + \sigma_S^2}} \tag{4.6}$$

Reliability index, β_c expresses the structural performance level corresponding to the specified limit state.

In FOSM method, if the limit state function is assumed as linear as shown in equation (4.7),

$$M = a_0 + a_1 X_1 + \cdots + a_n X_n \tag{4.7}$$

where,

$a_0, a_1, \ldots a_n$ = constants, then the corresponding mean and variance of the limit state functions will be

$$\mu_M = a_0 + a_1 \mu_1 + \cdots + a_n \mu_n \tag{4.8}$$

$$\sigma_M^2 = a_1^2 \sigma_1^2 + \cdots + a_n^2 \sigma_n^2 + \sum_{i=1}^{n} \sum_{j=1}^{n} \rho_{ij} a_i a_j \sigma_i \sigma_j \tag{4.9}$$

where,

$i \neq j$

μ_i = mean of the i^{th} random variable

σ_i = standard deviation of the i^{th} random variable

ρ_{ij} = correlation coefficient between random variables X_i and X_j

Nonlinear limit state functions are linearized by Taylor series expansion at the mean values by keeping only the first-order terms. However, this method has two shortcomings:

- When limit state function is nonlinear, significant errors may be introduced at increasing distances from the linearization point by neglecting higher order terms.
- Mean point expansion lacks limit state function invariance property. In other words, mechanically equivalent formulations of the same failure criterion may give different reliability index values.

4.2.3 Advanced First Order Second Moment Method

In order to overcome the shortcomings of the FOSM method, Hasofer and Lind (1974) proposed Advanced First Order Second Moment (AFOSM) method which is also known as First Order Reliability Method (FORM). In this method, the reliability index has the failure function invariance property. The first step of this method is to normalize all random variables using equation (4.10) to satisfy the condition that they have zero mean and unit standard deviation.

$$Z_i = \frac{X_i - \mu_{X_i}}{\sigma_{X_i}} \tag{4.10}$$

where,

Z_i = reduced (transformed) i^{th} basic variable

This process transforms the coordinate system of the original random variables to the coordinate system of the reduced variables. In this case, reliability index expresses the shortest distance from the origin of the reduced random variable coordinate system to the failure surface. Point corresponding to this shortest distance is called the checking or design point.

In the present case, reliability index, β_{HL} is expressed by the following formulation:

$$\beta_{HL} = \min\left(\sum_{i=1}^{n} Z_i^2\right)^{\frac{1}{2}} \quad subjected\ to\ \bar{z} \in \partial g \tag{4.11}$$

where,

∂g = failure surface in the z coordinate system

The reliability index of Cornell (1969) is the same as the reliability index of Hasofer and Lind (1974), when the failure function is linear. The two definitions of β also coincide for nonlinear functions if the Taylor series expansion is made at the design point.

In the general case, an iterative technique is used for the nonlinear failure surfaces. The distance vector from origin to the design point is expressed as in equation (4.12).

$$\beta_{HL}\bar{\alpha} \tag{4.12}$$

where,

$\bar{\alpha} = \alpha_1, \ldots, \alpha_n$ is unit vector

and

$$\sum_{i=1}^{n} \alpha_i^2 = 1.0 \tag{4.13}$$

here,

$$\alpha_i = \frac{-\frac{\partial g}{\partial Z_i}(\beta_{HL}\bar{\alpha})}{\sqrt{\sum_{i=1}^{n}\left(\frac{\partial g}{\partial Z_i}(\beta_{HL}\bar{\alpha})\right)^2}} \tag{4.14}$$

and the failure surface is given by equation (4.15).

$$g(z_1, z_2, \dots, z_n) = 0 \tag{4.15}$$

4.3 Multiple Failure Modes

For a structural element, there may be several failure modes due to the complicated load configurations which are also related with the geometric properties and material properties of the component. For example, a concrete column may fail under the combined compression and shear forces. One advantage of the probabilistic approach is the fact that different failure modes are considered and their effect on the failure probability is reflected.

Assume a structural element has k different failure modes and failure event in the i^{th} mode is represented by E_i. The failure event of i^{th} failure mode is defined as in equation (4.16).

$$E_i = [\, g_i(\tilde{X}) < 0] \tag{4.16}$$

here,

$g_i(\tilde{X})$ = limit state function for the i^{th} failure mode

Based on equation (4.16), survival for the i^{th} failure mode, $\bar{E}_i$ is described as

$$\bar{E}_i = [\, g_i(\tilde{X}) > 0] \tag{4.17}$$

Survival in all failure modes which means no failure will occur in any mode, is expressed as follows:

$$\bar{E} = \{\bar{E}_1 \cap \bar{E}_2 \cap \dots \cap \bar{E}_k\} \tag{4.18}$$

where,

$\bar{E}_i$ = survival event in the i[th] mode

∩ = intersection of events

Accordingly, the failure in at least one mode is expressed as

$$E = \{E_1 \cup E_2 \cup \ldots \cup E_k\} \tag{4.19}$$

where,

∪ = union of events

Assuming S is the load on the structural element and R_i is the capacity of the component in the i[th] failure mode, then the probability of survival is given as shown in equation (4.20).

$$P_S = \int_0^\infty \left[\int_{c_1 s}^\infty \ldots \int_{c_k s}^\infty f_{R_1,\ldots,R_k}(r_1, \ldots, r_k) d_{r_1} \ldots d_{r_k} \right] f_S(s) d_s \tag{4.20}$$

where,

$c_1s,\ldots,c_ks$ = load effects in different failure modes

$f_{R_1,\ldots,R_k}(r_1, \ldots, r_k)$ = joint probability density function of k-modal resistances

$f_S(s)$ = probability density function of load

However, two problems are faced in computing the integration given in equation (4.20), namely: There is no sufficient information and data to obtain $f_{R_1,\ldots,R_k}(r_1, \ldots, r_k)$ and it is quite hard to evaluate the multiple integrals. This problem

is handled by establishing bounds on probability of survival rather than computing the exact value.

If failure modes are perfectly correlated, minimum of the probability of survivals, P_S' is taken into consideration.

$$P_S' = \min(P_{S_1}, P_{S_2}, \dots, P_{S_k}) \tag{4.21}$$

Survival probabilities for each failure mode can be calculated based on the following equation.

$$P_{S_i} = \Pr(\bar{E}_i) = \int_0^\infty \int_{c_i s}^\infty f_{R_i}(r_i) f_S(s) d_{r_i} d_s \tag{4.22}$$

where,

P_{S_i}= survival probability in the ith failure mode

Assuming k modal resistances are statically independent but loads are dependent, probability of survival, P_S'' is computed as in equation (4.23).

$$P_S'' = \int_0^\infty \left[\int_{c_1 s}^\infty f_{R_1}(r_1) d_{r_1} \int_{c_2 s}^\infty f_{R_2}(r_2) d_{r_2} \dots \int_{c_k s}^\infty f_{R_k}(r_k) d_{r_k} \right] f_S(s) d_s \tag{4.23}$$

Equation (4.23) can also be expressed as follows:

$$P_S'' = \int_0^{\infty} [\Pr(R_1 > c_1 s) \Pr(R_2 > c_2 s) \dots \Pr(R_k > c_k s)] f_S(s) d_s \qquad (4.24)$$

If modal resistances and modal loads are independent (modal failures are independent), then probability of survival, P_S^* is calculated from equation (4.25)

$$P_S^* = \prod_{i=1}^{k} P_{S_i} = \prod_{i=1}^{k} \int_0^{\infty} \int_{c_i s}^{\infty} f_{R_i}(r_i) f_S(s) \, d_{r_i} d_s \qquad (4.25)$$

As a result, the bounds which are also called the fundamental inequalities of reliability are given in equation (4.26) for the true value of probability of survival, P_S.

$$P_S' \geq P_S \geq P_S'' \geq P_S^* \qquad (4.26)$$

In terms of probability of failure, bounds are as follows:

$$P_F' \leq P_F \leq P_F'' \leq P_F^* \qquad (4.27)$$

4.4 Reliability of Structural Systems

Highway system reliability is evaluated based on the reliability of its components in the system. To compute component reliability, bounds are established easily by calculating P_S' and P_S^* as explained in the previous section.

Dealing with the system reliability, it is important to distinguish the following two concepts: System damage and system failure. System damage means at least one component of the system fails and probability of damage to the system is expressed by P_{D_S}. System failure means collapse of the system and probability of system failure is denoted by P_{F_S}.

Reliability of a highway system like any structural system depends on the reliability of its components.

Let E_i be the failure of i^{th} member. For a structure having m members, probability of system damage is expressed by equation (4.28).

$$P_{D_S} = \Pr(E_1 \cup E_2 \cup \dots E_m) \tag{4.28}$$

Therefore, no damage probability is as follows:

$$1 - P_{D_S} = \Pr(\bar{E}_1 \cap \bar{E}_2 \cap \dots \bar{E}_m) \tag{4.29}$$

Here, it is assumed that structural elements fail in their weakest modes. Therefore, survival of the i^{th} component requires that:

$$R_i' \geq e_i S \tag{4.30}$$

where,

R_i' = capacity of i^{th} member in the weakest mode

e_i = factor of transforming load to the load effect in the i^{th} member in the weakest mode

S = load acting on the structure

Under the applied load S, forces in different members must satisfy certain laws of mechanics. Therefore member forces '$e_i S$'s will be perfectly correlated. Load effects ($e_i S$) and resistances (R_i') can be assumed independent. The only exception is the dead load since higher dead load means stronger member due to larger sections and more reinforcements. R_i''s are expected to be partially correlated as a result of similar manufacturing, construction design and material properties. This correlation is expected to be positive.

Under these observations, survival probability of the system, P_{s_s} is stated as in the following equation.

$$P_{S_S} = \int_0^\infty \left[\int_{e_1 s}^\infty \dots \int_{e_m s}^\infty f_{R_1', \dots, R_m'}(r_1, \dots, r_m) d_{r_1} \dots d_{r_m} \right] f_S(s) d_s \tag{4.31}$$

where,

$f_{R_1', \dots, R_m'}(r_1, \dots, r_m)$ = joint probability density function of member resistance in the weakest mode

Equation (4.31) is the same expression as the modal survival probability definition given in equation (4.20). Thus, same computational problem and difficulty in the assessment of joint probability density function are also valid here. For this reason, the same inequalities, i.e. fundamental inequalities of reliability are employed.

P_{S_S}' represents no damage probability for the system based on perfectly correlated resistances which is:

$$P_{S_S}' = min\{P_{S_1}', P_{S_2}', \dots, P_{S_m}'\} \tag{4.32}$$

and system damage probability is shown as:

$$P'_{D_S} = 1 - P'_{S_S} = max\{P'_{F_1}, P'_{F_2}, \dots, P'_{F_m}\} \tag{4.33}$$

Since load effects are also perfectly correlated, this assumption implies failure (or survival) of different members are perfectly correlated.

P''_{S_S} states no damage probability for the system based on the assumption that member resistances are independent which is shown in equation (4.34)

$$P''_{S_S} = \int_0^{\infty} \left[\prod_{i=1}^{m} \int_{e_i s}^{\infty} f_{R'_i}(r_i) d_{r_i} \right] f_S(s) d_s \tag{4.34}$$

and probability of system damage is defined as:

$$P''_{D_S} = 1 - P''_{S_S} \tag{4.35}$$

$P^*_{S_S}$ stands for no damage probability for the system based on the assumption that member failures are independent. The expression is shown by equation (4.36)

$$P^*_{S_S} = \prod_{i=1}^{m} \left[\int_0^{\infty} \int_{e_i s}^{\infty} f_{R'_i}(r_i) d_{r_i} f_S(s) d_s \right] = \prod_{i=1}^{m} P'_{S_i} \tag{4.36}$$

Then the system damage probability is expressed as

$$P_{D_S}^{*} = 1 - \prod_{i=1}^{m}(1 - P'_{F_i}) \tag{4.37}$$

Consequently, bounds of system reliability in terms of component reliabilities are established as given in equations (4.38) and (4.39).

$$P'_{S_S} \geq P_{S_S} \geq P''_{S_S} \geq P^{*}_{S_S} \tag{4.38}$$

$$P'_{D_S} \leq P_{D_S} \leq P''_{D_S} \leq P^{*}_{D_S} \tag{4.39}$$

The lower bound $P^{*}_{S_S}$ is a conservative estimate of P_{S_S}. Besides, $P^{*}_{S_S}$ depends on the component reliability. Therefore, if lower bound $P^{*}_{S_i}$'s are taken as component reliabilities, $P^{*}_{S_S}$ becomes a strictly conservative estimate for the system reliability.

If variability in R'_i is small and variability in S is large, then S dominates the system reliability. Then system reliability converges to the upper bound ($P_{S_S} \cong P'_{S_S}$).

On the other hand, if variability in R'_i is large whereas variability in S is small, then system reliability converges to the lower bounds ($P_{S_S} \cong P''_{S_S} \cong P^{*}_{S_S}$).

4.4.1 Series and Parallel Systems

From the system reliability point of view, two basic types of systems are considered namely: Series and parallel systems. The characteristics and the corresponding reliabilities of these two systems are summarized in the following.

4.4.1.1 Reliability of Series Systems

For series systems, failure of one member in the system means failure of the whole system. In other words, reliability of the system requires that none of the components in the system fail. Series systems are also called as weakest link systems. For series systems, probability of system damage equals to the probability of system failure which is expressed as:

$$P_{F_S} = P_{D_S} \tag{4.40}$$

4.4.1.2 Reliability of Parallel Systems

For parallel systems, the probability of failure of the system is not necessarily equal to the system damage, because after the failure of some components, remaining components may maintain the functions of the structure.

Additionally, failure of the parallel systems may occur due to the failure of different number of components and component failures may occur in different orders. Each failure pattern is called a failure path. If there are k failure paths in a parallel system, an upper bound estimate of system failure probability is

$$P_{F_S}^{*} = \sum P_{F_{S_i}} \tag{4.41}$$

where,

$P_{F_{S_i}}$ = probability of system failure through the i^{th} path

Grigorium and Turkstra (1979) are derived the following relation between the reliability index of a single element and reliability index of the parallel system, where the reliability indices of all elements are the same and equal to β_e .

$$\beta_{system} = \beta_e \sqrt{\frac{n}{1 + \bar{\rho}(n-1)}} \tag{4.42}$$

where,

β_e = reliability index of a single element, same for all elements

n = number of elements

$\bar{\rho}$ = average correlation coefficient among member failures

In parallel systems with unequally correlated elements, average correlation coefficient, $\bar{\rho}$ is determined by the following equation (Nowak and Collins, 2012).

$$\bar{\rho} = \frac{1}{n(n-1)} \sum_{i}^{n} \sum_{j}^{n} \rho_{ij} \tag{4.43}$$

where,

i≠j

CHAPTER 5

CASE STUDY

5.1 Introduction

In the previous chapters, probabilistic seismic hazard analysis is explained in detail, behavior of highway systems under earthquake loads is discussed and basic concepts of reliability calculations are presented. In this chapter, a case study is carried out based on real life data in order to illustrate the implementation of these methods.

The aim of this chapter is to evaluate the system reliability of a certain highway system. After a destructive earthquake, it is important to reach main places as soon as possible, especially where human population is concentrated. Therefore, components of a highway system should not be damaged during or after an intensive earthquake. Besides, there should be alternative highway paths in case seismic damage on some of the components of the highway system happens. In this respect, evaluation of the reliability of a highway system is very crucial.

For this case study, a region is selected which is located too close to the city center of Bursa Province in Turkey. A highway system is selected by considering vital services to be reached after an earthquake and alternative paths are determined to connect the industrial zone to the vital services.

In conducting the case study, firstly, a multisite probabilistic seismic hazard analysis is performed for the region to determine the seismic loads due to earthquake. Then, resistances of the system components are evaluated. Based on loads and resistances, reliability of each component is obtained and then system reliability is determined

for 75, 475, 1000 and 2475 years return period by constructing upper and lower bounds for series and parallel systems. At the final stage, reliability indices for the overall system are determined and the resulting reliability results are compared with the damage probability matrices (DPM's) to evaluate the level of expected seismic damage the whole system may experience.

5.1.1 General Information about the Bursa Province

Bursa Province is located on the south of the Marmara Region and the Middle Strand of the North Anatolian Fault (NAFMS) Zone (Gok and Polat, 2012). According to the current seismic zoning map of Turkey, which was prepared by the Ministry of Public Works and Settlements, General Directorate of Disaster Affairs (1996), the city center of Bursa falls within 1st degree seismic zone. Therefore, it can be concluded that the city is located in a highly active seismic region.

Bursa is among the most populated cities in Turkey. Furthermore, it is one of the most industrialized centers in the country. For this reason, population in industrial regions is also quite high.

5.2 Information on the Highway System and Description of the Problem

For this study, a disaster scenario is constituted by considering populations and locations of important services. The scenario is to reach one of the two major city hospitals from an industrial zone after the occurrence of a major earthquake. Thus, a proper highway system is designated in order to create highway links between the industrial zone and the two major hospitals, which are namely Bursa State Hospital and Bursa High Specialty Hospital.

After a major earthquake, it can be very difficult to use byroads due to the chaotic atmosphere that may occur. Therefore, selected highway system includes only major roads and highways; boulevards and main streets. In other words, byroads are not considered in this study. In addition, there are three highway bridges on the selected highway system, namely: Balıklı Bridge, Panayır Bridge and Demirtaş Viaduct.

General view of the selected region is shown in Figure 5.1 together with the layout of the highway system, locations of the industrial zone, hospitals and the bridges.

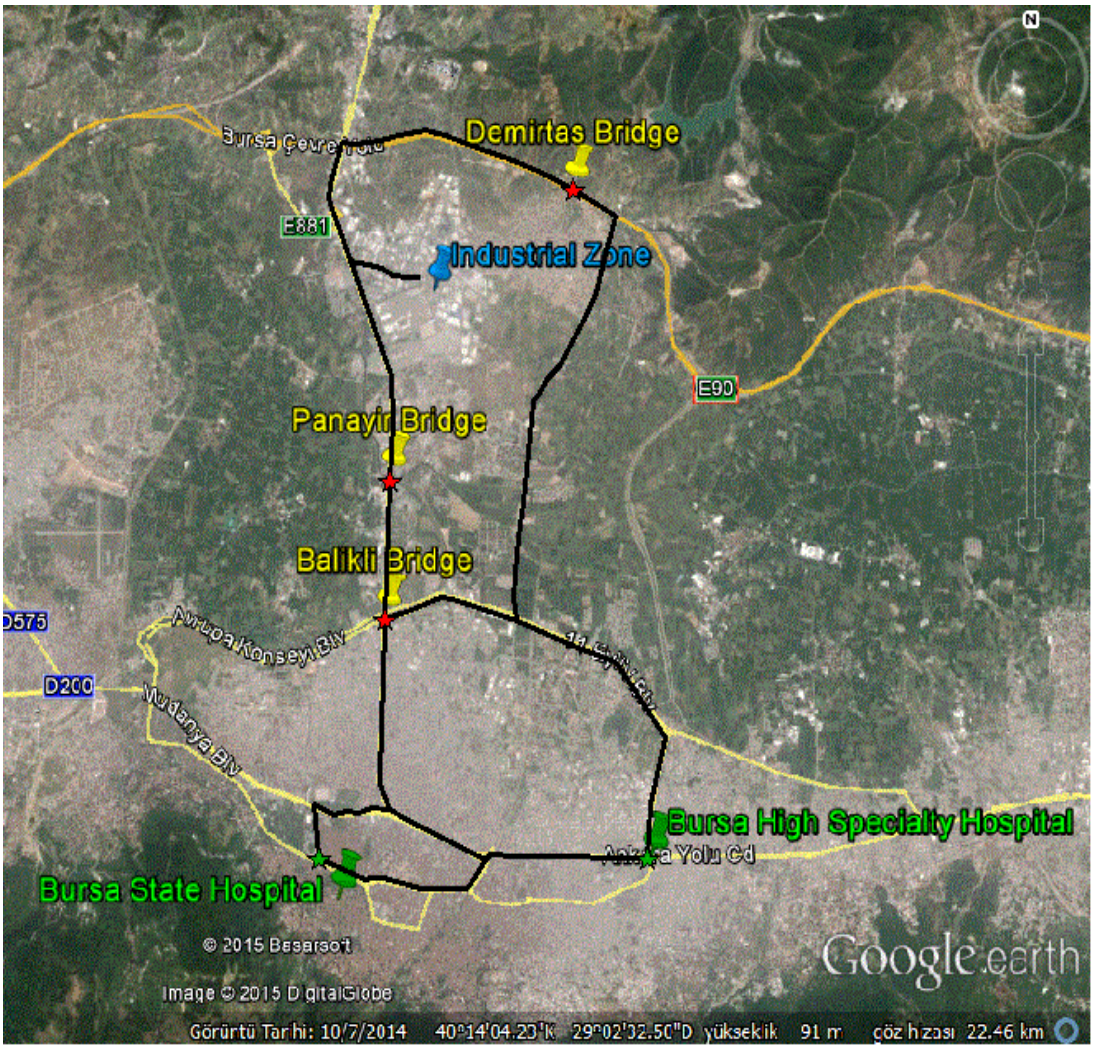

Figure 5.1 General View of the Selected Region, Layout of the Highway System, Locations of Industrial Zone, Hospitals and Bridges

As seen in Figure 5.1, except the selected highway system, there are also several alternative ways to reach the two hospitals from industrial zone. However, the aim of this case study is to reach to the hospitals as soon as possible, and so only closest main roads among these locations are selected to construct the highway system.

To reach the target hospitals from the industrial zone, different alternative paths in the selected highway system can be used. To specify these alternative paths, firstly roads and highways are divided into segments at their intersection points. Segments are marked by a capital letter and nodes are marked by numbers as seen in Figure 5.2. Bridges are also treated as intersection points and they are evaluated individually. Bridges are marked by their original names.

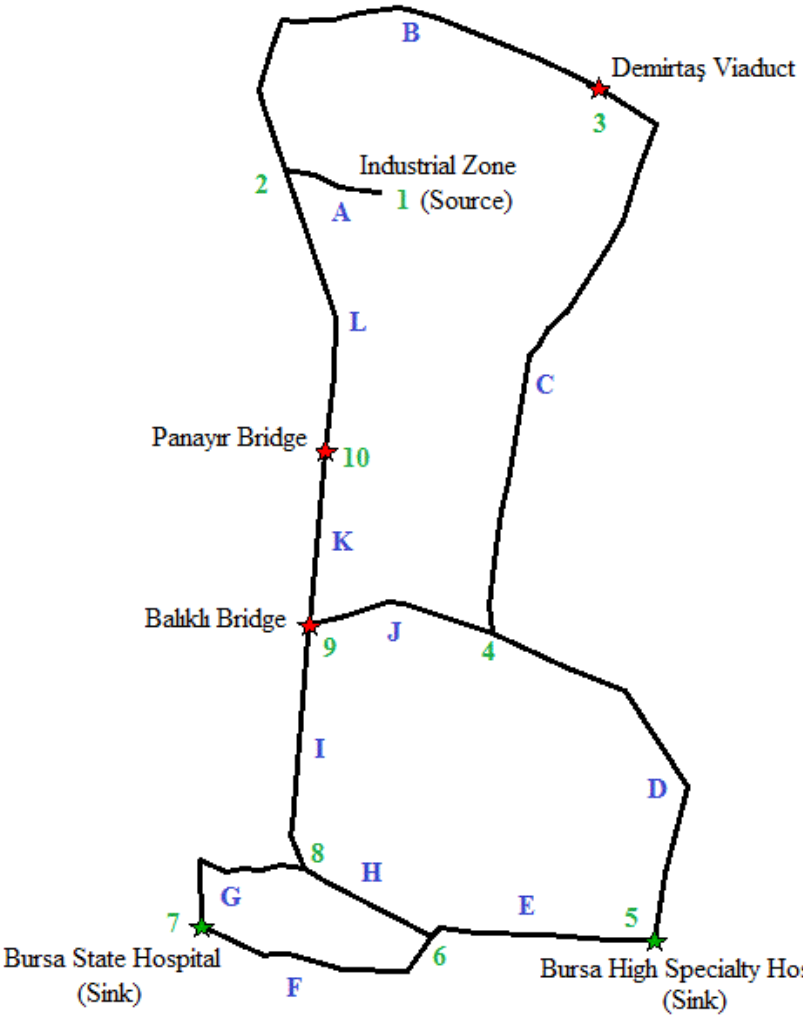

Figure 5.2 Segment Names and Node Numbers Defined for the Lifeline Transportation System

Lengths of each segment are determined by using Map Info Professional 11.0 as given in Table 5.1.

Table 5.1 Lengths of Each Segment Defined in the Highway System

Segment Name	Length of the Segment (km)
A	1.26
B	6.09
C	7.26
D	4.92
E	3.03
F	3.32
G	2.17
H	1.81
I	2.75
J	2.50
K	1.97
L	3.19

By considering all segments and nodes, all possible alternative paths (arcs) from the industrial zone (source) to the two main hospitals (sinks) are obtained.

5.2.1 Consideration of Alternative Paths

Based on the disaster scenario, alternative paths are generated by considering all nodes and segments between nodes. All possible routes from node 1 (industrial zone) to node 7 (Bursa State Hospital) and to node 5 (Bursa High Specialty Hospital) are shown in Table 5.2.

Corresponding path lengths are determined by using MapInfo and lengths of each path are also shown in Table 5.2.

Table 5.2 Alternative Paths with Corresponding Nodes, Segments and Their Lengths

Scenario	Paths	Nodes	Segments	Total Length (km)
Reach from Industrial Zone to Bursa State Hospital	Path 1	1-2-10-9-8-7	A-L-K-I-G	11.34
	Path 2	1-2-10-9-8-6-7	A-L-K-I-H-F	14.30
	Path 3	1-2-10-9-4-5-6-7	A-L-K-J-D-E-F	20.19
	Path 4	1-2-10-9-4-5-6-8-7	A-L-K-J-D-E-H-G	20.85
	Path 5	1-2-3-4-5-6-7	A-B-C-D-E-F	25.88
	Path 6	1-2-3-4-5-6-8-7	A-B-C-D-E-H-G	26.54
	Path 7	1-2-3-4-9-8-7	A-B-C-J-I-G	22.03
	Path 8	1-2-3-4-9-8-6-7	A-B-C-J-I-H-F	24.99
Reach from Industrial Zone to Bursa High Specialty Hospital	Path 9	1-2-3-4-5	A-B-C-D	19.53
	Path 10	1-2-3-4-9-8-6-5	A-B-C-J-I-H-E	24.70
	Path 11	1-2-3-4-9-8-7-6-5	A-B-C-J-I-G-F-E	28.38
	Path 12	1-2-10-9-4-5	A-L-K-J-D	13.84
	Path 13	1-2-10-9-8-7-6-5	A-L-K-I-G-F-E	17.69
	Path 14	1-2-10-9-8-6-5	A-L-K-I-H-E	14.01

5.3 Probabilistic Seismic Hazard Analysis for the Specified Region

Bursa city is located nearby the southwest branch of the North Anatolian Fault zone. Therefore, it becomes more important to determine seismic hazard in this region (Polat, 1997). Destructive historical earthquakes are known to occur in Bursa region even though epicenter locations are not exactly identified. According to Topal et al. (2003), two significant damaging earthquakes occurred in 1855. The next destructive earthquake occurred in Bursa is Manyas Earthquake with M_S 7.0 (Erentöz and Kurtman, 1964).

In the literature, there are several studies available on the probabilistic seismic hazard analysis performed for Bursa Province. Yücemen et al. (2006) conducted a

comprehensive probabilistic seismic hazard analysis for the city center of Bursa. Moreover, one of the most detailed analyses was carried out by Yılmaz (2008).

In this study, multisite probabilistic seismic hazard analysis is performed for the selected region which is located in Bursa based on PGA values by considering V_{s30}, the average shear wave velocity down to 30 m, as 760 m/sec.

Ground motion prediction equations proposed by Boore et al. (1997), Kalkan and Gülkan (2004), Abrahamson and Silva (2008) and Gülerce et al. (2015) are used in the study. Results are obtained for 75, 475, 1000 and 2475 years return periods (50%, 10%, 5% and 2% probability of exceedance in 50 years, respectively).

For the analysis, each segment is divided into 1 km unit length called as a subsegment. Depending on the length of the segments, lengths of subsegments are adjusted between 800 m – 1200 m. The purpose of dividing these segments into subsegments is to increase the precision of the results in the system analysis, and also to take the correlation into consideration.

Probabilistic seismic hazard computations are executed by using EZ-FRISK 7.52 (Risk Engineering, 2011) and results of analyses are combined for different alternatives by using the logic tree approach.

5.3.1 Seismic Database and Seismic Sources

In this thesis, seismic database compiled by Yücemen et al. (2006) is used to determine the hazard in the region. In this seismic database, the region is bounded by a rectangular area with 28°- 30° E longitudes and 39.75°- 40.75° N latitudes where city center of Bursa is also located approximately in the center of this rectangular area. In this area, a total of 46 fault segments are identified which are modelled as line sources. These faults are assumed to produce only characteristic earthquakes based on the Poisson model as stated in section 2.5.3.2 and 2.6.1. The locations of these faults are given in Appendix A. Besides, fault parameters such as type of the faults, minimum and maximum magnitudes etc. for each one of these 46 faults are also given in Appendix A.

Earthquakes which are not related to any of the fault segments are modelled as background activity within a rectangular area. Background activity is defined with the truncated exponential distribution with a magnitude range 4.5- 6.0 as explained in section 2.5.3.1 and modelled as an area source.

Line sources and the area source are modelled based on the recommendations of Yılmaz (2008).

The locations of line sources (faults) and the background seismic source are shown in Figure 5.3.

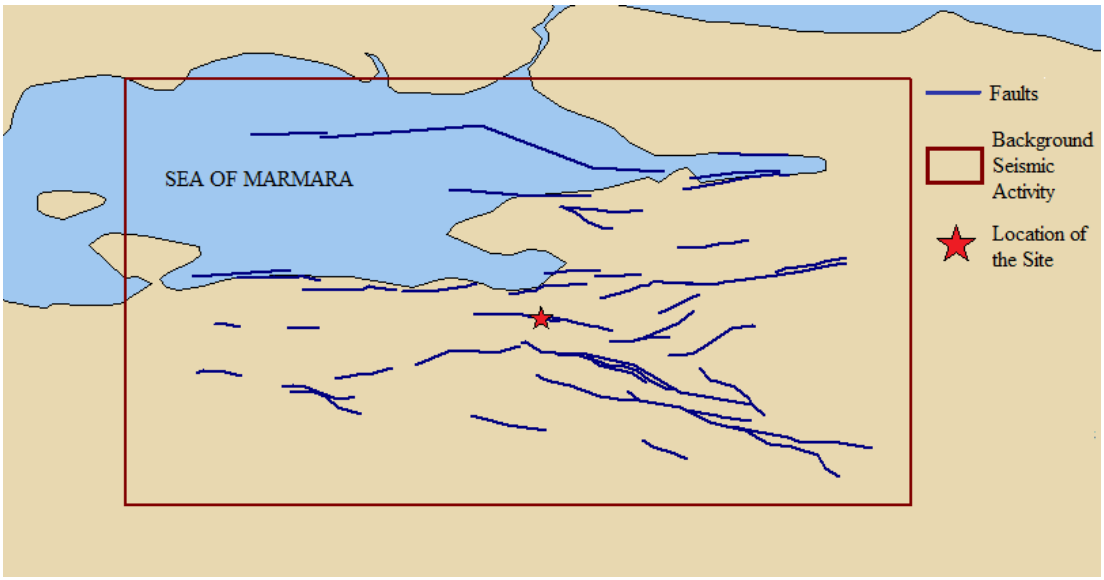

Figure 5.3 Line Sources and Background Area Source Defined for the Bursa Region

In this study, the seismic database compiled from the catalogs of Earthquake Research Department of General Directorate of Disaster Affairs by Yücemen et al. (2006) is used. In the provided database, all magnitudes have been converted into a common magnitude scale which is the moment magnitude (M_W) and only magnitudes 4.5 or greater are considered.

Since there is no information about the return periods of the characteristic earthquakes in the earthquake catalogs, Yücemen et al. (2006) classified faults into four categories based on their activity rating to estimate return periods as given in

Table 5.3. Lower bounds for the return periods are taken as best estimate return period (BERP) values and return periods of the fault segments are determined based on this information.

Table 5.3 Classification of Faults According to Their Activities and the Corresponding Mean Recurrence Intervals for the Characteristic Earthquakes (from Yücemen et al., 2006)

Fault category	**Return period (RP) (in years)**	**Best Estimate Return Period (BERP) in years**
Very high active fault	RP < 200	150
High active fault	200 < RP ≤ 500	200
Active fault	500 < RP ≤ 1000	500
Potentially active fault	RP ≥ 1000	1000

To calculate β and ν values for the background activity, correction for incompleteness and dependence of the earthquakes are considered as shown in Table 5.4.

Table 5.4 β and ν Values Computed for the Background Seismic Zone According to Different Assumptions (from Yücemen et al., 2006)

Main shock/ secondary shock analyses	**Correction for incompleteness**	**β**	**ν**
All earthquakes	No	1.184	0.657
	Yes	1.734	1.382
Main shocks	No	2.026	0.402
	Yes	1.529	0.794

In order to take into account the epistemic uncertainties, logic tree method explained in section 2.9.2.1 is used. Different alternatives are considered and different subjective probabilities are assigned to them as presented in Table 5.5

Table 5.5 Different Alternatives Considered and the Subjective Probabilities Assigned to Them

Alternatives	Subjective probabilities
The whole seismic database	0.4
Only main shocks	0.6
Incomplete seismic database	0.3
Artificially completed seismic database	0.7
Boore et al. (1997)	0.25
Kalkan and Gülkan (2004)	0.25
Abrahamson and Silva (2008)	0.25
Gülerce et al. (2015)	0.25

5.3.2 A Short Note on Near Fault Effects

Since chosen site is located within the close vicinity of some faults as seen in Figure 5.3, it is desirable to take into consideration the near fault effects on the highway components.

However, in this study, near fault effects are not considered. In the PSHA, only PGA values in the region are calculated and PGA is not a suitable indicator itself to assess near fault effects.

5.3.3 Probabilistic Seismic Hazard Results

PSHA is carried out following the steps and the methods explained in Chapter 2. In Table 5.6, seismic hazard results are presented for 75, 475, 1000 and 2475 years

return periods (50%, 10%, 5% and 2% probability of exceedance in 50 years, respectively). It is to be noted that these values correspond to the PGA expected at the midpoints of the subsegments and bridges.

Table 5.6 Seismic Hazard Results Obtained for Each Subsegment in Terms of PGA for Different Return Periods (in g)

Segment Name	Latitude	Longitude	75 years	475 years	1000 years	2475 years
A	40.2661	29.0668	0.1698	0.3925	0.5171	0.6910
	40.2663	29.0533	0.1689	0.3913	0.5157	0.6884
B	40.2671	29.0528	0.1689	0.3913	0.5159	0.6889
	40.2754	29.0492	0.1690	0.3906	0.5159	0.6905
	40.2818	29.0549	0.1698	0.3900	0.5145	0.6878
	40.2842	29.0661	0.1705	0.3887	0.5115	0.6814
	40.2839	29.0781	0.1711	0.3877	0.5096	0.6776
	40.2825	29.0903	0.1715	0.3873	0.5088	0.6764
	40.2813	29.1013	0.1720	0.3870	0.5082	0.6753
C	40.2810	29.1024	0.1720	0.3871	0.5083	0.6756
	40.2763	29.1093	0.1722	0.3893	0.5120	0.6828
	40.2678	29.1055	0.1719	0.3929	0.5174	0.6923
	40.2605	29.0991	0.1715	0.3934	0.5168	0.6889
	40.2531	29.0927	0.1710	0.3921	0.5123	0.6774
	40.2443	29.0917	0.1707	0.3897	0.5060	0.6622
	40.2346	29.0905	0.1704	0.3874	0.5004	0.6494
	40.2249	29.0893	0.1699	0.3868	0.4983	0.6452
D	40.2248	29.0905	0.1700	0.3869	0.4984	0.6453
	40.2232	29.1024	0.1710	0.3896	0.5015	0.6494
	40.2202	29.1131	0.1718	0.3926	0.5049	0.6545
	40.2138	29.1212	0.1723	0.3958	0.5089	0.6614
	40.2059	29.1193	0.1717	0.3996	0.5157	0.6750
	40.1980	29.1174	0.1710	0.4040	0.5253	0.6950
E	40.1979	29.1162	0.1709	0.4039	0.5254	0.6953
	40.1967	29.1046	0.1697	0.4025	0.5249	0.6963
	40.1955	29.0931	0.1685	0.4001	0.5223	0.6932
	40.1935	29.0827	0.1673	0.3981	0.5206	0.6910
F	40.1927	29.0820	0.1672	0.3984	0.5214	0.6928
	40.1886	29.0714	0.1658	0.3984	0.5240	0.6999
	40.1884	29.0594	0.1646	0.3958	0.5218	0.6977
	40.1895	29.0468	0.1634	0.3926	0.5192	0.6952

Table 5.6 (cont'd) Seismic Hazard Results Obtained for Each Subsegment in Terms of PGA for Different Return Periods (in g)

Segment Name	Latitude	Longitude	75 years	475 years	1000 years	2475 years
G	40.1904	29.0466	0.1635	0.3924	0.5188	0.6941
	40.1954	29.0501	0.1643	0.3919	0.5159	0.6869
	40.1974	29.0621	0.1657	0.3931	0.5149	0.6822
H	40.1972	29.0633	0.1658	0.3934	0.5152	0.6825
	40.1955	29.0724	0.1665	0.3955	0.5174	0.6859
	40.1935	29.0827	0.1673	0.3981	0.5206	0.6910
I	40.1982	29.0616	0.1657	0.3927	0.5142	0.6807
	40.2057	29.0602	0.1662	0.3895	0.5079	0.6676
	40.2137	29.0606	0.1668	0.3867	0.5022	0.6555
	40.2217	29.0611	0.1674	0.3850	0.4983	0.6476
J	40.2221	29.0622	0.1675	0.3850	0.4982	0.6473
	40.2250	29.0708	0.1684	0.3854	0.4976	0.6454
	40.2254	29.0800	0.1692	0.3860	0.4979	0.6451
	40.2249	29.0893	0.1699	0.3868	0.4983	0.6452
K	40.2226	29.0611	0.1675	0.3848	0.4980	0.6471
	40.2315	29.0615	0.1680	0.3846	0.4974	0.6457
	40.2394	29.0619	0.1684	0.3857	0.5002	0.6508
L	40.2403	29.0619	0.1685	0.3859	0.5006	0.6518
	40.2492	29.0622	0.1689	0.3884	0.5062	0.6644
	40.2576	29.0591	0.1690	0.3904	0.5118	0.6779
	40.2663	29.0533	0.1689	0.3913	0.5157	0.6884
Panayır Br.	40.2400	29.0600	0.1683	0.3856	0.5003	0.6677
Balıklı Br.	40.2200	29.0600	0.1672	0.3852	0.4990	0.6658
Demirtaş Via.	40.2800	29.1000	0.1719	0.3879	0.5098	0.6755

It is to be noted that since the geographical extend of the highway system is relatively small, the PGA values are quite close to each other.

5.4 Resistances of Highway System Components

The selected highway system consists of a viaduct, two bridges and a number of roads and highways. For roads and highways subjected to earthquake loads, two failure modes, namely; fault crossing and embankment failure are considered. On the

other hand, only one failure mode, which is the pier column failure, is taken into consideration for the viaduct and the two bridges.

In this study, roads and highways are divided into subsegments and it is assumed that they have the same seismic capacity against earthquake effects.

Since bridges have different characteristics; resistances of them are not generalized and structural analyses are performed for each one of them. In the following, resistance of the highway segments and bridges are evaluated.

5.4.1 Seismic Resistance of Highway Bridges

There are three bridges on the selected highway system. Two of them (Balıklı and Panayır Bridges) are standard highway bridges whereas one of them (Demirtaş Viaduct) is a viaduct with many spans. Since Balıklı Bridge, Panayır Bridge and Demirtaş Viaduct have different characteristics, such as number of spans, span lengths and pier heights etc. as shown in Table 5.7, they have different capacities when subjected to earthquake loads.

Table 5.7 Characteristics of the Bridges in the Highway System

Name	Number of spans	Average pier height (m)	Average span length (m)
Balıklı Bridge	2	6.5	22.5
Panayır Bridge	3	6.3	28.0
Demirtaş Viaduct	28	30.0	39.0

In Chapter 3, it is stated that pier columns are the critical components of the bridges during an earthquake. In this case study, it is assumed that if capacity of one pier column of the bridge is reached, the bridge becomes dysfunctional. In order to have an idea about the resistances of pier columns against earthquake excitation in terms of PGA, a simple approach is followed. Firstly, force-deformation graphs of the piers are obtained with a single degree of freedom pushover analysis by using USC_RC

1.0.2 program (Esmaeily, 2008) to comprehend the deflection capacities of the columns. Then, 3D structural models of the bridges are used to perform elastic dynamic analyses (response spectra analyses). To perform response spectra analyses, spectral response values for 2475 years return period with 5% damping are derived for the each bridge and only low period spectral acceleration parts are taken into consideration to obtain the capacities of the bridges in terms of PGA. Spectral response values obtained for the three bridges are presented in Appendix B. In the structural analyses, effective moments of inertia of the pier sections in their weak directions are considered to find the deflection capacity. An iterative procedure is followed to reach the deflection limits by scaling the spectral response values. Response spectra analyses are performed several times with different scale factors until the deflection limit of the columns are reached. When deflection limits of the columns are reached, corresponding peak ground acceleration values are accepted as the capacity values for the bridges. 3D structural analyses are performed with LARSA 4D 7.07 program (LARSA Inc., 2014).

Capacities are found by considering weak directions of piers which are placed in the longitudinal direction of the bridges. Therefore, only periods and displacements in the longitudinal direction are checked.

5.4.1.1 Resistance of Balıklı Bridge

Balıklı Bridge is a part of Bursa – Yalova State Highway. It is a two span bridge with a total length 47.20 m. Pier columns are oval shaped as shown in Figure 5.4 with an average height of 6.50 m. In Figure 5.5 reinforcement scheme of the pier is presented.

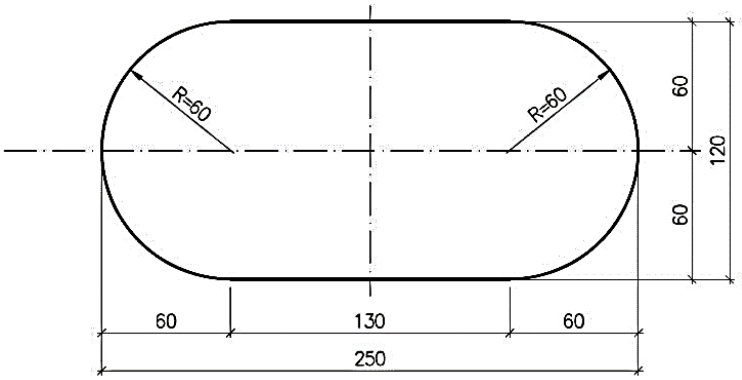

Figure 5.4 Cross Section of the Piers of Balıklı Bridge (in cm)

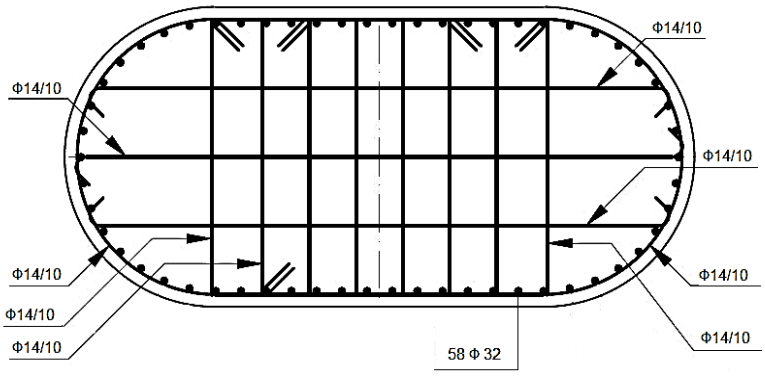

Figure 5.5 Reinforcement Scheme for the Piers of Balıklı Bridge

Superstructure of Balıklı Bridge is composed of I girders with a height of 120 cm and a slab with 25 cm thickness. Force-displacement graph for a pier column of the Balıklı Bridge is given in Figure 5.6.

3D model of the Balıklı Bridge is presented in Figure 5.7.

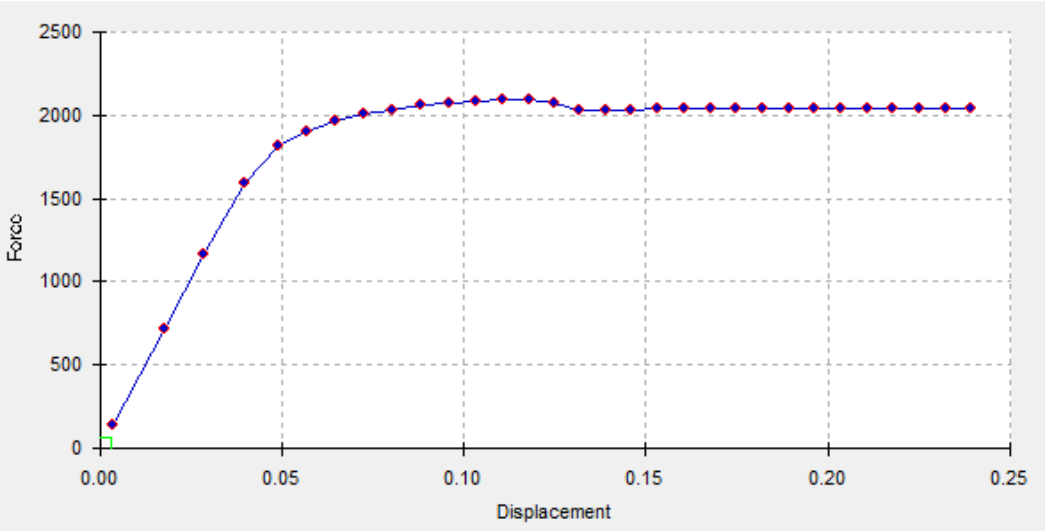

Figure 5.6 Force-Displacement Graph for the Piers of Balıklı Bridge

(Displacements in m and Force in kN)

Deflection limit of the pier column is obtained as 24 cm from the graph.

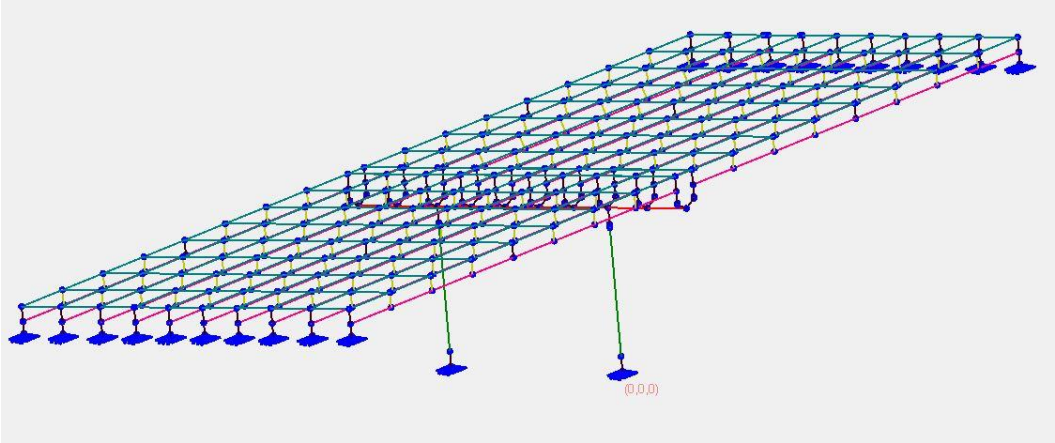

Figure 5.7 3D Model of Balıklı Bridge on LARSA 4D

Fundamental period for the longitudinal direction is obtained as 0.67 sec and 24 cm deflection is reached when peak ground acceleration is 1.62 g. Therefore, resistance of Balıklı Bridge is assumed as 1.62 g.

5.4.1.2 Resistance of Panayır Bridge

Panayır Bridge is a part of Bursa – Yalova State Highway. It is a three span bridge with span lengths 27.50, 28.25 and 27.50 m, respectively. Total length of the Panayır Bridge is 85.57 m. Pier columns are oval shaped as shown in Figure 5.8 with an average height of 6.30 m. In Figure 5.9 reinforcement scheme of the pier is presented.

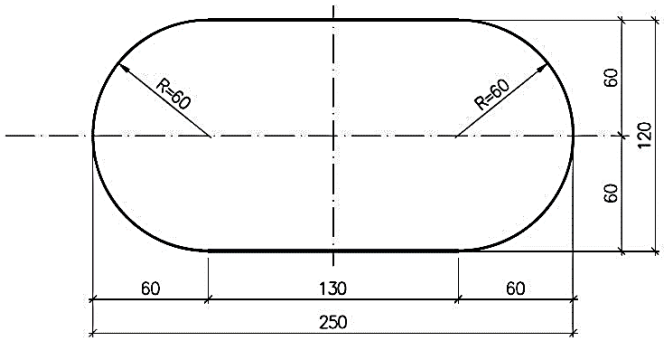

Figure 5.8 Cross Section of the Piers of Panayır Bridge (in cm)

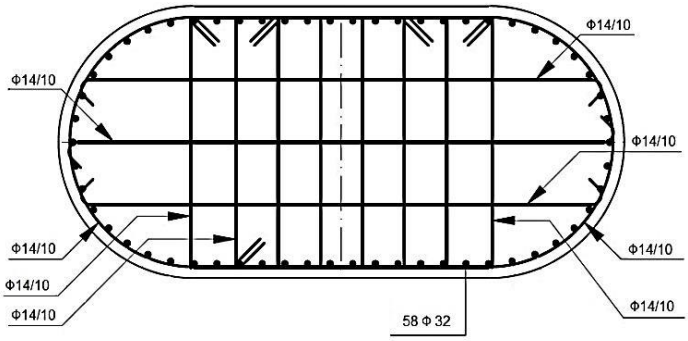

Figure 5.9 Reinforcement Scheme for the Piers of Panayır Bridge

Superstructure of Panayır Bridge is composed of I girders with a height of 120 cm and a slab with 25 cm thickness. Force-displacement graph for a pier column of the Panayır Bridge is given in Figure 5.10.

3D model of the Panayır Bridge is presented in Figure 5.11.

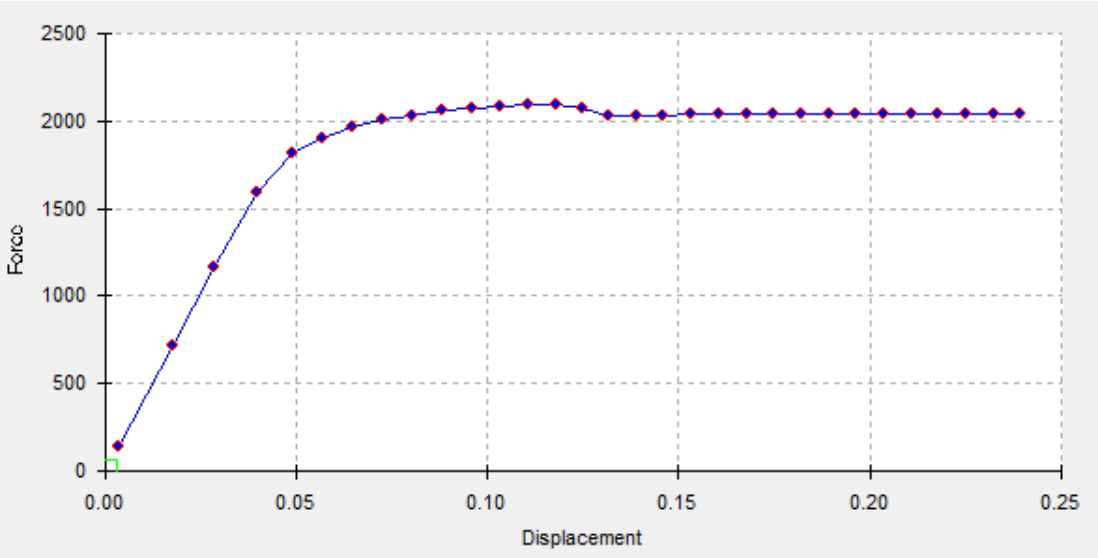

Figure 5.10 Force-Displacement Graph for the Piers of Panayır Bridge

(Displacements in m and Force in kN)

Deflection limit of the pier column is obtained as 24 cm from the graph.

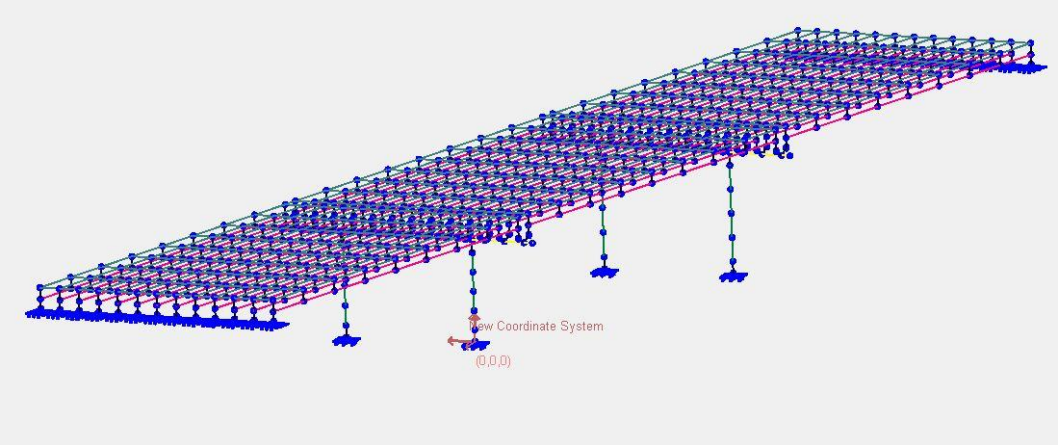

Figure 5.11 3D Model of the Panayır Bridge on LARSA 4D

Fundamental period for the longitudinal direction is obtained as 0.74 sec and 24 cm deflection is reached when peak ground acceleration is 1.26 g. Therefore, resistance of Panayır Bridge is assumed as 1.26 g.

5.4.1.3 Demirtaş Viaduct

Demirtaş Viaduct is a part of İstanbul-Bursa-Balıkesir-İzmir Motorway. It is a twenty eight span viaduct with span lengths 37.00 m between abutments and columns and 39.00 m between interior columns. Total length of the Demirtaş Viaduct is 1088 m. Pier columns of the viaduct are H shaped as shown in Figure 5.12 with an average height of 30 m. In Figure 5.13 reinforcement scheme of the pier is presented.

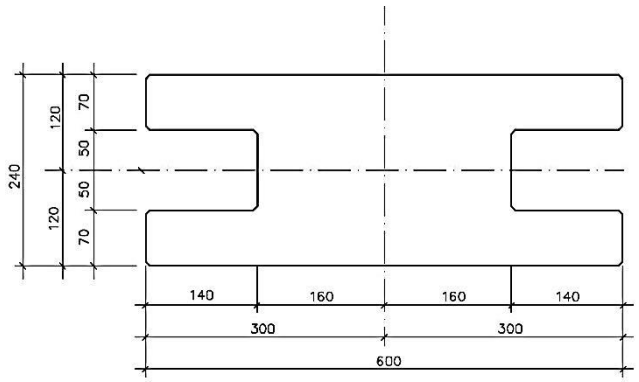

Figure 5.12 Cross Section of the Piers of Demirtaş Viaduct (in cm)

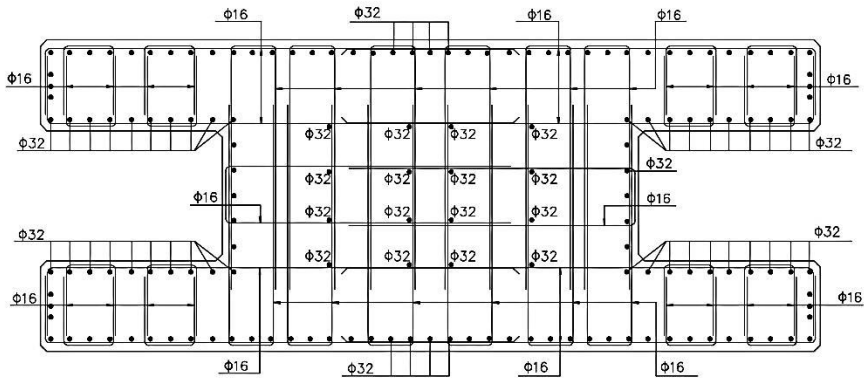

Figure 5.13 Reinforcement Scheme for the Piers of Demirtaş Viaduct

Superstructure of Demirtaş Viaduct is composed of I girders with a height of 160 cm and a slab with 20 cm thickness. Force-displacement graph for one pier column of the Demirtaş Viaduct is given in Figure 5.14.

3D model of the Demirtaş Viaduct is presented in Figure 5.15. Only 5 columns between two expansion joints in the middle of the viaduct are modelled to represent the whole viaduct.

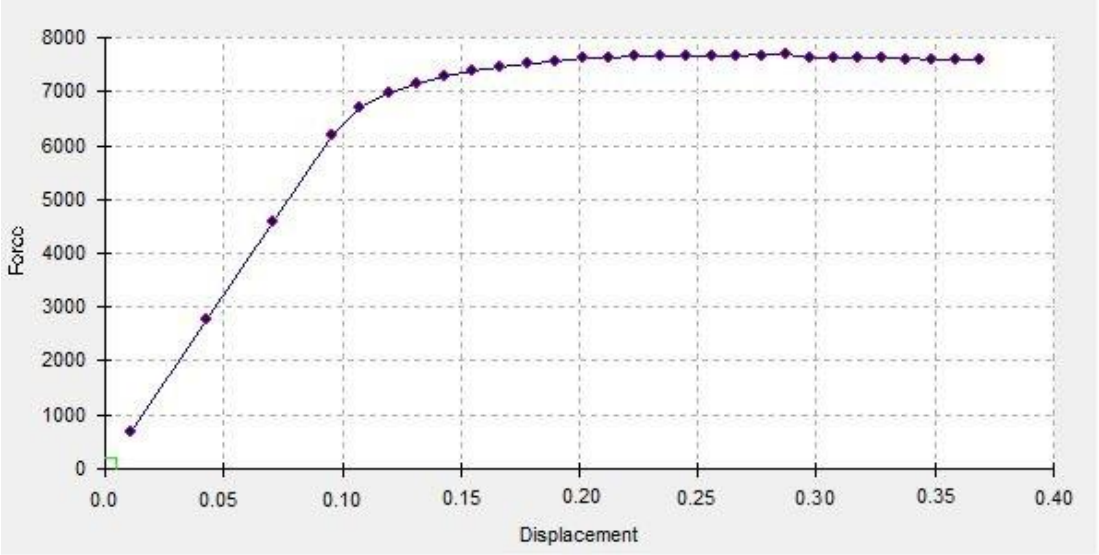

Figure 5.14 Force-Displacement Graph for the Piers of Demirtaş Viaduct

(Displacements in m and Force in kN)

Deflection limit of the pier column is obtained as 37 cm from the graph.

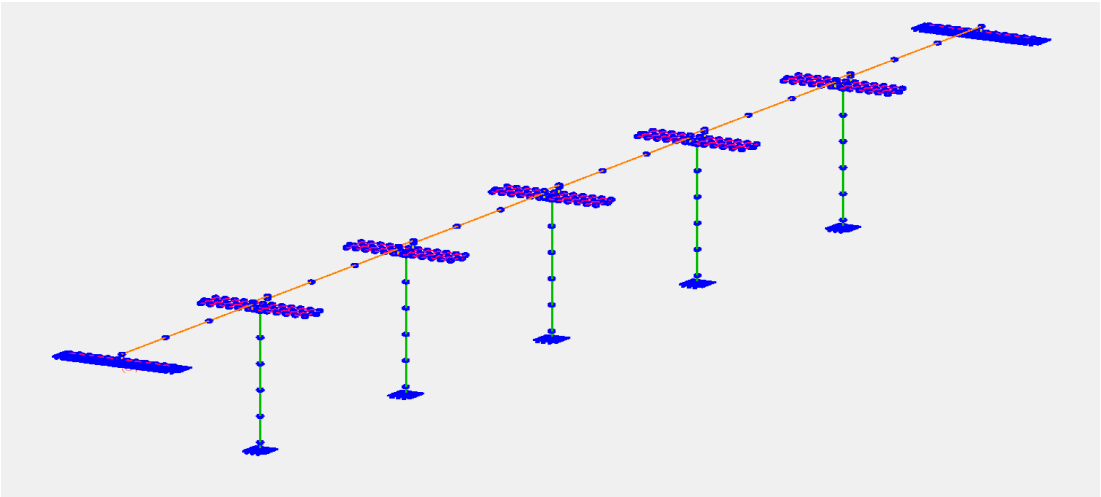

Figure 5.15 3D Model of the Demirtaş Viaduct on LARSA 4D

Fundamental period for the longitudinal direction is obtained as 2.01 sec and 37 cm deflection is reached when peak ground acceleration is 0.88 g. Therefore, resistance of Demirtaş Viaduct is assumed as 0.88 g.

5.4.2 Resistances of Asphalt Roads and Highways

For this study, it is assumed that, there are two failure modes for asphalt roads. First one is failure due to fault crossing and the other is based on embankment failure.

Faults are assumed to produce characteristic earthquakes and their activity is described by the characteristic earthquake model as explained in section 2.5.3.2. As stated here, a fault produces a characteristic earthquake if whole segment ruptures. If a fault crossing a road or highway ruptures, the corresponding road or highway becomes out of service.

In the study, Demirtaş Fault directly crosses the highway system. It passes through the segments C and L. Accordingly, if Demirtaş Fault ruptures, the highway system will fail, and there is no chance of reaching from the industrial zone to the two hospitals.

As discussed in Chapter 3, asphalts roads are flexible pavements and so, failure may occur due to failure of the embankments under the asphalt roads. In this study, parameters of numerical fragility curves are used to determine the capacities of embankments which are shown in the Table 5.8. Although PGA's are given as median values in Table 5.8, they are taken as mean values since resistances are assumed to have a normal distribution.

Table 5.8 Parameters of Numerical Fragility Curves for Embankments (SYNER-G Project 244061, 2011)

Damage State	Median Peak Ground Acceleration (g)			
	Soil Type C		Soil Type D	
	h = 2m	h = 4m	h = 2m	h = 4m
Minor	0.33	0.31	0.20	0.15
Moderate	0.54	0.54	0.42	0.31
Extensive	0.89	0.92	0.77	0.58
Complete	1.84	1.95	1.71	1.29

According to pavement performance report of U.S. Department of Transportation Federal Highway Administration (2004), heights of standard roadway sections vary between 660 mm and 820 mm for flexible pavements. In this study, it is approximately taken as 750 mm as an average value.

When fill dirt quality is considered in Turkey, soil type is assumed as D. Extensive damage on the embankments is considered for the failure of the asphalt pavements. As a result, resistance of the embankments is approximately taken as 0.9 g by extrapolating the height of embankment for 0.75 cm.

5.5 Assessment of the Reliability of Highway Systems

Reliability of the highway systems can be calculated step by step based on the concepts of the reliability of series and parallel systems. In the highway system, subsegments are in series and constitute segments. Segments and bridges constitute the paths. Paths are in parallel since they form alternatives and create redundancies. Paths finally form the highway system.

Reliability of the highway system is determined according to the flow chart given in Figure 5.16.

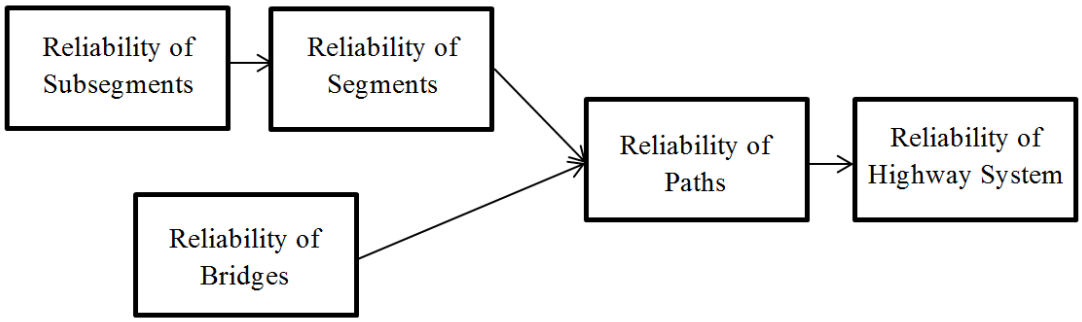

Figure 5.16 Steps to be Followed in the Calculation of Highway System Reliability

Survival probabilities of the elements of the highway system are basically calculated from equation (4.4). To calculate the Ps, mean values and variances (or standard deviations) of the loads and resistances should be known.

In the previous sections, loads and resistances for the highway elements are obtained. These values are assumed as the mean values for the loads and resistances. To determine variances or standard deviations or coefficients of variation (COV), information given in the literature are used.

Coefficient of variation is defined as the ratio of the standard deviation to the mean as given in equation (5.1)

$$COV = \frac{\sigma}{\mu} \tag{5.1}$$

Nowak (1999) uses a COV of 15.5% for columns which are reinforced with steel. Besides, Liu et al. (2001) states that in multicolumn systems, after a column reaches its ultimate bending capacity, other columns with confined reinforcements are able to withstand 30% additional load. Based on this information, they proposed a COV in the order of 12.5%.

Therefore, COV's of 15.5% can be used for Panayır and Balıklı Bridges due to the fact that these bridges are not multicolumn systems. On the other hand, since

Demirtaş Viaduct is a multicolumn system, COV of 12.5 % can be adopted. However, in this study, COV of 20% is used for Panayır and Balıklı Bridges and COV of 15% is used for Demirtaş Viaduct due to the expected lower construction quality in Turkey.

Because most of the roads are under cyclic loading, the approach of Bea (1983) is taken into consideration to determine the COV of embankments, which is 15%. Again due to construction quality, COV is increased to 20% in this study.

For seismic load demand, PGA, Yılmaz (2014) proposed a COV of 30% for Bursa region. However, Lallemant et al. (2015) states that combined uncertainty due to intra-event and inter-event uncertainties in the GMPE's can be significant. Therefore, for PGA, COV of 35% is used.

Fırat and Yücemen (2015) state that although dead and live loads acting on a structure are independent of the geographical location of the structure, environmental loads, such as earthquake loads are highly dependent on the location of the structure.

For bridges, only one failure mode, which is the failure of pier column, is considered. On the other hand, two failure modes are taken into consideration for roads and highways, namely: fault crossing and embankment failure.

5.5.1 System Reliability Due to Fault Crossing

Demirtaş Fault crosses the highway system by intersecting segments C and L. For this reason, if Demirtaş Fault ruptures, the highway system becomes out of service. In other words, in case of rupturing of Demirtaş Fault, probability of failure of the highway system equals to 1.0. In that case, it is more rational to calculate the probability of system failure due to fault crossing based on the activity rate of the Demirtaş Fault.

The probability that an event will occur at least once within a T year time period is as follows:

$$P_T = 1-(1-p)^T \quad (5.2)$$

where,

p = annual probability of occurrence

Since Demirtaş Fault is considered as potentially active (see Appendix A), activity rate for Demirtaş Fault is 1/1000 based on Table 5.3. Accordingly, annual probability of rupture of the Demirtaş fault will be 1/1000 =0.001.

From equation (5.2), probability of rupture of Demirtaş Fault is calculated for time intervals of 50 and 75 years, which are assumed as the alternative economical lifetimes for the transportation lifelines giving priority to the viaduct and the bridges. The computed probabilities are shown in Table 5.9. Since rupturing of the fault means failure of the highway system, these probabilities also correspond to the failure probabilities of the highway system due to fault crossing failure mode during its assumed lifetime of 50 or 75 years. In the same table the probability of survival of the highway system is also presented.

Table 5.9 Rupture Probability of Demirtaş Fault and Failure and Survival Probabilities of the Highway System Corresponding to Different Economical Lifetimes

Economical Lifetime	**Failure Probability of the Highway System (Rupture Probability of Demirtaş Fault)**	**Survival Probability of the Highway System**
50 years	0.0488	0.9512
75 years	0.0723	0.9277

5.5.2 System Reliability Due to Embankment and Pier Failures

Survival probability of subsegments and bridges are also calculated for different return periods as explained in the next sections.

5.5.2.1 System Reliability for a Return Period of 75 Years

In Table 5.10, PGA's corresponding to 75 years return period for each subsegment and bridges are given as well as the resistances (see Chapter 3.4), reliability indices and probabilities of survival.

Table 5.10 PGA Values Obtained for the Midpoints of Road Subsegments and Bridges for 75 Years Return Period (RP), Resistance Values in Terms of PGA, β and Probability of Survival for Subsegments and Bridges

Segment Name	Latitude	Longitude	Loads PGA (g) RP =75 years	Resistances PGA (g)	σ_S	σ_R	β	P_S
A	40.2661	29.0668	0.1698	0.9000	0.0594	0.1800	3.8524	0.999942
	40.2663	29.0533	0.1689	0.9000	0.0591	0.1800	3.8589	0.999943
B	40.2671	29.0527	0.1689	0.9000	0.0591	0.1800	3.8589	0.999943
	40.2754	29.0492	0.1690	0.9000	0.0592	0.1800	3.8578	0.999943
	40.2818	29.0549	0.1698	0.9000	0.0594	0.1800	3.8524	0.999942
	40.2842	29.0661	0.1705	0.9000	0.0597	0.1800	3.8469	0.999940
	40.2839	29.0781	0.1711	0.9000	0.0599	0.1800	3.8427	0.999939
	40.2825	29.0903	0.1715	0.9000	0.0600	0.1800	3.8391	0.999938
	40.2813	29.1013	0.1720	0.9000	0.0602	0.1800	3.8358	0.999937
C	40.2810	29.1024	0.1720	0.9000	0.0602	0.1800	3.8355	0.999937
	40.2763	29.1093	0.1722	0.9000	0.0603	0.1800	3.8338	0.999937
	40.2678	29.1055	0.1719	0.9000	0.0602	0.1800	3.8363	0.999938
	40.2605	29.0991	0.1715	0.9000	0.0600	0.1800	3.8397	0.999938
	40.2531	29.0927	0.1710	0.9000	0.0598	0.1800	3.8435	0.999939
	40.2443	29.0917	0.1707	0.9000	0.0597	0.1800	3.8454	0.999940
	40.2346	29.0905	0.1704	0.9000	0.0596	0.1800	3.8480	0.999940
	40.2249	29.0893	0.1699	0.9000	0.0595	0.1800	3.8514	0.999941
D	40.2248	29.0905	0.1700	0.9000	0.0595	0.1800	3.8507	0.999941
	40.2232	29.1023	0.1710	0.9000	0.0598	0.1800	3.8434	0.999939
	40.2202	29.1131	0.1718	0.9000	0.0601	0.1800	3.8370	0.999938
	40.2138	29.1212	0.1723	0.9000	0.0603	0.1800	3.8337	0.999937
	40.2059	29.1193	0.1717	0.9000	0.0601	0.1800	3.8379	0.999938
	40.1980	29.1174	0.1710	0.9000	0.0599	0.1800	3.8431	0.999939
E	40.1979	29.1162	0.1709	0.9000	0.0598	0.1800	3.8439	0.999939
	40.1967	29.1046	0.1697	0.9000	0.0594	0.1800	3.8528	0.999942
	40.1954	29.0931	0.1685	0.9000	0.0590	0.1800	3.8620	0.999944
	40.1935	29.0827	0.1673	0.9000	0.0586	0.1800	3.8709	0.999946

Table 5.10 (cont'd) PGA Values Obtained for the Midpoints of Road Subsegments and Bridges for 75 Years Return Period (RP), Resistance Values in Terms of PGA, β and Probability of Survival for Subsegments and Bridges

Segment Name	Latitude	Longitude	Loads PGA (g) RP =75 years	Resistances PGA (g)	σ_S	σ_R	β	P_S
F	40.1927	29.0819	0.1672	0.9000	0.0585	0.1800	3.8719	0.999946
	40.1886	29.0714	0.1658	0.9000	0.0580	0.1800	3.8821	0.999948
	40.1884	29.0594	0.1646	0.9000	0.0576	0.1800	3.8912	0.999950
	40.1895	29.0467	0.1634	0.9000	0.0572	0.1800	3.9003	0.999952
G	40.1904	29.0466	0.1635	0.9000	0.0572	0.1800	3.8997	0.999952
	40.1954	29.0501	0.1643	0.9000	0.0575	0.1800	3.8934	0.999951
	40.1974	29.0621	0.1657	0.9000	0.0580	0.1800	3.8830	0.999948
H	40.1972	29.0632	0.1658	0.9000	0.0580	0.1800	3.8823	0.999948
	40.1954	29.0724	0.1665	0.9000	0.0583	0.1800	3.8768	0.999947
	40.1935	29.0827	0.1673	0.9000	0.0586	0.1800	3.8709	0.999946
I	40.1982	29.0615	0.1657	0.9000	0.0580	0.1800	3.8829	0.999948
	40.2057	29.0602	0.1662	0.9000	0.0582	0.1800	3.8793	0.999948
	40.2137	29.0606	0.1668	0.9000	0.0584	0.1800	3.8745	0.999947
	40.2217	29.0611	0.1674	0.9000	0.0586	0.1800	3.8701	0.999946
J	40.2221	29.0622	0.1675	0.9000	0.0586	0.1800	3.8692	0.999945
	40.2250	29.0708	0.1684	0.9000	0.0589	0.1800	3.8625	0.999944
	40.2254	29.0800	0.1692	0.9000	0.0592	0.1800	3.8567	0.999943
	40.2249	29.0893	0.1699	0.9000	0.0595	0.1800	3.8514	0.999941
K	40.2226	29.0611	0.1675	0.9000	0.0586	0.1800	3.8697	0.999946
	40.2315	29.0615	0.1680	0.9000	0.0588	0.1800	3.8656	0.999945
	40.2394	29.0619	0.1684	0.9000	0.0589	0.1800	3.8625	0.999944
L	40.2403	29.0619	0.1685	0.9000	0.0590	0.1800	3.8622	0.999944
	40.2492	29.0622	0.1689	0.9000	0.0591	0.1800	3.8593	0.999943
	40.2576	29.0591	0.1690	0.9000	0.0591	0.1800	3.8585	0.999943
	40.2663	29.0533	0.1689	0.9000	0.0591	0.1800	3.8589	0.999943
Panayır Br.	40.2400	29.0600	0.1683	1.2600	0.0589	0.2520	4.2184	0.999988
Balıklı Br.	40.2200	29.0600	0.1672	1.6200	0.0585	0.3240	4.4126	0.999995
Demirtaş Via	40.2800	29.1000	0.1719	0.8800	0.0602	0.1320	4.8814	0.999999

Since segments are formed by subsegments in series, upper and lower bounds for the probability of survival for the segments in 75 years return period are determined as given is Table 5.11.

Table 5.11 Upper (P_S') and Lower (P_S^*) Bounds for the Probability of Survival of Each Segment (Subsegments in Series) for 75 Years Return Period

Segment	**A**	**B**	**C**	**D**	**E**	**F**
$\mathbf{P_S^*}$	0.999885	0.999582	0.999511	0.999632	0.999771	0.999796
$\mathbf{P_S'}$	0.999942	0.999937	0.999937	0.999937	0.999939	0.999948

Segment	**G**	**H**	**I**	**J**	**K**	**L**
$\mathbf{P_S^*}$	0.999851	0.999841	0.999788	0.999773	0.999834	0.999773
$\mathbf{P_S'}$	0.999948	0.999946	0.999946	0.999941	0.999944	0.999943

Paths consist of different segments. Upper and lower bounds of probability of survival of each path for 75 years return period are presented in Table 5.12

Table 5.12 Upper and Lower Bounds for the Probability of Survival of Each Path (Segments in Series) for 75 Years Return Period

	Nodes	**Segments**	$\mathbf{P_S^*}$	$\mathbf{P_S'}$
Bursa State Hospital	1-2-10-9-8-7	A-L-K-I-G	0.999114	0.999942
	1-2-10-9-8-6-7	A-L-K-I-H-F	0.999066	0.999942
	1-2-10-9-4-5-6-7	A-L-K-J-D-E-F	0.998448	0.999937
	1-2-10-9-4-5-6-8-7	A-L-K-J-D-E-H-G	0.998343	0.999937
	1-2-3-4-5-6-7	A-B-C-D-E-F	0.998178	0.999937
	1-2-3-4-5-6-8-7	A-B-C-D-E-H-G	0.998074	0.999937
	1-2-3-4-9-8-7	A-B-C-J-I-G	0.998386	0.999937
	1-2-3-4-9-8-6-7	A-B-C-J-I-H-F	0.998173	0.999937
Bursa High Specialty Hospital	1-2-3-4-5	A-B-C-D	0.998611	0.999937
	1-2-3-4-9-8-6-5	A-B-C-J-I-H-E	0.998147	0.999937
	1-2-3-4-9-8-7-6-5	A-B-C-J-I-G-F-E	0.997954	0.999937
	1-2-10-9-4-5	A-L-K-J-D	0.998880	0.999937
	1-2-10-9-8-7-6-5	A-L-K-I-G-F-E	0.998681	0.999939
	1-2-10-9-8-6-5	A-L-K-I-H-E	0.998875	0.999939

Survival probabilities of the paths reaching from the industrial zone to the two hospitals are given in Table 5.13 for 75 years return period.

Table 5.13 Upper and Lower Reliability Bounds for Reaching from the Industrial Zone to the Hospitals for 75 Years Return Period (Paths in Parallel)

	P_S^*	P_S'
Bursa State Hospital	0.998074	≈1.000000*
Bursa High Specialty Hospital	0.997954	≈1.000000

*Actual Value: 0.999999999999999999999999999999999784

Bounds on the reliability of highway system for reaching from the industrial zone to the hospitals for 75 years return period are

$$1.000000 \geq P_{S_S} \geq 0.997954$$

$$2.16\text{x}10^{-34} \leq P_{F_S} \leq 0.002046$$

5.5.2.2 System Reliability for a Return Period of 475 Years

In Table 5.14, PGA's corresponding to 475 years return period for each subsegment and bridges are given as well as the resistances (see Chapter 3.4), reliability indices and probabilities of survival.

Table 5.14 PGA Values Obtained for the Midpoints of Road Subsegments and Bridges for 475 Years Return Period (RP), Resistance Values in Terms of PGA, β and Probability of Survival for Subsegments and Bridges

Segment Name	Latitude	Longitude	Loads PGA (g) RP =475 years	Resistances PGA (g)	σ_S	σ_R	β	P_S
A	40.2661	29.0668	0.3925	0.9000	0.1374	0.1800	2.2414	0.987500
	40.2663	29.0533	0.3913	0.9000	0.1370	0.1800	2.2490	0.987745
B	40.2671	29.0527	0.3913	0.9000	0.1370	0.1800	2.2490	0.987745
	40.2754	29.0492	0.3906	0.9000	0.1367	0.1800	2.2534	0.987884
	40.2818	29.0549	0.3900	0.9000	0.1365	0.1800	2.2573	0.988007
	40.2842	29.0661	0.3887	0.9000	0.1360	0.1800	2.2663	0.988284
	40.2839	29.0781	0.3877	0.9000	0.1357	0.1800	2.2727	0.988479
	40.2825	29.0903	0.3873	0.9000	0.1355	0.1800	2.2755	0.988562
	40.2813	29.1013	0.3870	0.9000	0.1354	0.1800	2.2775	0.988621

Table 5.14 (cont'd) PGA Values Obtained for the Midpoints of Road Subsegments and Bridges for 475 Years Return Period (RP), Resistance Values in Terms of PGA, β and Probability of Survival for Subsegments and Bridges

Segment Name	Latitude	Longitude	Loads PGA (g) RP =475 years	Resistances PGA (g)	σ_S	σ_R	β	P_S
C	40.2810	29.1024	0.3871	0.9000	0.1355	0.1800	2.2768	0.988601
	40.2763	29.1093	0.3893	0.9000	0.1363	0.1800	2.2621	0.988155
	40.2678	29.1055	0.3929	0.9000	0.1375	0.1800	2.2389	0.987418
	40.2605	29.0991	0.3934	0.9000	0.1377	0.1800	2.2352	0.987299
	40.2531	29.0927	0.3921	0.9000	0.1372	0.1800	2.2442	0.987591
	40.2443	29.0917	0.3897	0.9000	0.1364	0.1800	2.2594	0.988072
	40.2346	29.0905	0.3874	0.9000	0.1356	0.1800	2.2744	0.988528
	40.2249	29.0893	0.3868	0.9000	0.1354	0.1800	2.2787	0.988658
D	40.2248	29.0905	0.3869	0.9000	0.1354	0.1800	2.2779	0.988632
	40.2232	29.1023	0.3896	0.9000	0.1364	0.1800	2.2604	0.988100
	40.2202	29.1131	0.3926	0.9000	0.1374	0.1800	2.2408	0.987481
	40.2138	29.1212	0.3958	0.9000	0.1385	0.1800	2.2201	0.986793
	40.2059	29.1193	0.3996	0.9000	0.1398	0.1800	2.1955	0.985936
	40.1980	29.1174	0.4040	0.9000	0.1414	0.1800	2.1671	0.984887
E	40.1979	29.1162	0.4039	0.9000	0.1414	0.1800	2.1676	0.984906
	40.1967	29.1046	0.4025	0.9000	0.1409	0.1800	2.1768	0.985252
	40.1954	29.0931	0.4001	0.9000	0.1400	0.1800	2.1920	0.985810
	40.1935	29.0827	0.3981	0.9000	0.1393	0.1800	2.2052	0.986281
F	40.1927	29.0819	0.3984	0.9000	0.1394	0.1800	2.2033	0.986213
	40.1886	29.0714	0.3984	0.9000	0.1395	0.1800	2.2028	0.986195
	40.1884	29.0594	0.3958	0.9000	0.1385	0.1800	2.2198	0.986782
	40.1895	29.0467	0.3926	0.9000	0.1374	0.1800	2.2404	0.987469
G	40.1904	29.0466	0.3924	0.9000	0.1374	0.1800	2.2417	0.987509
	40.1954	29.0501	0.3919	0.9000	0.1372	0.1800	2.2453	0.987624
	40.1974	29.0621	0.3931	0.9000	0.1376	0.1800	2.2374	0.987369
H	40.1972	29.0632	0.3934	0.9000	0.1377	0.1800	2.2357	0.987314
	40.1954	29.0724	0.3955	0.9000	0.1384	0.1800	2.2220	0.986857
	40.1935	29.0827	0.3981	0.9000	0.1393	0.1800	2.2052	0.986281
I	40.1982	29.0615	0.3927	0.9000	0.1374	0.1800	2.2400	0.987454
	40.2057	29.0602	0.3895	0.9000	0.1363	0.1800	2.2609	0.988119
	40.2137	29.0606	0.3867	0.9000	0.1354	0.1800	2.2790	0.988668
	40.2217	29.0611	0.3850	0.9000	0.1347	0.1800	2.2907	0.989009

Table 5.14 (cont'd) PGA Values Obtained for the Midpoints of Road Subsegments and Bridges for 475 Years Return Period (RP), Resistance Values in Terms of PGA, β and Probability of Survival for Subsegments and Bridges

Segment Name	Latitude	Longitude	Loads PGA (g) RP =475 years	Resistances PGA (g)	σ_S	σ_R	β	P_S
J	40.2221	29.0622	0.3850	0.9000	0.1347	0.1800	2.2905	0.989005
	40.2250	29.0708	0.3854	0.9000	0.1349	0.1800	2.2880	0.988931
	40.2254	29.0800	0.3860	0.9000	0.1351	0.1800	2.2836	0.988802
	40.2249	29.0893	0.3868	0.9000	0.1354	0.1800	2.2787	0.988658
K	40.2226	29.0611	0.3848	0.9000	0.1347	0.1800	2.2915	0.989034
	40.2315	29.0615	0.3846	0.9000	0.1346	0.1800	2.2932	0.989083
	40.2394	29.0619	0.3857	0.9000	0.1350	0.1800	2.2857	0.988863
L	40.2403	29.0619	0.3859	0.9000	0.1351	0.1800	2.2844	0.988825
	40.2492	29.0622	0.3884	0.9000	0.1359	0.1800	2.2681	0.988340
	40.2576	29.0591	0.3904	0.9000	0.1366	0.1800	2.2549	0.987931
	40.2663	29.0533	0.3913	0.9000	0.1370	0.1800	2.2490	0.987745
Panayır Br.	40.2400	29.0600	0.3856	1.2600	0.1350	0.2520	3.0586	0.998888
Balıklı Br.	40.2200	29.0600	0.3852	1.6200	0.1348	0.3240	3.5189	0.999783
Demirtaş Via	40.2800	29.1000	0.3879	0.8800	0.1358	0.1320	2.5991	0.995327

Since segments are formed by subsegments in series, upper and lower bounds for the probability of survival for the segments in 475 years return period are determined as given is Table 5.15.

Table 5.15 Upper (P_S') and Lower (P_S^*) Bounds for the Probability of Survival of Each Segment (Subsegments in Series) for 475 Years Return Period

Segment	A	B	C	D	E	F
P_S^*	0.975399	0.920435	0.908231	0.924327	0.943488	0.947716
P_S'	0.987500	0.987745	0.987299	0.984887	0.984906	0.986195

Segment	G	H	I	J	K	L
P_S^*	0.962969	0.960971	0.954062	0.956136	0.967342	0.953668
P_S'	0.987369	0.986281	0.987454	0.988658	0.988863	0.987745

Paths consist of different segments. Upper and lower bounds of probability of survival of each path for 475 years return period are presented in Table 5.16.

Table 5.16 Upper and Lower Bounds for the Probability of Survival of Each Path (Segments in Series) for 475 Years Return Period

	Nodes	Segments	P_S^*	P_S'
Bursa State Hospital	1-2-10-9-8-7	A-L-K-I-G	0.825602	0.987369
	1-2-10-9-8-6-7	A-L-K-I-H-F	0.807174	0.986195
	1-2-10-9-4-5-6-7	A-L-K-J-D-E-F	0.710137	0.984887
	1-2-10-9-4-5-6-8-7	A-L-K-J-D-E-H-G	0.693404	0.984887
	1-2-3-4-5-6-7	A-B-C-D-E-F	0.670777	0.984887
	1-2-3-4-5-6-8-7	A-B-C-D-E-H-G	0.654971	0.984887
	1-2-3-4-9-8-7	A-B-C-J-I-G	0.712773	0.987299
	1-2-3-4-9-8-6-7	A-B-C-J-I-H-F	0.674105	0.986195
Bursa High Specialty Hospital	1-2-3-4-5	A-B-C-D	0.750176	0.984887
	1-2-3-4-9-8-6-5	A-B-C-J-I-H-E	0.671098	0.984906
	1-2-3-4-9-8-7-6-5	A-B-C-J-I-G-F-E	0.637333	0.984906
	1-2-10-9-4-5	A-L-K-J-D	0.794196	0.984887
	1-2-10-9-8-7-6-5	A-L-K-I-G-F-E	0.738220	0.984906
	1-2-10-9-8-6-5	A-L-K-I-H-E	0.777330	0.984906

Survival probabilities of the paths reaching from the industrial zone to the two hospitals are given in Table 5.17 for 475 years return period.

Table 5.17 Upper and Lower Reliability Bounds for Reaching from the Industrial Zone to the Hospitals for 475 Years Return Period (Paths in Parallel)

	P_S^*	P_S'
Bursa State Hospital	0.654971	≈1.000000
Bursa High Specialty Hospital	0.637333	≈1.000000

Bounds on the reliability of highway system for reaching from the industrial zone to the hospitals for 475 years return period are

$$1.000000 \geq P_{S_S} \geq 0.637333$$

$$1.59\text{x}10^{-15} \leq P_{F_S} \leq 0.362667$$

5.5.2.3 System Reliability for a Return Period of 1000 Years

In Table 5.18, PGA's corresponding to1000 years return period for each subsegment and bridges are given as well as the resistances (see Chapter 3.4), reliability indices and probabilities of survival.

Table 5.18 PGA Values Obtained for the Midpoints of Road Subsegments and Bridges for 1000 Years Return Period (RP), Resistance Values in Terms of PGA, β and Probability of Survival for Subsegments and Bridges

Segment Name	Latitude	Longitude	Loads PGA (g) RP =1000 years	Resistances PGA (g)	σ_S	σ_R	β	P_S
A	40.2661	29.0668	0.5171	0.9000	0.1810	0.1800	1.5000	0.933187
	40.2663	29.0533	0.5157	0.9000	0.1805	0.1800	1.5076	0.934171
B	40.2671	29.0527	0.5159	0.9000	0.1806	0.1800	1.5066	0.934047
	40.2754	29.0492	0.5159	0.9000	0.1806	0.1800	1.5065	0.934026
	40.2818	29.0549	0.5145	0.9000	0.1801	0.1800	1.5139	0.934969
	40.2842	29.0661	0.5115	0.9000	0.1790	0.1800	1.5304	0.937037
	40.2839	29.0781	0.5096	0.9000	0.1783	0.1800	1.5409	0.938324
	40.2825	29.0903	0.5088	0.9000	0.1781	0.1800	1.5450	0.938826
	40.2813	29.1013	0.5082	0.9000	0.1779	0.1800	1.5484	0.939234
C	40.2810	29.1024	0.5083	0.9000	0.1779	0.1800	1.5476	0.939136
	40.2763	29.1093	0.5120	0.9000	0.1792	0.1800	1.5275	0.936687
	40.2678	29.1055	0.5174	0.9000	0.1811	0.1800	1.4985	0.932999
	40.2605	29.0991	0.5168	0.9000	0.1809	0.1800	1.5018	0.933431
	40.2531	29.0927	0.5123	0.9000	0.1793	0.1800	1.5258	0.936471
	40.2443	29.0917	0.5060	0.9000	0.1771	0.1800	1.5604	0.940662
	40.2346	29.0905	0.5004	0.9000	0.1751	0.1800	1.5910	0.944195
	40.2249	29.0893	0.4983	0.9000	0.1744	0.1800	1.6026	0.945492
D	40.2248	29.0905	0.4984	0.9000	0.1745	0.1800	1.6020	0.945418
	40.2232	29.1023	0.5015	0.9000	0.1755	0.1800	1.5848	0.943496
	40.2202	29.1131	0.5049	0.9000	0.1767	0.1800	1.5665	0.941383
	40.2138	29.1212	0.5089	0.9000	0.1781	0.1800	1.5443	0.938741
	40.2059	29.1193	0.5157	0.9000	0.1805	0.1800	1.5075	0.934164
	40.1980	29.1174	0.5253	0.9000	0.1839	0.1800	1.4561	0.927321
E	40.1979	29.1162	0.5254	0.9000	0.1839	0.1800	1.4558	0.927277
	40.1967	29.1046	0.5249	0.9000	0.1837	0.1800	1.4586	0.927665
	40.1954	29.0931	0.5223	0.9000	0.1828	0.1800	1.4721	0.929506
	40.1935	29.0827	0.5206	0.9000	0.1822	0.1800	1.4811	0.930709

Table 5.18 (cont'd) PGA Values Obtained for the Midpoints of Road Subsegments and Bridges for 1000 Years Return Period (RP), Resistance Values in Terms of PGA, β and Probability of Survival for Subsegments and Bridges

Segment Name	Latitude	Longitude	Loads PGA (g) RP =1000 years	Resistances PGA (g)	σ_S	σ_R	β	P_S
F	40.1927	29.0819	0.5214	0.9000	0.1825	0.1800	1.4769	0.930152
	40.1886	29.0714	0.5240	0.9000	0.1834	0.1800	1.4634	0.928328
	40.1884	29.0594	0.5218	0.9000	0.1826	0.1800	1.4750	0.929894
	40.1895	29.0467	0.5192	0.9000	0.1817	0.1800	1.4887	0.931715
G	40.1904	29.0466	0.5188	0.9000	0.1816	0.1800	1.4912	0.932039
	40.1954	29.0501	0.5159	0.9000	0.1806	0.1800	1.5063	0.934006
	40.1974	29.0621	0.5149	0.9000	0.1802	0.1800	1.5118	0.934701
H	40.1972	29.0632	0.5152	0.9000	0.1803	0.1800	1.5105	0.934536
	40.1954	29.0724	0.5174	0.9000	0.1811	0.1800	1.4983	0.932971
	40.1935	29.0827	0.5206	0.9000	0.1822	0.1800	1.4811	0.930709
I	40.1982	29.0615	0.5142	0.9000	0.1800	0.1800	1.5156	0.935188
	40.2057	29.0602	0.5079	0.9000	0.1778	0.1800	1.5499	0.939418
	40.2137	29.0606	0.5022	0.9000	0.1758	0.1800	1.5811	0.943068
	40.2217	29.0611	0.4983	0.9000	0.1744	0.1800	1.6026	0.945492
J	40.2221	29.0622	0.4982	0.9000	0.1744	0.1800	1.6033	0.945571
	40.2250	29.0708	0.4976	0.9000	0.1742	0.1800	1.6064	0.945907
	40.2254	29.0800	0.4979	0.9000	0.1743	0.1800	1.6052	0.945773
	40.2249	29.0893	0.4983	0.9000	0.1744	0.1800	1.6026	0.945492
K	40.2226	29.0611	0.4980	0.9000	0.1743	0.1800	1.6043	0.945675
	40.2315	29.0615	0.4974	0.9000	0.1741	0.1800	1.6080	0.946078
	40.2394	29.0619	0.5002	0.9000	0.1751	0.1800	1.5923	0.944338
L	40.2403	29.0619	0.5006	0.9000	0.1752	0.1800	1.5899	0.944071
	40.2492	29.0622	0.5062	0.9000	0.1772	0.1800	1.5590	0.940506
	40.2576	29.0591	0.5118	0.9000	0.1791	0.1800	1.5286	0.936822
	40.2663	29.0533	0.5157	0.9000	0.1805	0.1800	1.5076	0.934171
Panayır Br.	40.2400	29.0600	0.5003	1.2600	0.1751	0.2520	2.4757	0.993352
Balıklı Br.	40.2200	29.0600	0.4990	1.6200	0.1746	0.3240	3.0456	0.998839
Demirtaş Via	40.2800	29.1000	0.5098	0.8800	0.1784	0.1320	1.6682	0.952357

Since segments are formed by subsegments in series, upper and lower bounds for the probability of survival for the segments in 1000 years return period are determined as given is Table 5.19.

Table 5.19 Upper (P_S') and Lower (P_S^*) Bounds for the Probability of Survival of Each Segment (Subsegments in Series) for 1000 Years Return Period

Segment	**A**	**B**	**C**	**D**	**E**	**F**
$\mathbf{P_S^*}$	0.871757	0.632403	0.602467	0.682856	0.744160	0.748121
$\mathbf{P_S'}$	0.933187	0.934026	0.932999	0.927321	0.927277	0.928328

Segment	**G**	**H**	**I**	**J**	**K**	**L**
$\mathbf{P_S^*}$	0.813685	0.811481	0.783355	0.799811	0.844883	0.777051
$\mathbf{P_S'}$	0.932039	0.930709	0.935188	0.945492	0.944338	0.934171

Paths consist of different segments. Upper and lower bounds of probability of survival of each path for 1000 years return period are presented in Table 5.20

Table 5.20 Upper and Lower Bounds for the Probability of Survival of Each Path (Segments in Series) for 1000 Years Return Period

	Nodes	**Segments**	$\mathbf{P_S^*}$	$\mathbf{P_S'}$
Bursa State Hospital	1-2-10-9-8-7	A-L-K-I-G	0.361955	0.932039
	1-2-10-9-8-6-7	A-L-K-I-H-F	0.319633	0.928328
	1-2-10-9-4-5-6-7	A-L-K-J-D-E-F	0.172661	0.927277
	1-2-10-9-4-5-6-8-7	A-L-K-J-D-E-H-G	0.152390	0.927277
	1-2-3-4-5-6-7	A-B-C-D-E-F	0.120251	0.927277
	1-2-3-4-5-6-8-7	A-B-C-D-E-H-G	0.106134	0.927277
	1-2-3-4-9-8-7	A-B-C-J-I-G	0.161072	0.932039
	1-2-3-4-9-8-6-7	A-B-C-J-I-H-F	0.120175	0.928328
Bursa High Specialty Hospital	1-2-3-4-5	A-B-C-D	0.215999	0.927321
	1-2-3-4-9-8-6-5	A-B-C-J-I-H-E	0.119539	0.927277
	1-2-3-4-9-8-7-6-5	A-B-C-J-I-G-F-E	0.089672	0.927277
	1-2-10-9-4-5	A-L-K-J-D	0.310139	0.927321
	1-2-10-9-8-7-6-5	A-L-K-I-G-F-E	0.201508	0.927277
	1-2-10-9-8-6-5	A-L-K-I-H-E	0.268623	0.927277

Survival probabilities of the paths reaching from the industrial zone to the two hospitals are given in Table 5.21 for 1000 years return period.

Table 5.21 Upper and Lower Reliability Bounds for Reaching from the Industrial Zone to the Hospitals for 1000 Years Return Period (Paths in Parallel)

	P_S^*	P_S'
Bursa State Hospital	0.106134	0.999999
Bursa High Specialty Hospital	0.089672	0.999998

Bounds on the reliability of highway system for reaching from the industrial zone to the hospitals for 1000 years return period are

$$0.999999 \geq P_{S_S} \geq 0.089672$$

$$1.48\text{x}10^{-7} \leq P_{F_S} \leq 0.910328$$

5.5.2.4 System Reliability for a Return Period of 2475 Years

In Table 5.22, PGA's corresponding to 2475 years return period for each subsegment and bridges are given as well as the resistances (see Chapter 3.4), reliability indices and probabilities of survival.

Table 5.22 PGA Values Obtained for the Midpoints of Road Subsegments and Bridges for 2475 Years Return Period (RP), Resistance Values in Terms of PGA, β and Probability of Survival for Subsegments and Bridges

Segment Name	Latitude	Longitude	Loads PGA (g) RP =2475 years	Resistances PGA (g)	σ_S	σ_R	β	P_S
A	40.2661	29.0668	0.6910	0.9000	0.2419	0.1800	0.6931	0.755884
	40.2663	29.0533	0.6884	0.9000	0.2409	0.1800	0.7037	0.759186
B	40.2671	29.0527	0.6889	0.9000	0.2411	0.1800	0.7015	0.758517
	40.2754	29.0492	0.6905	0.9000	0.2417	0.1800	0.6951	0.756505
	40.2818	29.0549	0.6878	0.9000	0.2407	0.1800	0.7060	0.759905
	40.2842	29.0661	0.6814	0.9000	0.2385	0.1800	0.7317	0.767833
	40.2839	29.0781	0.6776	0.9000	0.2372	0.1800	0.7468	0.772413
	40.2825	29.0903	0.6764	0.9000	0.2367	0.1800	0.7519	0.773943
	40.2813	29.1013	0.6753	0.9000	0.2364	0.1800	0.7562	0.775250
C	40.2810	29.1024	0.6756	0.9000	0.2365	0.1800	0.7550	0.774884
	40.2763	29.1093	0.6828	0.9000	0.2390	0.1800	0.7262	0.766134
	40.2678	29.1055	0.6923	0.9000	0.2423	0.1800	0.6881	0.754304
	40.2605	29.0991	0.6889	0.9000	0.2411	0.1800	0.7016	0.758529
	40.2531	29.0927	0.6774	0.9000	0.2371	0.1800	0.7476	0.772658
	40.2443	29.0917	0.6622	0.9000	0.2318	0.1800	0.8103	0.791115
	40.2346	29.0905	0.6494	0.9000	0.2273	0.1800	0.8642	0.806252
	40.2249	29.0893	0.6452	0.9000	0.2258	0.1800	0.8825	0.811235
D	40.2248	29.0905	0.6453	0.9000	0.2258	0.1800	0.8821	0.811131
	40.2232	29.1023	0.6494	0.9000	0.2273	0.1800	0.8644	0.806323
	40.2202	29.1131	0.6545	0.9000	0.2291	0.1800	0.8428	0.800343
	40.2138	29.1212	0.6614	0.9000	0.2315	0.1800	0.8138	0.792109
	40.2059	29.1193	0.6750	0.9000	0.2363	0.1800	0.7574	0.775592
	40.1980	29.1174	0.6950	0.9000	0.2433	0.1800	0.6773	0.750889
E	40.1979	29.1162	0.6953	0.9000	0.2434	0.1800	0.6761	0.750515
	40.1967	29.1046	0.6963	0.9000	0.2437	0.1800	0.6725	0.749366
	40.1954	29.0931	0.6932	0.9000	0.2426	0.1800	0.6846	0.753208
	40.1935	29.0827	0.6910	0.9000	0.2419	0.1800	0.6932	0.755896
F	40.1927	29.0819	0.6928	0.9000	0.2425	0.1800	0.6862	0.753694
	40.1886	29.0714	0.6999	0.9000	0.2450	0.1800	0.6582	0.744787
	40.1884	29.0594	0.6977	0.9000	0.2442	0.1800	0.6667	0.747529
	40.1895	29.0467	0.6952	0.9000	0.2433	0.1800	0.6768	0.750739
G	40.1904	29.0466	0.6941	0.9000	0.2429	0.1800	0.6809	0.752024
	40.1954	29.0501	0.6869	0.9000	0.2404	0.1800	0.7095	0.760983
	40.1974	29.0621	0.6822	0.9000	0.2388	0.1800	0.7285	0.766849

Table 5.22 (cont'd) PGA Values Obtained for the Midpoints of Road Subsegments and Bridges for 2475 Years Return Period (RP), Resistance Values in Terms of PGA, β and Probability of Survival for Subsegments and Bridges

Segment Name	Latitude	Longitude	Loads PGA (g) RP =2475 years	Resistances PGA (g)	σ_S	σ_R	β	P_S
H	40.1972	29.0632	0.6825	0.9000	0.2389	0.1800	0.7273	0.766479
	40.1954	29.0724	0.6859	0.9000	0.2401	0.1800	0.7135	0.762220
	40.1935	29.0827	0.6910	0.9000	0.2419	0.1800	0.6932	0.755896
I	40.1982	29.0615	0.6807	0.9000	0.2383	0.1800	0.7343	0.768608
	40.2057	29.0602	0.6676	0.9000	0.2336	0.1800	0.7881	0.784690
	40.2137	29.0606	0.6555	0.9000	0.2294	0.1800	0.8385	0.799135
	40.2217	29.0611	0.6476	0.9000	0.2267	0.1800	0.8719	0.808370
J	40.2221	29.0622	0.6473	0.9000	0.2265	0.1800	0.8735	0.808802
	40.2250	29.0708	0.6454	0.9000	0.2259	0.1800	0.8814	0.810956
	40.2254	29.0800	0.6451	0.9000	0.2258	0.1800	0.8829	0.811363
	40.2249	29.0893	0.6452	0.9000	0.2258	0.1800	0.8825	0.811235
K	40.2226	29.0611	0.6471	0.9000	0.2265	0.1800	0.8743	0.809012
	40.2315	29.0615	0.6457	0.9000	0.2260	0.1800	0.8803	0.810642
	40.2394	29.0619	0.6508	0.9000	0.2278	0.1800	0.8582	0.804610
L	40.2403	29.0619	0.6518	0.9000	0.2281	0.1800	0.8542	0.803493
	40.2492	29.0622	0.6644	0.9000	0.2325	0.1800	0.8011	0.788474
	40.2576	29.0591	0.6779	0.9000	0.2373	0.1800	0.7456	0.772057
	40.2663	29.0533	0.6884	0.9000	0.2409	0.1800	0.7037	0.759186
Panayır Br.	40.2400	29.0600	0.6677	1.2600	0.2337	0.1980	1.0521	0.957580
Balıklı Br.	40.2200	29.0600	0.6658	1.6200	0.2337	0.2520	1.7233	0.957580
Demirtaş Via	40.2800	29.1000	0.6755	0.8800	0.2330	0.3240	2.3909	0.991597

Since segments are formed by subsegments in series, upper and lower bounds for the probability of survival for the segments in 2475 years return period are determined as given is Table 5.23.

Table 5.23 Upper ($\mathbf{P_S'}$) and Lower ($\mathbf{P_S^*}$) Bounds for the Probability of Survival of Each Segment (Subsegments in Series) for 2475 Years Return Period

Segment	**A**	**B**	**C**	**D**	**E**	**F**
$\mathbf{P_S^*}$	0.573857	0.155169	0.135802	0.241474	0.320207	0.315024
$\mathbf{P_S'}$	0.755884	0.756505	0.754304	0.750889	0.749366	0.744787

Segment	**G**	**H**	**I**	**J**	**K**	**L**
$\mathbf{P_S^*}$	0.438850	0.441614	0.389613	0.431719	0.527678	0.371336
$\mathbf{P_S'}$	0.752024	0.755896	0.768608	0.808802	0.804610	0.759186

Paths consist of different segments. Upper and lower bounds of probability of survivals of each segment for 2475 years return period are presented in Table 5.24.

Table 5.24 Upper and Lower Bounds for the Probability of Survival of Each Path (Segments in Series) for 2475 Years Return Period

	Nodes	**Segments**	$\mathbf{P_S^*}$	$\mathbf{P_S'}$
Bursa State Hospital	1-2-10-9-8-7	A-L-K-I-G	0.018256	0.752024
	1-2-10-9-8-6-7	A-L-K-I-H-F	0.010967	0.744787
	1-2-10-9-4-5-6-7	A-L-K-J-D-E-F	0.001123	0.744787
	1-2-10-9-4-5-6-8-7	A-L-K-J-D-E-H-G	0.000691	0.749366
	1-2-3-4-5-6-7	A-B-C-D-E-F	0.000228	0.744787
	1-2-3-4-5-6-8-7	A-B-C-D-E-H-G	0.000140	0.749366
	1-2-3-4-9-8-7	A-B-C-J-I-G	0.000686	0.752024
	1-2-3-4-9-8-6-7	A-B-C-J-I-H-F	0.000217	0.744787
Bursa High Specialty Hospital	1-2-3-4-5	A-B-C-D	0.002263	0.750889
	1-2-3-4-9-8-6-5	A-B-C-J-I-H-E	0.000221	0.749366
	1-2-3-4-9-8-7-6-5	A-B-C-J-I-G-F-E	0.000069	0.744787
	1-2-10-9-4-5	A-L-K-J-D	0.011131	0.750889
	1-2-10-9-8-7-6-5	A-L-K-I-G-F-E	0.001842	0.744787
	1-2-10-9-8-6-5	A-L-K-I-H-E	0.005882	0.749366

Survival probabilities of the paths reaching from the industrial zone to the two hospitals are given in Table 5.25 for 2475 years return period.

Table 5.25 Upper and Lower Reliability Bounds for Reaching from the Industrial Zone to the Hospitals for 2475 Years Return Period (Paths in Parallel)

	P_S^*	P_S'
Bursa State Hospital	0.000140	0.999984
Bursa High Specialty Hospital	0.000069	0.999746

Bounds on the reliability of highway system for reaching from the industrial zone to the hospitals for 2475 years return period are

$$0.999984 \geq P_{S_S} \geq 0.000069$$

$$0.000016 \leq P_{F_S} \leq 0.999931$$

5.6 Reliability of the Highway System Considering the Correlation Among Different Paths

As mentioned earlier an exact determination of system survival (or failure) probability requires extensive numerical integration of multiple integrals. In the previous sections in order to avoid this problem, instead of computing the exact system survival probability (reliability), very simple upper and lower bounds were established. In computing these bounds two extreme assumptions were made with respect to the correlation among paths; namely: perfectly correlated (ρ=1) and completely independent (ρ=0) paths. In reality it is expected that these paths to be partially correlated due to the correlation resulting from the similar construction process and materials used in different segments of the highway and also due to the fact that the whole highway system is subjected to the same earthquake excitation. Besides, since the spatial extent of the area where the highway system is located is rather small, the underlying soil conditions will be highly spatially correlated. Another important source of correlation is the existence of the same segments in different paths. Here this source of correlation is directly taken into consideration as explained in the following.

To evaluate the overall system reliability, reliability indices of the highway system for different return periods can be calculated based on the average correlation coefficient of the system and average reliability indices of the paths by using equation (4.42). In order to calculate average correlation coefficient for the system comprised of alternative paths, a correlation matrix should be established.

Correlation is a statistical tool to describe the degree of relationship between variables. For more than two variables, relationships among all of them should be estimated. In other words, unique correlations between all possible pairs of variables should be identified. For this reason, correlation matrices are used to describe the relationships among all of the variables. Since a variable always perfectly correlated with itself, the numbers on diagonal of a correlation matrix will always be 1. Also, a correlation matrix is always symmetric.

In the light of this information, a correlation matrix for the highway system is constructed showing the degree of correlation among the alternative paths. Since there are common segments in different paths, there exists a certain degree of correlation among all of the paths.

In Table 5.26, relationship between paths and segments are shown. If a path includes the corresponding segment, 1 is assigned to the intersection cell. On the other hand, if a path does not include a segment, 0 is assigned to the intersection cell.

Table 5.26 Relationships Among Alternative Paths and Segments

	A	**B**	**C**	**D**	**E**	**F**	**G**	**H**	**I**	**J**	**K**	**L**
Path 1 (P1)	1	0	0	0	0	0	1	0	1	0	1	1
Path 2 (P2)	1	0	0	0	0	1	0	1	1	0	1	1
Path 3 (P3)	1	0	0	1	1	1	0	0	0	1	1	1
Path 4 (P4)	1	0	0	1	1	0	1	1	0	1	1	1
Path 5 (P5)	1	1	1	1	1	1	0	0	0	0	0	0
Path 6 (P6)	1	1	1	1	1	0	1	1	0	0	0	0
Path 7 (P7)	1	1	1	0	0	0	1	0	1	1	0	0
Path 8 (P8)	1	1	1	0	0	1	0	1	1	1	0	0
Path 9 (P9)	1	1	1	1	0	0	0	0	0	0	0	0
Path 10 (P10)	1	1	1	0	1	0	0	1	1	1	0	0
Path 11 (P11)	1	1	1	0	1	1	1	0	1	1	0	0
Path 12 (P12)	1	0	0	1	0	0	0	0	0	1	1	1
Path 13 (P13)	1	0	0	0	1	1	1	0	1	0	1	1
Path 14 (P14)	1	0	0	0	1	0	0	1	1	0	1	1

There are 12 segments in the system and based on the disaster scenario, 14 different alternative paths are created. After identifying the path and segment relationships, the common segments in the paths are listed in Table 5.27.

Table 5.27 Number of Common Segments in Different Paths

	P1	**P2**	**P3**	**P4**	**P5**	**P6**	**P7**	**P8**	**P9**	**P10**	**P11**	**P12**	**P13**	**P14**
P1	12	4	3	4	1	2	3	2	1	2	3	3	5	4
P2	4	12	4	4	2	2	2	4	1	3	3	3	5	5
P3	3	4	12	6	4	3	2	3	2	3	4	5	5	4
P4	4	4	6	12	3	5	3	3	2	4	4	5	5	5
P5	1	2	4	3	12	5	3	4	4	3	5	2	3	2
P6	2	2	3	5	5	12	4	4	4	5	5	2	3	3
P7	3	2	2	3	3	4	12	5	3	5	6	2	3	2
P8	2	4	3	3	4	4	5	12	3	6	6	2	2	3
P9	1	1	2	2	4	4	3	3	12	3	3	2	1	1
P10	2	3	3	4	3	5	5	6	3	12	6	2	3	4
P11	3	3	4	4	5	5	6	6	3	6	12	2	5	3
P12	3	3	5	5	2	2	2	2	2	2	2	12	3	3
P13	5	5	5	5	3	3	3	2	1	3	5	3	12	5
P14	4	5	4	5	2	3	2	3	1	4	3	3	5	12

Since there are 12 segments in the system, to obtain the correlation coefficients among different paths, values in Table 5.27 are divided by 12. As a result the correlation matrix for the system is obtained as presented in Table 5.28. It is to be noted that this correlation matrix quantifies only the correlation resulting from the existence of common segments in different paths.

Table 5.28 Correlation Matrix for the Highway System

	P1	**P2**	**P3**	**P4**	**P5**	**P6**	**P7**	**P8**	**P9**	**P10**	**P11**	**P12**	**P13**	**P14**
P1	1.00	0.33	0.25	0.33	0.08	0.17	0.25	0.17	0.08	0.17	0.25	0.25	0.42	0.33
P2	0.33	1.00	0.33	0.33	0.17	0.17	0.17	0.33	0.08	0.25	0.25	0.25	0.42	0.42
P3	0.25	0.33	1.00	0.50	0.33	0.25	0.17	0.25	0.17	0.25	0.33	0.42	0.42	0.33
P4	0.33	0.33	0.50	1.00	0.25	0.42	0.25	0.25	0.17	0.33	0.33	0.42	0.42	0.42
P5	0.08	0.17	0.33	0.25	1.00	0.42	0.25	0.33	0.33	0.25	0.42	0.17	0.25	0.17
P6	0.17	0.17	0.25	0.42	0.42	1.00	0.33	0.33	0.33	0.42	0.42	0.17	0.25	0.25
P7	0.25	0.17	0.17	0.25	0.25	0.33	1.00	0.42	0.25	0.42	0.50	0.17	0.25	0.17
P8	0.17	0.33	0.25	0.25	0.33	0.33	0.42	1.00	0.25	0.50	0.50	0.17	0.17	0.25
P9	0.08	0.08	0.17	0.17	0.33	0.33	0.25	0.25	1.00	0.25	0.25	0.17	0.08	0.08
P10	0.17	0.25	0.25	0.33	0.25	0.42	0.42	0.50	0.25	1.00	0.50	0.17	0.25	0.33
P11	0.25	0.25	0.33	0.33	0.42	0.42	0.50	0.50	0.25	0.50	1.00	0.17	0.42	0.25
P12	0.25	0.25	0.42	0.42	0.17	0.17	0.17	0.17	0.17	0.17	0.17	1.00	0.25	0.25
P13	0.42	0.42	0.42	0.42	0.25	0.25	0.25	0.17	0.08	0.25	0.42	0.25	1.00	0.42
P14	0.33	0.42	0.33	0.42	0.17	0.25	0.17	0.25	0.08	0.33	0.25	0.25	0.42	1.00

From equation (4.42), the average correlation coefficient for the different paths of the system is calculated as

$$\bar{\rho} = 0.28$$

To calculate a reliability index for the highway system, maximum and minimum reliability indices of each path, β_e are taken into consideration for different return periods. By using average correlation coefficient and reliability indices calculated for each path, system reliability for different return periods are calculated from equation (4.42) as displayed in Tables 5.29 and 5.30.

Table 5.29 Minimum Reliability Indices and the Corresponding Survival Probabilities for the Highway System Obtained for Different Return Periods Based on Partial Correlation Among the Paths ($\bar{\rho}$ = 0.28)

	75 years	**475 years**	**1000 years**	**2475 years**
Min β_S	**5.3730**	**3.0373**	**2.0403**	**0.9225**
Min P_{S_S}	≈1.000000	0.998806	0.979342	0.821863
Max P_{F_S}	3.87×10^{-8}	0.001194	0.020658	0.178137

Table 5.30 Maximum Reliability Indices and the Corresponding Survival Probabilities for the Highway System Obtained for Different Return Periods Based on Partial Correlation Among the Paths ($\bar{\rho}$ = 0.28)

	75 years	**475 years**	**1000 years**	**2475 years**
Max β_S	**6.8414**	**4.9318**	**4.2685**	**3.3509**
Max P_{S_S}	≈1.000000	0.999999	0.999990	0.999597
Min P_{F_S}	3.92×10^{-12}	4.67×10^{-7}	0.000010	0.000403

5.7 Combination of the Different Failure Modes in Evaluating the Overall Reliability of the Transportation Lifeline System

The main failure modes to be considered in the evaluation of the reliability of highways and roads subjected to earthquake loads are the failure of the road segments by fault rupture named as the "fault crossing" failure mode and the embankment failure mode. For bridges and the viaduct only one failure mode is considered; namely failure of the pier columns. In reflecting the effect of these failure modes to the reliability of the highway system, it is assumed that the bridges and the viaduct are quantified in a combined way and in terms of the system reliability values computed in sections 5.5 and 5.6. For this "combined failure modes", the upper bound system failure probabilities given in Tables 5.29 and 5.30 for $\bar{\rho}$ = 0.28 corresponding to 1000 years return period are selected. Taking into account this combined failure modes together with the fault crossing failure mode, the overall failure probability of this transportation lifeline system is calculated based on the theorem of total probability as follows:

P_T (Failure / T = t) = P (Failure | Rupture of Demirtaş Fault)

x P (Rupture of Demirtaş Fault in t years)

+ $P_{\text{upper bound}}$ (Failure of highways and roads due to embankment failure and/or Failure of bridges due to failure of pier columns | PGA $\geq y_{1000}$)

x P (PGA $\geq y_{1000}$ in t years)

For economical lifetimes of T = 50 and 75 years, the corresponding highway system failure probabilities are computed from the above expression, respectively as:

P_{50} (Failure / T = 50) = 1.0 x 0.0488 + 0.0207 x 0.0488 = 0.0488 + 0.0010 = 0.0498 $\simeq$ 0.050

P_{75} (Failure / T = 75) = 1.0 x 0.0723 + 0.0207 x 0.0723 = 0.0723 + 0.0015 = 0.0738 $\simeq$ 0.075

As observed from these computations, the reliability of the lifeline transportation system considered in the case study is approximately 95% and 92.5%, respectively, for economic lifetimes of 50 and 75 years if designed for a PGA level having a 1000 year return period. The dominant mode of failure is expected to be the fault crossing mode resulting from the rupturing of the Demirtaş Fault. The contribution of this mode of failure to the highway system failure is expected to be almost 50 times more than the combined contribution of other failure modes.

5.8 Sensitivity of the Lower Bound Reliability Value of the Transportation Lifeline Systems to the Length of Subsegments

In the previous sections, reliability bounds of the transportation lifeline system are established based on the reliability of subsegments which are obtained by dividing each segment into subsegments of 1 km unit length. In the case study, due to the fact

that both seismic capacity and seismic demand are almost the same for each subsegment, the upper bound reliability of the transportation lifeline system does not change with the change of the length of subsegments since the minimum probability of survival value is taken as the upper bound system reliability. On the other hand, the lower bound reliability of the transportation lifeline system depends on the number of subsegments since lower bound system reliability is obtained by taking the products of reliabilities of subsegments.

To check the sensitivity of the lower bound system reliability to this effect, the length of each subsegment is increased to 2 km. Because the segment lengths are short in this study, longer subsegmentation is not feasible for this case. The calculations are repeated for 1000 year return period to examine the variation in lower bound system reliability by taking the subsegment length equal to 2 km.

In Table 5.31, PGA's corresponding to 1000 years return period for each subsegment of 2 km length and bridges are given as well as the resistances, reliability indices and probabilities of survival.

Table 5.31 PGA Values Obtained for the Midpoints of Road Subsegments and Bridges for 1000 Years Return Period (RP), Resistance Values in Terms of PGA, β and Probability of Survival for Subsegments and Bridges (Subsegment Length=2km)

Segment Name	Latitude	Longitude	Loads PGA (g) RP =1000 years	Resistances PGA (g)	σ_S	σ_R	β	P_S
A	40.2662	29.0600	0.5164	0.9000	0.1805	0.1800	1.5076	0.934171
B	40.2713	29.0510	0.5159	0.9000	0.1806	0.1800	1.5065	0.934026
	40.2830	29.0605	0.5130	0.9000	0.1790	0.1800	1.5304	0.937037
	40.2832	29.0842	0.5092	0.9000	0.1781	0.1800	1.5450	0.938826
C	40.2811	29.1018	0.5083	0.9000	0.1779	0.1800	1.5476	0.939136
	40.2721	29.1074	0.5147	0.9000	0.1811	0.1800	1.4985	0.932999
	40.2568	29.0959	0.5146	0.9000	0.1793	0.1800	1.5258	0.936471
	40.2395	29.0911	0.5032	0.9000	0.1751	0.1800	1.5910	0.944195
D	40.2248	29.0899	0.4984	0.9000	0.1745	0.1800	1.6020	0.945418
	40.2217	29.1077	0.5032	0.9000	0.1767	0.1800	1.5665	0.941383
	40.2099	29.1202	0.5123	0.9000	0.1805	0.1800	1.5075	0.934164
E	40.1980	29.1168	0.5254	0.9000	0.1839	0.1800	1.4558	0.927277
	40.1961	29.0989	0.5236	0.9000	0.1828	0.1800	1.4721	0.929506
F	40.1931	29.0823	0.5210	0.9000	0.1825	0.1800	1.4769	0.930152
	40.1885	29.0654	0.5229	0.9000	0.1826	0.1800	1.4750	0.929894
G	40.1900	29.0467	0.5190	0.9000	0.1816	0.1800	1.4912	0.932039
	40.1964	29.0561	0.5154	0.9000	0.1802	0.1800	1.5118	0.934701
H	40.1963	29.0678	0.5163	0.9000	0.1811	0.1800	1.4983	0.932971
I	40.1958	29.0721	0.5174	0.9000	0.1800	0.1800	1.5156	0.935188
	40.2097	29.0604	0.5051	0.9000	0.1758	0.1800	1.5811	0.943068
J	40.2219	29.0616	0.4983	0.9000	0.1744	0.1800	1.6033	0.945571
	40.2252	29.0754	0.4978	0.9000	0.1743	0.1800	1.6052	0.945773
K	40.2237	29.0752	0.4982	0.9000	0.1743	0.1800	1.6043	0.945675
	40.2354	29.0617	0.4988	0.9000	0.1751	0.1800	1.5923	0.944338
L	40.2448	29.0620	0.5034	0.9000	0.1772	0.1800	1.5590	0.940506
	40.2619	29.0562	0.5138	0.9000	0.1805	0.1800	1.5076	0.934171
Panayır Br.	40.2400	29.0600	0.5003	1.2600	0.1751	0.2520	2.4757	0.993352
Balıklı Br.	40.2200	29.0600	0.4990	1.6200	0.1746	0.3240	3.0456	0.998839
Demirtaş Via	40.2800	29.1000	0.5098	0.8800	0.1784	0.1320	1.6682	0.952357

Since segments are formed by subsegments in series, upper and lower bounds for the probability of survival for the segments in 1000 years return period are determined as given is Table 5.32.

Table 5.32 Upper ($\mathbf{P_S'}$) and Lower ($\mathbf{P_S^*}$) Bounds for the Probability of Survival of Each Segment (Subsegments in Series) for 1000 Years Return Period (Subsegment Length = 2 km)

Segment	A	B	C	D	E	F
$\mathbf{P_S^*}$	0.934171	0.821677	0.774758	0.831407	0.861910	0.864943
$\mathbf{P_S'}$	0.934171	0.934026	0.932999	0.934164	0.927277	0.929894

Segment	G	H	I	J	K	L
$\mathbf{P_S^*}$	0.871178	0.932971	0.881946	0.894296	0.893037	0.878594
$\mathbf{P_S'}$	0.932039	0.932971	0.935188	0.945571	0.944338	0.934171

Paths consist of different segments. Upper and lower bounds of probability of survival of each path for 1000 years return period are presented in Table 5.33

Table 5.33 Upper and Lower Bounds for the Probability of Survival of Each Path (Segments in Series) for 1000 Years Return Period (Subsegment Length = 2 km)

	Nodes	Segments	$\mathbf{P_S^*}$	$\mathbf{P_S^{'}}$
Bursa State Hospital	1-2-10-9-8-7	A-L-K-I-G	0.558768	0.932039
	1-2-10-9-8-6-7	A-L-K-I-H-F	0.579577	0.928328
	1-2-10-9-4-5-6-7	A-L-K-J-D-E-F	0.403113	0.927277
	1-2-10-9-4-5-6-8-7	A-L-K-J-D-E-H-G	0.378804	0.927277
	1-2-3-4-5-6-7	A-B-C-D-E-F	0.351040	0.927277
	1-2-3-4-5-6-8-7	A-B-C-D-E-H-G	0.329871	0.927277
	1-2-3-4-9-8-7	A-B-C-J-I-G	0.388704	0.932039
	1-2-3-4-9-8-6-7	A-B-C-J-I-H-F	0.360054	0.928328
Bursa High Specialty Hospital	1-2-3-4-5	A-B-C-D	0.470876	0.927321
	1-2-3-4-9-8-6-5	A-B-C-J-I-H-E	0.358791	0.927277
	1-2-3-4-9-8-7-6-5	A-B-C-J-I-G-F-E	0.289780	0.927277
	1-2-10-9-4-5	A-L-K-J-D	0.540727	0.927321
	1-2-10-9-8-7-6-5	A-L-K-I-G-F-E	0.416563	0.927277
	1-2-10-9-8-6-5	A-L-K-I-H-E	0.515768	0.927277

Survival probabilities of the paths reaching from the industrial zone to the two hospitals are given in Table 5.34 for 1000 years return period.

Table 5.34 Upper and Lower Reliability Bounds for Reaching from the Industrial Zone to the Hospitals for 1000 Years Return Period (Paths in Parallel) (Subsegment Length = 2 km)

	P_S^*	P_S'
Bursa State Hospital	0.329871	0.999999
Bursa High Specialty Hospital	0.289780	0.999998

Bounds on the reliability of highway system for reaching from the industrial zone to the hospitals for 1000 years return period with the 2 km subsegment lengths are

$$0.999999 \geq P_{S_S} \geq 0.289780$$

$$1.24\text{x}10^{-7} \leq P_{F_S} \leq 0.710220$$

In Table 5.35, upper and lower bound system reliability values are presented for 1000 years return period for subsegment lengths of 1 km and 2 km, for comparison purpose.

Table 5.35 Comparison of Upper and Lower Bound System Reliabilities with Different Subsegment Lengths for Reaching from the Industrial Zone to the Hospitals for 1000 Years Return Period

Probabilities of Survival RP =1000 years	**Subsegment Length = 1 km**	**Subsegment Length = 2 km**
Upper Bound	≈0.999999	≈0.999999
Lower Bound	0.089672	0.289780

As observed from Table 5.35, the upper bound system reliability is practically the same for subsegment lengths of 1 km and 2 km, but the difference in the lower bound is almost more than 3 times which is quite significant. Reliability of the system is higher when subsegment length is increased.

Combination of different failure modes is not considered in this comparison.

5.9 Evaluation of the Damage State of the Highway System Using the Damage Probability Matrices

The Damage Probability Matrix (DPM) is an alternative way to express the damage states of the structures. DPM's are used to state the discrete probabilities for certain damage states. There are a number of DPM's derived for different structure types by many researchers in the literature. In this study, to correlate the system reliability with the appropriate damage state the DPM's are utilized. DPM's reflect the correlation between intensity, generally Modified Mercalli Intensity (MMI), and the damage states. Accordingly, here it is necessary to convert the average PGA values affecting the highway system to MMI. The average PGA values corresponding to different return periods, as obtained earlier, are given in Table 5.36 below.

Table 5.36 The Average PGA Values (in g) Affecting the Highway System as Computed for Different Return Periods

75 years	475 years	1000 years	2475 years
0.1688	0.3913	0.5105	0.6739

A number of conversion equations were developed by different researchers, some of which are shown in Table 5.37. Averaging over these conversion equations the MMI values corresponding to the average PGA's shown in Table 5.36 are calculated and listed in Table 5.37.

Table 5.37 MMI Values Corresponding to the Average PGA Values Affecting the Highway System as Computed for Different Return Periods

Reference	75 years	475 years	1000 years	2475 years
Bilal and Askan (2014)	8.33	9.65	10.07	10.51
Arıoğlu et al. (2001)	7.85	9.32	9.79	10.27
Tselentis and Danciu (2008)	6.96	8.26	8.67	9.10
Faenza and Michelini (2010)	7.41	8.35	8.64	8.96
Murphy and O'Brien (1977)	7.88	9.34	9.80	10.28
Trifunac and Brady (1975)	6.93	8.15	8.53	8.93
Wald et al. (1999)	6.46	7.80	8.22	8.66
Average MMI	**7.40**	**8.69**	**9.10**	**9.53**
Approximated as	**MMI=VII**	**MMI=VIII**	**MMI=IX**	**MMI=X**

The average MMI values shown in Table 5.37 are used to evaluate damage state for the system by utilizing DPM's. In assessing the earthquake insurance rate for Gumusova-Gerede motorway, Yucemen et al. (2008) obtained a best estimate DPM for viaducts and highways based on expert opinion and based on the reports of Applied Technology Council (ATC) namely: ATC-13 and ATC-25. Best estimate values are based on these DPM's in terms of mean damage ratio (MDR). MDR expresses the average damage ratio for a given structure subjected to earthquake of a specified intensity level.

Best estimate MDR values derived by Yücemen et al. (2008) for different highway system components are presented in Table 5.38.

Table 5.38 ''Best Estimate'' Mean Damage Ratio (MDR) Values (%) for Different Transportation System Components (Yücemen et al.,2008)

Structure Type	MMI = V	MMI = VI	MMI = VII	MMI = VIII	MMI = IX
Viaducts	0	0.0021	0.146	1.023	10.19
Tunnel	0	0.10	0.325	1.16	5.20
Cut and Cover	0	0	0.19	1.22	5.72
"Other" Structures	0	0.02	0.25	1.30	6.03

Corresponding MDR values are determined from Table 5.38 for viaducts and cut and cover (embankments) by using average MMI values which take place in Table 5.37.

Damage ratios corresponding to different damage states for the highway system components are given in Table 5.39. This table is presented in HAZUS Technical Manual (2003) and developed by the U.S. Department of Homeland Security Emergency Preparedness & Response Directorate. Here, the values given in table are used to determine damage states of the highways system components involved in the case study.

Table 5.39 Best Estimate Damage Ratios and the Corresponding Damage States for Highway System Components (from HAZUS Technical Manual, 2003)

Classification	Damage State	Best Estimate Damage Ratio	Range of Damage Ratios
Roadways	slight moderate extensive/ complete	0.05 0.20 0.70	0.01 to 0.15 0.15 to 0.4 0.4 to 1.0
Tunnel's Lining	slight moderate extensive complete	0.01 0.30 0.70 1.00	0.01 to 0.15 0.15 to 0.4 0.4 to 0.8 0.8 to 1.0
Bridges	slight moderate extensive complete	0.03 0.08 0.25 1.00	0.01 to 0.03 0.02 to 0.15 0.10 to 0.40 0.30 to 1.00

Based on Tables 5.38 and 5.39, it can be concluded that for return periods of 75 and 475 years, damage state for roads and bridges are “slight”. On the other hand, for a return period of 1000 years, damage state of the bridges is “extensive”, whereas damage state of roads and highways is rated as “slight”. For 2475 years return period, MMI is approximated as X. Although MDR values are not given for MMI =X in Table 5.38, it is estimated based on extrapolation that for 2475 years return period, damage on the roads and highways will be “moderate” and damage on the bridges will be “extensive”.

In Section 5.5, reliabilities of highway system components in the case study are calculated based on classical reliability approach for different return periods. It is observed that bridges are more reliable than the roads and highways. Although resistance of the Demirtaş Viaduct is lower than the resistances of roads and highways, probability of survival is higher due to the smaller coefficient of variation, reflecting better quality control in the viaduct. However, in damage state estimations, it is observed that bridges are more vulnerable under earthquake loads. If DPM's are used to estimate system reliability of the transportation lifeline, then the probabilities of survival will be close to the lower bound which is a conservative estimate.

CHAPTER 6

SUMMARY AND CONCLUSIONS

6.1 Summary

The main objective of this study is to investigate the system reliability of lifelines subjected to earthquake loads within the context of transportation lifeline systems. Although in the explanation of the methodology and in the case study only transportation lifeline systems consisting of viaducts, bridges, roads and highways are considered, the methodology presented here can be applied to other lifeline network systems. After a major earthquake it is extremely important that transportation lifeline systems are operative so that an effective management of post-disaster operations is possible without any interruption. This is the main reason why transportation lifeline systems are selected as the main theme.

Evaluation of the seismic reliability of a lifeline system requires firstly the assessment of the seismic hazard at the region where the lifeline is located. Considering the various sources of uncertainties, epistemic and aleatory in nature, the seismic hazard analysis is carried out based on probabilistic methods. The concepts and main steps of the probabilistic seismic hazard analysis are explained in detail in the thesis.

The second main input in the evaluation of the seismic reliability of a lifeline system is the tools of reliability. In this thesis the basic concepts of structural reliability, namely: parallel and series systems, failure and survival probabilities, fundamental inequalities of reliability, reliability index, correlation among components are applied

to the lifeline systems in computing the reliability of the components and the overall system reliability of a transportation lifeline system. Again the methodology implemented and the main concepts are covered in detail.

The third main input involves the assessment of the vulnerability of the components of the highway system. In this respect, component reliability is calculated by assessing the seismic capacity and demand of the associated element. Both seismic capacity and demand are quantified in terms of PGA. Highway system elements may fail due to different causes. Seismic capacity of the elements in a highway system can be determined based on analyses as well as by using available fragility curves for the elements. For bridges and the viaduct, the most critical failure mechanism due to earthquake loads is the failure of pier columns. For roads and highways, there are two failure modes namely, fault crossing and embankment failure.

In order to illustrate the reliability analysis of highway systems subjected to earthquake loads, a case study is presented. In this case study, a region is selected in Bursa Province. A disaster scenario is constituted in which the aim is to reach one of the two major city hospitals (sinks) from the industrial zone (source) after the occurrence of a major earthquake. A proper highway system is designated and alternative paths (arcs) are generated. On this basis, firstly, a multisite probabilistic seismic hazard analysis is performed for the region to determine the seismic loads due to expected earthquakes. Then, resistances of the system components are evaluated. Based on loads and resistances, firstly reliability of each component is obtained and then system reliability is determined for 75, 475, 1000 and 2475 years return periods by constructing upper and lower bounds of the system survival probability for series and parallel systems. At the final stage, correlation among the different transportation paths is taken into consideration and reliability indices for the overall system are determined with the help of the correlation matrix derived for the system. Damage probability matrices are used to evaluate the level of expected damage to the highway system components, with respect to the different return periods.

The system reliability values computed for the transportation lifeline system considered in the case study under different assumptions and for different return

periods are summarized in Table 6.1. It is appropriate to base the reliability of this highway network system for a 1000 year return period earthquake. In this case, the system reliability lies between 0.089672 and almost 1.0, corresponding to $\rho = 0$ and $\rho = 1.0$, respectively, for both segments and paths. On the other hand, for partial correlation among the paths, which is more representative of the actual condition and quantified by $\bar{\rho} = 0.28$, the lower and upper bounds of the system reliability is obtained as 0.979342 and 0.999990, respectively. It is to be emphasized that $\bar{\rho} = 0.28$ is applied only with respect to correlation among the paths, but in computing the bounds on the reliability of segments forming the paths, still it is assumed that $\rho = 0$ and $\rho = 1.0$. This is the reason why we have upper and lower bounds for system reliability also in the case where correlation coefficient is single valued and specified as $\bar{\rho} = 0.28$.

Table 6.1 The System Reliability Values Computed for the Transportation Lifeline System Considered in the Case Study Under Different Assumptions for Different Return Periods

Return Period	Completely Independent ($\rho = 0$)	Partially Correlated ($\rho = 0.28$)		Perfectly Correlated ($\rho = 1$)
	Lower Bound	Lower Bound	Upper Bound	Upper Bound
75 years	0.997954	≈1.000000*	≈1.000000*	≈1.000000*
475 years	0.637333	0.998806	0.999999	≈1.000000
1000 years	0.089672	0.979342	0.999990	0.999999
2475 years	0.000069	0.821863	0.999597	0.999931

*For corresponding probabilities of failure, see Sections 5.5 and 5.6

6.2 Conclusions

The main conclusions and contributions of the study can be listed as follows:

An original contribution of the study is the implementation of the basic concepts and methods of structural reliability to evaluate the reliability of a transportation network system subjected to earthquake excitation. Another original contribution is the consideration of the correlation among different transportation paths by a simple

procedure based on upper and lower bounds of the system reliability (fundamental inequalities of reliability). Also a convenient method is developed to obtain the correlation matrix among the different paths connecting the source to sinks based on the existence of common segments. A representative average correlation coefficient is obtained from this correlation matrix and the reliability indices for the system is computed based on this correlation coefficient. This way a more realistic result for the system reliability is acquired, since this correlation coefficient is more likely than the values 0 and 1 imposed in forming the lower and upper bound reliability values.

With respect to the case study presented in the thesis the following comments can be made:

System reliability due to fault crossing depends on the probability of rupturing of the Demirtaş Fault. If this fault ruptures, since it crosses both alternative paths (involving segments C and L) connecting the industrial zone to the two hospitals, there will be no connectivity left; hence probability of survival of the system equals to zero which means failure of the whole system. After fault rupture, it is quite hard to respond to the bridge (Panayır and Balıklı Bridges and Demirtaş Viaduct) failures. However, roads and highways can be repaired in a shorter time.

With respect to embankment and pier column failures, reliability of the highway components is rather high; accordingly the upper bound system reliability is also high.

Lower bound system reliability estimations are quite low since the products of the survival probabilities of the subsegments are taken into consideration. Accordingly, lower bound system reliability is dependent on the number of subsegments. Lower bound system reliability increases significantly as the length of subsegments increases. On the other hand, since there are fourteen alternative paths in the highway system, it is a highly redundant transportation lifeline. Accordingly the upper bound probability of survival is close to 1.0.

Besides the mean values of resistances, the uncertainties involved (quantified in terms of variances and/or coefficients of variation) also affect the reliabilities of components. This is observed especially in the in the assessment of the reliability of bridges and the viaduct.

Reliabilities of the paths are governed by the reliability of roads and highways since bridges are more reliable than the roads and highways.

As a result of combination of failure modes, the reliability of the lifeline transportation system considered in the case study is approximately 95% and 92.5%, respectively, for economic lifetimes of 50 and 75 years if designed for a PGA level having a 1000 year return period. The dominant mode of failure is the fault crossing mode resulting from the rupturing of the Demirtaş Fault. The contribution of this mode of failure to the highway system failure is expected to be almost 50 times more than the combined contribution of other failure modes.

It is also observed that as the return period increases the range of the bounds (i.e. difference between upper and lower bounds) increases as expected.

Based on the DPM's considered in the study for a return period of 1000 years, the damage state of bridges is expected to be extensive (MDR ≈ 0.25), whereas damage state of roads and highways is estimated as slight (MDR ≈ 0.05).

6.3 Future Work and Recommendations

The main topics of the future work that can be conducted related to this thesis are as follows:

It is desirable to use more realistic resistance values for the components and these should be consistent with the seismic response of the different components. Also more failure modes can be considered.

Correlation resulting from similar material, construction procedure, soil conditions as well as excitation due to the same earthquake should also be quantified. In this respect the spatial correlation proportional to the distance between subsegments and components should be taken into consideration.

Lower bound of system survival probability is sensitive to the partitioning of the segments involved. A more comprehensive sensitivity study may be conducted with respect to the lengths of the subsegments, i.e. number of subsegments. In selecting

the length of subsegments, the concepts of spatial correlation and scale of fluctuation can be utilized.

The probabilistic seismic hazard analysis can be performed for the region by using alternative stochastic models, like the renewal model and regional and up-to-date GMPE's. Also near fault effects can be considered consistent with the existence of active faults crossing the transportation lifeline system.

REFERENCES

Abrahamson, N. A., & Bommer, J. J. (2005). Probability and Uncertainty in Seismic Hazard Analysis. *Earthquake Spectra, 21*(2), 603-607.

Abrahamson, N. A., and W. J. Silva (2008), Summary of the Abrahamson & Silva NGA Ground-Motion Relations, *Earthquake Spectra, 24*(1), 67-97.

Abrahamson, N.A. (2006). Notes on Probabilistic Seismic Hazard Analysis – An Overview. *Rose School, Pavia, Italy.*

Adlinge, S. S., & Gupta, A. K. (2013). Pavement Deterioration and its Causes. *International Journal of Innovative Research and Development*, *2*(4), 437-450.

Aki, K. (1966). Generation and Propagation of G Waves from the Niigata Earthquake of June 16, 1964: Part 1. A statistical analysis.

Arıoğlu, E., Arıoğlu, B. M., & Girgin, C. (2001). Doğu Marmara Depreminin Yer İvme Değerleri Açısından Değerlendirilmesi. *Beton Prefabrikasyon*, *57*(58), 5-15.

Avsar, O., Caner, A., & Yakut, A. (2008). Effect of Cap Beam to Column Inertia Ratio on Transverse Seismic Response of Multi Column Bridge Bents. *In Proceedings of the 14th world conference on earthquake engineering* (pp. 12-17).

Bea, R. G. (1983). Characterization of the reliability of offshore piles subjected to axial loadings. In *Session ST-12, Bias and Uncertainty in Loadings and Resistance of Offshore Structures, American Society of Civil Engineers (ASCE) Structural Congres, Houston, TX*.

Bilal, M., & Askan, A. (2014). Relationships between Felt Intensity and Recorded Ground-Motion Parameters for Turkey. *Bulletin of the Seismological Society of America, 104*, 484-486.

Boore, D. M., Joyner, W. B., & Fumal, T. E. (1997). Equations for Estimating Horizontal Response Spectra and Peak Acceleration from Western North American Earthquakes: A Summary of Recent Work. *Seismological Research Letters*, *68*(1), 128-153.

Chang, K. C., Chang, D. W., Tsai, M. H., & Sung, Y. C. (2000). Seismic Performance of Highway Bridges. *Earthquake Engineering and Engineering Seismology*, *2*(1), 55-77.

Cornell, C. A. (1968). Engineering Seismic Risk Analysis. *Bulletin of the Seismological Society of America*, *58*(5), 1583-1606.

Cornell, C. A. (1969). A Normative Second Moment Reliability Theory for Structural Design: Seminar No. 6, December 15, 1969. Solid Mechanics Division, University of Waterloo.

Cornell, C. A., & Winterstein, S. R. (1988). Temporal and Magnitude Dependence in Earthquake Recurrence Models. *Bulletin of the Seismological Society of America*, *78*(4), 1522-1537.

Deniz, A., & Yucemen, M. S. (2010). Magnitude Conversion Problem for the Turkish Earthquake Data. *Natural hazards*, *55*(2), 333-352.

Erentöz, C. and Kurtman, F. (1964). Report on 1964 Manyas Earthquake, *Bulletin of the Mineral Research and Exploration Institute of Turkey. 63(1), 1-5.*

Esmaeily, A. (2008). USC_RC Version 1.0.2. Civil Engineering Department of University of Southern California.

Faenza, L., & Michelini, A. (2010). Regression Analysis of MCS Intensity and Ground Motion Parameters in Italy and its Application in Shake Map. *Geophysical Journal International*, *180*(3), 1138-1152.

Fırat, F.K. and Yücemen, M.S. (2015), Comparison of Loads in Turkish Earthquake code with Those Computed Statistically. *Earthquakes and Structures*, Vol.8, No.5, pp.977-994.

Gok, E., & Polat, O. (2012). An Assessment of the Seismicity of the Bursa Region from a Temporary Seismic Network. *Pure and Applied Geophysics*, *169*(4), 659-675.

Grigoriu, M., & Turkstra, C. (1979). Safety of Structural Systems with Correlated Resistances. *Applied Mathematical Modelling*, *3*(2), 130-136.

Gutenberg, B., & Richter, C. (1954). *Seismicity of the Earth and Associated Phenomena*. Princeton University Press.

Gutenberg, B., & Richter, C. F. (1944). Frequency of Earthquakes in California. *Bulletin of the Seismological Society of America*, *34*(4), 185-188.

Gülerce, Z., Kargioglu, B., & Abrahamson, N. A. (2015). Turkey-Adjusted NGA-W1 Horizontal Ground Motion Prediction Models. *Earthquake Spectra*. (In Press)

Han, Q., Du, X., Liu, J., Li, Z., Li, L., & Zhao, J. (2009). Seismic Damage of Highway Bridges During the 2008 Wenchuan Earthquake. *Earthquake Engineering and Engineering Vibration*, *8*(2), 263-273.

Hanks, T. C., & Kanamori, H. (1979). A Moment Magnitude Scale. *Journal of Geophysical Research B*, *84*(B5), 2348-2350.

Hasofer, A. M., & Lind, N. C. (1974). Exact and Invariant Second-Moment Code Format. *Journal of the Engineering Mechanics division*, *100*(1), 111-121.

HAZUS Technical Manual (2003). *Multi-Hazard Loss Estimation Methodology: Earthquake Model.* Department of Homeland Security, FEMA, Washington, DC.

Hsu, Y. T., & Fu, C. C. (2004). Seismic Effect on Highway Bridges in Chi Chi Earthquake. *Journal of Performance of Constructed Facilities*, *18*(1), 47-53.

Jara, J. M., Reynoso, J. R., Olmos, B. A., & Jara, M. (2015). Expected Seismic Performance of Irregular Medium-Span Simply Supported Bridges on Soft and Hard Soils. *Engineering Structures*, *98*, 174-185.

Kalkan, E., & Gulkan, P. (2004). Site-Dependent Spectra Derived from Ground Motion Records in Turkey. *Earthquake Spectra*, *20*(4), 1111-1138.

Kawashima, K., & Unjoh, S. (1997). The Damage of Highway Bridges in the 1995 Hyogo-Ken Nanbu Earthquake and Its Impact on Japanese Seismic Design. *Journal of Earthquake Engineering*, *1*(03), 505-541.

Lallemant, D., Kiremidjian, A., & Burton, H. (2015). Statistical Procedures for Developing Earthquake Damage Fragility Curves. *Earthquake Engineering & Structural Dynamics*, *44(9)*, 1373-1389.

LARSA Inc. (2014). *LARSA 4D User's Manual*, Version 7.07, New York

Liu, W. D., Neuenhoffer, A., Ghosn, M., & Moses, F. (2001). *Redundancy in Highway Bridge Substructures.* National Cooperative Highway Research Program. NCHRP Report 458, Transportation Research Board, National Academy Press, Washington DC.

MCEER Highway Project 094 (2000). *Seismic Vulnerability of the Highway System.* FHWA Contract DTFH61-98-C-00094.

Mohseni, M. (2012). *Dynamic Vulnerability Assessment of Highway and Railway Bridges.* University of Nebraska-Lincoln, PhD Dissertation.

Monteiro, R., Delgado, R., & Pinho, R. (2015). Probabilistic Seismic Assessment of RC Bridges: Part I—Uncertainty Models. In *Structures*, 5, 258-273

Murphy, J. U., & O'brien, L. J. (1977). The Correlation of Peak Ground Acceleration Amplitude with Seismic Intensity and Other Physical Parameters. *Bulletin of the Seismological Society of America*, *67*(3), 877-915.

Nowak, A. S. (1999). *Calibration of LRFD Bridge Design Code*. National Cooperative Highway Research Program. NCHRP Report 368, Transportation Research Board, National Academy Press, Washington DC.

Nowak, A. S., & Collins, K. R. (2012). *Reliability of Structures.* CRC Press.

O'Rourke, T. D. (1998). An Overview of Geotechnical and Lifeline Earthquake Engineering. In *Geotechnical Earthquake Engineering and Soil Dynamics*, 1392-1426).

O'Rourke, T. D., & Jeon, S. S. (2000). Seismic Zonation for Lifelines and Utilities. In *Proceedings of The Sixth International Conference on Seismic Zonation. Palm Springs, CA.*

Polat, O. (1997). Estimation of the Source Parameters from the Earthquake Records of Bursa Acceleration Network (BUSNET), *Jeofizik*,11 (1-2), 65-79.

Reid, H. F. (1911). *The Elastic-Rebound Theory of Earthquakes*. University Press.

Reiter, L. (1991). *Earthquake Hazard Analysis: Issues and Insights*. Columbia University Press.

Risk Engineering Inc. (2011). *EZ-FRISK: 2005, User's Manual*, Version 7.52, Colorado

Schwartz, D. P., & Coppersmith, K. J. (1984). Fault Behavior and Characteristic Earthquakes: Examples from the Wasatch and San Andreas Fault Zones. *Journal of Geophysical Research: Solid Earth (1978–2012)*, *89*(B7), 5681-5698.

Selcuk-Kestel, A. S., Duzgun, H. S., & Oduncuoglu, L. (2012). A GIS-Based Software for Lifeline Reliability Analysis under Seismic Hazard. *Computers & Geosciences*, *42*, 37-46.

SYNER-G Project Report. (2011). Systemic Seismic Vulnerability and Risk Analysis for Buildings, Lifeline Networks and Infrastructures Safety Gain. Project No 244061. European Community's Seventh Framework Program (FP7/2007-2013)

Thenhaus, P. C., & Campbell, K. W. (2003). Seismic Hazard Analysis. *Earthquake Engineering Handbook*, *8*, 1-50.

Topal, T., Doyuran, V., Karahanoğlu, N., Toprak, V., Süzen, M. L., & Yeşilnacar, E. (2003). Microzonation for Earthquake Hazards: Yenişehir Settlement, Bursa, Turkey. *Engineering Geology*, *70*(1), 93-108.

Trifunac, M. D., & Brady, A. G. (1975). On the Correlation of Seismic Intensity Scales with the Peaks of Recorded Strong Ground Motion. *Bulletin Of The Seismological Society of America*, *65*(1), 139-162.

Tselentis, G. A., & Danciu, L. (2008). Empirical Relationships Between Modified Mercalli Intensity and Engineering Ground-Motion Parameters in Greece. *Bulletin of The Seismological Society of America*, *98*(4), 1863-1875.

Wald, D. J., Quitoriano, V., Heaton, T. H., & Kanamori, H. (1999). Relationships Between Peak Ground Acceleration, Peak Ground Velocity, and Modified Mercalli Intensity in California. *Earthquake Spectra*, *15*(3), 557-564.

Wardhana, K., & Hadipriono, F. C. (2003). Analysis of Recent Bridge Failures in the United States. *Journal of Performance of Constructed Facilities*, *17*(3), 144-150.

Weichert, D. H. (1980). Estimation of the Earthquake Recurrence Parameters for Unequal Observation Periods for Different Magnitudes. *Bulletin of the Seismological Society of America*, *70*(4), 1337-1346.

Yılmaz-Öztürk, N. (2008). *Probabilistic Seismic Hazard Analysis: A Sensitivity Study with Respect to Different Models*. Middle East Technical University, PhD Dissertation.

Yilmaz, S. A. (2014). *Reliability Based Evaluation of Seismic Design of Turkish Bridges by Using Load and Resistance Factor Method*. Middle East Technical University, Master Dissertation.

Yilmaz, T., & Caner, A. (2012). Target Damage Level Assessment for Seismic Performance Evaluation of Two-Column Reinforced Concrete Bridge Bents. *Bridge Structures-Assessment, Design & Construction*, *8*, 3-4.

Youngs, R. R., & Coppersmith, K. J. (1985). Implications of Fault Slip Rates and Earthquake Recurrence Models to Probabilistic Seismic Hazard Estimates. *Bulletin of the Seismological society of America*, *75*(4), 939-964.

Yücemen, M. S., Kocyigit, A., Yakut, A., & Gencoglu, S. (2006). *Guidelines for the Development of Seismic Hazard Maps*. Technical Report Prepared for General Directorate of Disaster Affairs, Ankara.

Yücemen, M. S., Yilmaz, C., & Erdik, M. (2008). Probabilistic Assessment of Earthquake Insurance Rates for Important Structures: Application to Gumusova–Gerede Motorway. *Structural Safety*, *30*(5), 420-435.

Yücemen, S. (1982). *Seismic Risk Analysis.* Publication of Middle East Technical University, Ankara (in Turkish).

APPENDIX A

FAULT PARAMETERS FOR THE BURSA REGION

Table A. 1 Parameters for the Faults Identified in the Vicinity of Bursa City Center Resulting from the Field Surveys (from Yücemen et al., 2006)

Fault Name	Fault Mechanism	Direction	Dip Angle	Length (km)	Activity	Vertical and Horizontal Displ.(km)	Slip Rate mm/year	Max. Mag.	Reccurence Rate
Adalar	Normal	N 50° W	75° - 80° NE	35	Very active	?	?	6.9	?
Akçabük	Normal	N 66° W	69° SW	20	Potentialy active	?	?	6.5	≥ 1000
Alaçam	Normal Oblique	N 57° W	84° E	27	Active		?	6.7	
Altıntaş-Kurşunlu	Strike Slip	N 66° E	84° NW	9	Active	?	?	6.2	
Ayaz	Normal Oblique	N 60° W	76° NE	15	Potentialy active	~0.5 (V)	?	6.4	≥ 1000
Bandırma	Strike Slip	N 86° E	80° NW	42	Potentialy active	?	?	7	ε 1000
Boğazköy	Normal Oblique	N 70° E	85° NW	25	Potentialy active	0.4 (V)	?	6.7	≥ 1000
Boğazköy-Ekinli	Strike Slip	N 83° E	72° NW	25	Active	2 (H)		6.7	
Bursa	Normal Oblique	N 59° E	37° NW	63	Potentialy active	2.7 (V)	1	7.2	≥ 1000
Çalı	Normal Oblique	N 82° W	46° NE	29	Potentialy active	~1 (V)	?	6.8	≥ 1000
Çamdibi	Strike Slip	N 41° E	81° NW	42	Potentialy active	22 (H)	8,5	7	≥ 1000
Çavuşköy	Normal Oblique	N 86° E	52° NW	7	Potentialy active	?	?	6	≥ 1000
Çınarcık	Strike Slip	N 85° E	79° NW	36	Very active	4 (H)	5,7	6.9	≥ 400
Darıca	Strike Slip	E – W	Sub vert.	19	Active	?	?	6.5	?
Demirtaş	Normal Oblique	N 85° E	46° SE	22	Potentialy active	?	?	6.6	≥ 1000
Derecik	Normal Oblique	N 85° W	83° SW	19	Potentialy active	?	?	6.5	≥ 1000
Dodurga	Normal Oblique	N 64° W	78° SW	10	Potentialy active	0.05 (V)	?	6.2	≥ 1000
Erikli	Normal Oblique	N 70° W	75° NE	37	Potentialy active	0.3 (V)	?	6.9	≥ 1000

Table A.1 (cont'd) Parameters for the Faults Identified in the Vicinity of Bursa City Center Resulting from the Field Surveys (from Yücemen et al., 2006)

Fault Name	Fault Mechanism	Direction	Dip Angle	Length (km)	Activity	Vertical and Horizontal Displ.(km)	Slip Rate mm/year	Max. Mag.	Reccurence Rate
Eskiköy	Normal Oblique	N 58° W	47° NE	35	Potentialy active	0.3 (V)	?	6.9	≥ 1000
Eymir	Normal Oblique	N 70° W	67° SW	23	Potentialy active	0.2 (V)		6.6	≥ 1000
Gemlik	Strike Slip	N 76° W	74° NE	14	Active	?	?	6.4	
Gençali	Strike Slip	N 85° E	82° NW	12	Active	?	?	6.3	
Gölcük	Strike Slip	N 82° E	80° NW	25	Very active	?	?	6.7	210-280
Gürle	Strike Slip	N 80° E	50° NW	12	Active	?	?	6.3	
Karadin	Strike Slip	N 70° E	85° SE	19	Active	?	?	6.5	
Karahıdır	Normal Oblique	N 82° W	52° SW	26	Potentialy active	0.5 (V)	?	6.7	≥ 1000
Karamürsel	Strike Slip	N 50° E	49° NW	28	Very active			6.7	250-300
Kavaklı	Strike Slip	N 44° E	77° SE	12	Active	?	?	6.3	
Kestel	Normal Oblique	N 76° W	76° NE	15	Potentialy active			6.4	≥ 1000
Koyunhisar	Strike Slip	N 60° E	88° NW	20	Active	?	?	6.5	
Kozpınar	Normal Oblique	N 30° W	71° NE	39	Potentialy active	0.2 (V)	?	7	≥ 1000
Körfez	Strike Slip	N 75° E	79° SE	16	Very active	?	?	6.4	250-300
Kumburgaz	Strike Slip	N 86° E	Sub vert.	18	Very active	?	?	6.5	257± 23
Kurşunlu	Strike Slip	N 55° W	54° NE	21	Active	?	?	6.6	
Kurtköy-Gökçedere	Normal Oblique	N 55° W	68° NE	15	Active	?	?	6.4	
Laledere	Strike Slip	N 80° E	82° NW	20	Active	1.5 (H)	1,5	6.5	< 1000
M. Kemalpaşa	Normal Oblique	N 87° E	73° N	20	Potentialy active	?	?	6.5	≥ 1000
Mudanya	Strike Slip	N 80° E	82° NW	20	Active	2 (H)		6.5	
Narlıca	Strike Slip	E-W	54° N	10	Active	?	?	6.2	
Orhaniye	Strike Slip	N 85 E	80° SE	18	Active	?	?	6.5	
Ortaca	Normal	N 70° W	64° SW	13	Potentialy active	?	?	6.3	≥ 1000
Sayfiye	Normal Oblique	N 50° W	44° NE	29	Potentialy active	~1 (V)	?	6.8	?
Soğukpınar	Normal Oblique	N 48° W	63° SW	28	Potentialy active	~1 (V)	?	6.7	
Şükrüye	Strike Slip	N 70° E	78° NW	20	Active	?	?	6.5	
Taşlık	Normal Oblique	N 65° E	70° SE	7	Potentialy active	?	?	6	
Yeniköy	Normal Oblique	N 56° W	75° NE	10	Potentialy active	?	?	6.2	≥ 1000
Yeşilköy	Strike Slip	N 85° E	Sub vert.	41	Very active	?	?	7	257± 23

Table A. 2 Seismic Hazard Input Parameters of the Faults Required by the EZ-FRISK Program

Fault Name	Fault Mechanism	Mag. Scale	Deter. Mag.	Dip Angle	Model Type	Rate Type	Rate	Min Mag.	Max Mag.	Δ 1	Δ 2
Adalar	Normal	Mw	6.9	75	Char.	Activity	0.00100	6.0	6.9	0.9	10
Akçabük	Normal	Mw	6.5	69	Char.	Activity	0.00100	6.0	6.5	0.5	10
Alaçam	Normal Oblique	Mw	6.7	84	Char.	Activity	0.00100	6.0	6.7	0.7	10
Ayaz	Normal Oblique	Mw	6.4	76	Char.	Activity	0.00100	6.0	6.4	0.4	10
Bandırma	Strike Slip	Mw	7.0	80	Char.	Activity	0.00100	6.0	7.0	1.0	10
Boğazköy	Normal Oblique	Mw	6.7	85	Char.	Activity	0.00100	6.0	6.7	0.7	10
Boğazköy-Ekinli	Strike Slip	Mw	6.7	72	Char.	Activity	0.00100	6.0	6.7	0.7	10
Bursa	Normal Oblique	Mw	7.2	127	Char.	Slip	1.00000	6.0	7.2	1.2	10
Çalı	Normal Oblique	Mw	6.8	46-66	Char.	Activity	0.00100	6.0	6.8	0.8	10
Çamdibi	Strike Slip	Mw	7.0	81	Char.	Activity	0.00100	6.0	7.0	1.0	10
Çavuşköy	Normal Oblique	Mw	6.0	142	Char.	Activity	0.00100	5.5	6.0	0.5	10
Çınarcık	Strike Slip	Mw	6.9	79	Char.	Slip	5.70000	6.0	6.9	0.9	10
Darıca	Strike Slip	Mw	6.5	90	Char.	Activity	0.00100	6.0	6.5	0.5	10
Demirtaş	Normal Oblique	Mw	6.6	46	Char.	Activity	0.00100	6.0	6.6	0.6	10
Derecik	Normal Oblique	Mw	6.5	173	Char.	Activity	0.00100	6.0	6.5	0.5	10
Dodurga	Normal Oblique	Mw	6.2	78	Char.	Activity	0.00100	6.0	6.2	0.2	10
Erikli	Normal Oblique	Mw	6.9	75	Char.	Activity	0.00100	6.0	6.9	0.9	10
Eskiköy	Normal Oblique	Mw	6.9	47	Char.	Activity	0.00100	6.0	6.9	0.9	10
Eymir	Normal Oblique	Mw	6.6	67	Char.	Activity	0.00100	6.0	6.6	0.6	10
Gemlik	Strike Slip	Mw	6.4	74	Char.	Activity	0.00100	6.0	6.4	0.4	10
Gencali-Altıntaş-Kurşunlu	Strike Slip	Mw	6.3	82	Char.	Activity	0.00100	6.0	6.3	0.3	10
Gölcük	Strike Slip	Mw	6.7	80	Char.	Activity	0.00400	6.0	6.7	0.7	10
Gürle	Strike Slip	Mw	6.3	50	Char.	Activity	0.00010	6.0	6.3	0.3	10
Karadin	Strike Slip	Mw	6.5	85	Char.	Activity	0.00100	6.0	6.5	0.5	10
Karahıdır	Normal Oblique	Mw	6.7	52	Char.	Activity	0.00100	6.0	6.7	0.7	10
Karamürsel	Strike Slip	Mw	6.7	49	Char.	Activity	0.00400	6.0	6.7	0.7	10
Kavaklı	Strike Slip	Mw	6.3	77	Char.	Activity	0.00100	6.0	6.3	0.3	10
Kestel	Normal Oblique	Mw	6.4	76	Char.	Activity	0.00100	6.0	6.4	0.4	10
Koyunhisar	Strike Slip	Mw	6.5	88	Char.	Activity	0.00100	6.0	6.5	0.5	10
Kozpınar	Normal Oblique	Mw	7.0	71	Char.	Activity	0.00100	6.0	7.0	1.0	10
Körfez	Strike Slip	Mw	6.4	79	Char.	Activity	0.00400	6.0	6.4	0.4	10
Kumburgaz	Strike Slip	Mw	6.5	90	Char.	Activity	0.00100	6.0	6.5	0.5	10
Kurşunlu	Strike Slip	Mw	6.6	54	Char.	Activity	0.00100	6.0	6.6	0.6	10
Kurtköy-Gökçedere	Normal Oblique	Mw	6.4	68	Char.	Activity	0.00100	6.0	6.4	0.4	10

Table A.2 (cont'd) Seismic Hazard Input Parameters of the Faults Required by the EZ-FRISK Program

Fault Name	Fault Mechanism	Mag. Scale	Deter. Mag.	Dip Angle	Model Type	Rate Type	Rate	Min Mag.	Max Mag.	Δ 1	Δ 2
Laledere	Strike Slip	Mw	6.5	82	Char.	Slip	1.50000	6.0	6.5	0.5	10
M.Kemal Paşa	Normal Oblique	Mw	6.5	163	Char.	Activity	0.00100	6.0	6.5	0.5	10
Mudanya	Strike Slip	Mw	6.5	82	Char.	Activity	0.00100	6.0	6.5	0.5	10
Narlıca	Strike Slip	Mw	6.2	54	Char.	Activity	0.00100	6.0	6.2	0.2	10
Orhaniye	Strike Slip	Mw	6.5	80	Char.	Activity	0.00100	6.0	6.5	0.5	10
Ortaca	Normal	Mw	6.3	64	Char.	Activity	0.00100	6.0	6.3	0.3	10
Sayfiye	Normal Oblique	Mw	6.8	44	Char.	Activity	0.00100	6.0	6.8	0.8	10
Soğukpınar	Normal Oblique	Mw	6.7	153	Char.	Activity	0.00100	6.0	6.7	0.7	10
Şükriye	Strike Slip	Mw	6.5	78	Char.	Activity	0.00100	6.0	6.5	0.5	10
Taşlık	Normal Oblique	Mw	6.0	70	Char.	Activity	0.00100	6.0	6.01	0.01	10
Yeniköy	Normal Oblique	Mw	6.2	75	Char.	Activity	0.00100	6.0	6.2	0.2	10
Yeşilköy	Strike Slip	Mw	7.0	90	Char.	Activity	0.00100	6.0	7.0	1.0	10

Table A. 3 Coordinates of the Faults Identified in the Vicinity of Bursa City Center (from Yücemen et al., 2006)

Fault Name	Longitude	Latitude
Bursa Fault	29.7135	40.0082
	29.4915	40.0450
	29.3498	40.1285
	29.2063	40.1622
	29.1104	40.1677
	29.0726	40.1649
	29.0188	40.1970
	29.0052	40.1950
Sayfiye Fault	29.3866	40.0741
	29.3444	40.1050
	29.2432	40.1280
	29.2210	40.1456
	29.1840	40.1573
	29.1306	40.1588
	29.1104	40.1677
Alaçam Fault	29.4746	40.0524
	29.4450	40.0575
	29.3957	40.0820
	29.3592	40.1117
	29.3226	40.1224
	29.2790	40.1246
	29.2490	40.1380
	29.2264	40.1465
	29.2063	40.1622
Soğukpınar Fault	29.3671	40.0224
	29.3297	40.0189
	29.2466	40.0347
	29.1558	40.0652
	29.0986	40.0784
	29.0731	40.0850
	29.0501	40.0977
Çalı Fault	28.9998	40.1878
	28.9257	40.1658
	28.8771	40.1699
	28.7800	40.1689
	28.6799	40.1294

Table A.3 (cont'd) Coordinates of the Faults Identified in the Vicinity of Bursa City Center (from Yücemen et al., 2006)

Fault Name	Longitude	Latitude
Ayaz Fault	28.6103	40.1181
	28.5539	40.1032
	28.5345	40.0982
	28.5024	40.0978
	28.4382	40.0851
Gençali and Altıntaş-Kurşunlu Faults	29.2045	40.3743
	29.1531	40.3736
	29.0732	40.3683
	29.0444	40.3533
	29.0127	40.3526
	28.9970	40.3490
	28.9690	40.3458
Narlıca Fault	29.5288	40.3780
	29.4370	40.3834
	29.4062	40.3821
Şükrüye Fault	29.4062	40.3821
	29.3979	40.3732
	29.3831	40.3682
	29.3650	40.3675
	29.3365	40.3572
	29.2480	40.3332
Çamdibi Fault	30.0000	40.4391
	29.9458	40.4322
	29.8643	40.4146
	29.7844	40.4038
	29.6242	40.3803
	29.5942	40.3742
	29.5082	40.3731
Karadin Fault	30.0000	40.4578
	29.9310	40.4446
	29.9059	40.4373
	29.8470	40.4283
	29.8133	40.4226
	29.7803	40.4108

Table A.3 (cont'd) Coordinates of the Faults Identified in the Vicinity of Bursa City Center (from Yücemen et al., 2006)

Fault Name	Longitude	Latitude
Orhaniye Fault	29.7012	40.5117
	29.6357	40.4966
	29.6069	40.4977
	29.5724	40.4911
	29.4851	40.4860
Kurtköy-Gökçedere Fault	29.2837	40.5422
	29.2639	40.5441
	29.2092	40.5625
	29.1715	40.5928
	29.1349	40.6082
Koyunhisar Fault	29.5330	40.2945
	29.4860	40.2575
	29.3801	40.2131
	29.3488	40.2026
M. Kemalpaşa Fault	28.4965	40.0336
	28.4664	40.0266
	28.4310	40.0274
	28.3443	40.0603
	28.3073	40.0643
	28.2735	40.0602
Derecik Fault	28.5168	39.9787
	28.4445	40.0002
	28.4084	40.0313
	28.3726	40.0452
	28.2998	40.0454
Yeniköy Fault	28.1510	40.0937
	28.0996	40.1072
	28.0359	40.1128
	28.0115	40.1033
Çavuşköy Fault	28.1482	40.2437
	28.1239	40.2481
	28.1030	40.2537
	28.0680	40.2548
Kestel Fault System	29.4571	40.2170
	29.3871	40.2094
	29.3488	40.2026
	29.2751	40.2009

Table A.3 (cont'd) Coordinates of the Faults Identified in the Vicinity of Bursa City Center (from Yücemen et al., 2006)

Fault Name	Longitude	Latitude
Taşlık Fault	28.3889	40.2428
	28.2935	40.2418
Demirtaş Fault	29.1206	40.2620
	29.0655	40.2694
	29.0108	40.2829
	28.8594	40.2852
Karahıdır Fault	29.2855	40.2307
	29.2419	40.2438
	29.2288	40.2440
	29.1984	40.2546
	29.1757	40.2562
	29.1474	40.2647
	29.1021	40.2731
	29.0598	40.2778
Eymir Fault	29.7488	39.9766
	29.7135	40.0082
	29.6988	40.0306
	29.6561	40.0627
	29.6027	40.0778
	29.5875	40.0796
	29.5501	40.1182
Boğazköy Fault	29.7188	40.2439
	29.7098	40.2508
	29.6477	40.2403
	29.5742	40.1926
	29.5342	40.1645
	29.4902	40.1593
	29.4560	40.1589
Eskiköy Fault	29.7056	39.9586
	29.6459	39.9654
	29.6282	39.9675
	29.6048	39.9746
	29.5086	39.9925
	29.4913	39.9986
	29.3671	40.0224
	29.3314	40.0503

Table A.3 (cont'd) Coordinates of the Faults Identified in the Vicinity of Bursa City Center (from Yücemen et al., 2006)

Fault Name	Longitude	Latitude
Kozpınar Fault	30.0789	39.8765
	29.9773	39.8901
	29.8889	39.8908
	29.8527	39.8970
	29.8198	39.9086
	29.7055	39.9286
	29.6685	39.9381
	29.6318	39.9402
Erikli Fault	29.9101	39.8528
	29.8320	39.8787
	29.7666	39.8884
	29.7625	39.8884
	29.6902	39.9273
	29.6318	39.9402
	29.5833	39.9530
	29.5086	39.9925
Dodurga Fault	29.9778	39.7864
	29.9363	39.8117
	29.9101	39.8528
Gemlik Fault	29.2474	40.4173
	29.1857	40.4139
	29.1421	40.4130
	29.0762	40.4069
Gürle Fault	29.3708	40.4021
	29.3202	40.4022
	29.2865	40.4003
	29.2285	40.4006
Kavaklı Fault	29.5484	40.3462
	29.5216	40.3308
	29.4940	40.3195
	29.4450	40.2931
	29.4235	40.2866
Mudanya Fault	28.8679	40.3764
	28.8399	40.3704
	28.7543	40.3559
	28.6839	40.3527
	28.6391	40.3515

Table A.3 (cont'd) Coordinates of the Faults Identified in the Vicinity of Bursa City Center (from Yücemen et al., 2006)

Fault Name	Longitude	Latitude
Boğazköy-Ekinli Fault	28.6251	40.3563
	28.5564	40.3670
	28.5391	40.3672
	28.5255	40.3606
	28.4453	40.3554
	28.3354	40.3623
Kurşunlu Fault	28.3902	40.3847
	28.3429	40.3962
	28.3240	40.3965
	28.2907	40.3921
	28.2487	40.3989
	28.2141	40.3960
	28.1322	40.3939
Karamürsel Fault	29.8241	40.7044
	29.7932	40.7092
	29.7722	40.7089
	29.6985	40.7005
	29.6187	40.6847
	29.5005	40.6658
Çınarcık Fault	29.2169	40.6470
	29.1906	40.6434
	28.9947	40.6467
	28.8540	40.6606
	28.7853	40.6647
Laledere Fault	29.3740	40.6004
	29.2986	40.5935
	29.2661	40.5955
	29.2390	40.6009
	29.1349	40.6082
	29.1234	40.6095
Gölcük Fault	29.7928	40.7204
	29.6476	40.7133
	29.5187	40.6983
Körfez Fault	29.8198	40.7728
	29.7770	40.7695
	29.6724	40.7701
	29.6078	40.7714

Table A.3 (cont'd) Coordinates of the Faults Identified in the Vicinity of Bursa City Center (from Yücemen et al., 2006)

Fault Name	Longitude	Latitude
Ortaca Fault	29.5110	39.8427
	29.4736	39.8600
	29.4099	39.8810
	29.3745	39.8998
Akçabük Fault	29.0800	39.9272
	29.0553	39.9313
	28.9945	39.9412
	28.9636	39.9457
	28.9024	39.9636
	28.8501	39.9753
Darıca Fault	29.2200	40.7300
	29.4400	40.7200
Adalar Fault	28.8800	40.8600
	29.2200	40.7300
Yeşilköy Fault	28.3900	40.8200
	28.8800	40.8600
Kumburgaz Fault	28.4100	40.8400
	28.1800	40.8300
Bandırma Fault	28.0000	40.4000
	28.5000	40.4200

APPENDIX B

PROBABILISTIC SPECTRA RESULTS COMPUTED FOR BRIDGES CORRESPONDING TO DIFFERENT RETURN PERIODS

Table B. 1 Probabilistic Spectra Results of Balıklı Bridge for a Return Period of 75 Years (50% Probability of Exceedance in 50 years)

75 Years Return Period					
Spectral Period (sn)	**Average Spectral Acceleration(g)**	**Abrahamson-Silva (2008)**	**Boore et al. (1997)**	**Gulerce et al. (2015)**	**Gülkan-Kalkan (2004)**
PGA	0.1672	0.1684	0.1683	0.1054	0.2042
0.10	0.3730	0.3532	0.3019	0.1988	0.5220
0.20	0.3827	0.4049	0.3879	0.2517	0.4484
0.30	0.3374	0.3247	0.3469	0.2259	0.4236
0.40	0.2918	0.2589	0.2868	0.1919	0.3948
0.50	0.2441	0.2088	0.2359	0.1616	0.3376
0.60	0.2134	0.1710	0.1937	0.1372	0.3189
0.70	0.1848	0.1448	0.1636	0.1199	0.2836
0.80	0.1623	0.1254	0.1411	0.1058	0.2554
0.90	0.1479	0.1104	0.1242	0.0937	0.2431
1.00	0.1386	0.0978	0.1105	0.0841	0.2429
1.50	0.0776	0.0568	0.0770	0.0505	0.1177
2.00	0.0572	0.0372	0.0662	0.0335	0.0837
2.50	0.0446	0.0277	0.0530	0.0252	0.0672
3.00	0.0361	0.0217	0.0436	0.0198	0.0558
3.50	0.0304	0.0172	0.0370	0.0157	0.0478
4.00	0.0264	0.0141	0.0323	0.0130	0.0411

Table B. 2 Probabilistic Spectra Results of Balıklı Bridge for a Return Period of 475 Years (10% Probability of Exceedance in 50 years)

475 Years Return Period					
Spectral Period (sn)	**Average Spectral Acceleration(g)**	**Abrahamson-Silva (2008)**	**Boore et al. (1997)**	**Gulerce et al. (2015)**	**Gülkan-Kalkan (2004)**
PGA	0.3851	0.3874	0.3630	0.3110	0.4594
0.10	0.8458	0.8137	0.7528	0.5881	1.0940
0.20	0.9289	0.9540	0.9324	0.7403	1.0460
0.30	0.8415	0.7616	0.8801	0.6391	1.0470
0.40	0.7309	0.6140	0.7671	0.5377	0.9344
0.50	0.6117	0.5043	0.6539	0.4529	0.7809
0.60	0.5493	0.4195	0.5474	0.3827	0.7648
0.70	0.4831	0.3578	0.4675	0.3308	0.6878
0.80	0.4295	0.3121	0.4039	0.2914	0.6245
0.90	0.3972	0.2746	0.3528	0.2558	0.5975
1.00	0.3816	0.2429	0.3138	0.2294	0.6111
1.50	0.2078	0.1410	0.2084	0.1342	0.3012
2.00	0.1492	0.0987	0.1653	0.0945	0.2170
2.50	0.1184	0.0732	0.1313	0.0705	0.1724
3.00	0.0989	0.0569	0.1103	0.0549	0.1429
3.50	0.0837	0.0457	0.0956	0.0436	0.1228
4.00	0.0729	0.0366	0.0834	0.0351	0.1082

Table B. 3 Probabilistic Spectra Results of Balıklı Bridge for a Return Period of 1000 Years (5% Probability of Exceedance in 50 years)

1000 Years Return Period					
Spectral Period (sn)	**Average Spectral Acceleration(g)**	**Abrahamson-Silva (2008)**	**Boore et al. (1997)**	**Gulerce et al. (2015)**	**Gülkan-Kalkan (2004)**
PGA	0.4990	0.4894	0.4696	0.4115	0.6010
0.10	1.0870	1.0420	0.9836	0.7798	1.3940
0.20	1.1910	1.2000	1.1670	1.0080	1.3670
0.30	1.1140	0.9944	1.1340	0.8634	1.4040
0.40	0.9802	0.8000	1.0310	0.7321	1.2400
0.50	0.8201	0.6610	0.8878	0.6128	1.0430
0.60	0.7452	0.5520	0.7556	0.5206	1.0340
0.70	0.6556	0.4768	0.6494	0.4518	0.9306
0.80	0.5841	0.4163	0.5623	0.3985	0.8471
0.90	0.5416	0.3674	0.5000	0.3505	0.8102
1.00	0.5267	0.3271	0.4433	0.3155	0.8342
1.50	0.2857	0.1955	0.2934	0.1883	0.4116
2.00	0.2090	0.1281	0.2280	0.1247	0.3006
2.50	0.1636	0.0997	0.1820	0.0964	0.2392
3.00	0.1350	0.0773	0.1495	0.0755	0.2004
3.50	0.1156	0.0625	0.1280	0.0607	0.1699
4.00	0.1016	0.0519	0.1129	0.0507	0.1480

Table B. 4 Probabilistic Spectra Results of Balıklı Bridge for a Return Period of 2475 Years (2% Probability of Exceedance in 50 years)

2475 Years Return Period					
Spectral Period (sn)	**Average Spectral Acceleration(g)**	**Abrahamson-Silva (2008)**	**Boore et al. (1997)**	**Gulerce et al. (2015)**	**Gülkan-Kalkan (2004)**
PGA	0.6490	0.6158	0.6064	0.5300	0.8024
0.10	1.4090	1.3250	1.2140	1.0240	1.8720
0.20	1.5710	1.5600	1.4880	1.2930	1.8950
0.30	1.4900	1.2540	1.4610	1.1390	2.0050
0.40	1.3020	1.0490	1.3230	0.9879	1.7270
0.50	1.1120	0.8685	1.1740	0.8243	1.4160
0.60	1.0320	0.7344	1.0330	0.7050	1.4280
0.70	0.9127	0.6314	0.8959	0.6069	1.2880
0.80	0.8181	0.5524	0.7838	0.5351	1.1800
0.90	0.7621	0.4933	0.7013	0.4761	1.1290
1.00	0.7513	0.4386	0.6227	0.4271	1.1700
1.50	0.4054	0.2602	0.4152	0.2543	0.5804
2.00	0.2983	0.1751	0.3193	0.1710	0.4293
2.50	0.2361	0.1295	0.2539	0.1266	0.3430
3.00	0.1968	0.1046	0.2125	0.1031	0.2860
3.50	0.1662	0.0848	0.1807	0.0830	0.2443
4.00	0.1444	0.0708	0.1561	0.0697	0.2143

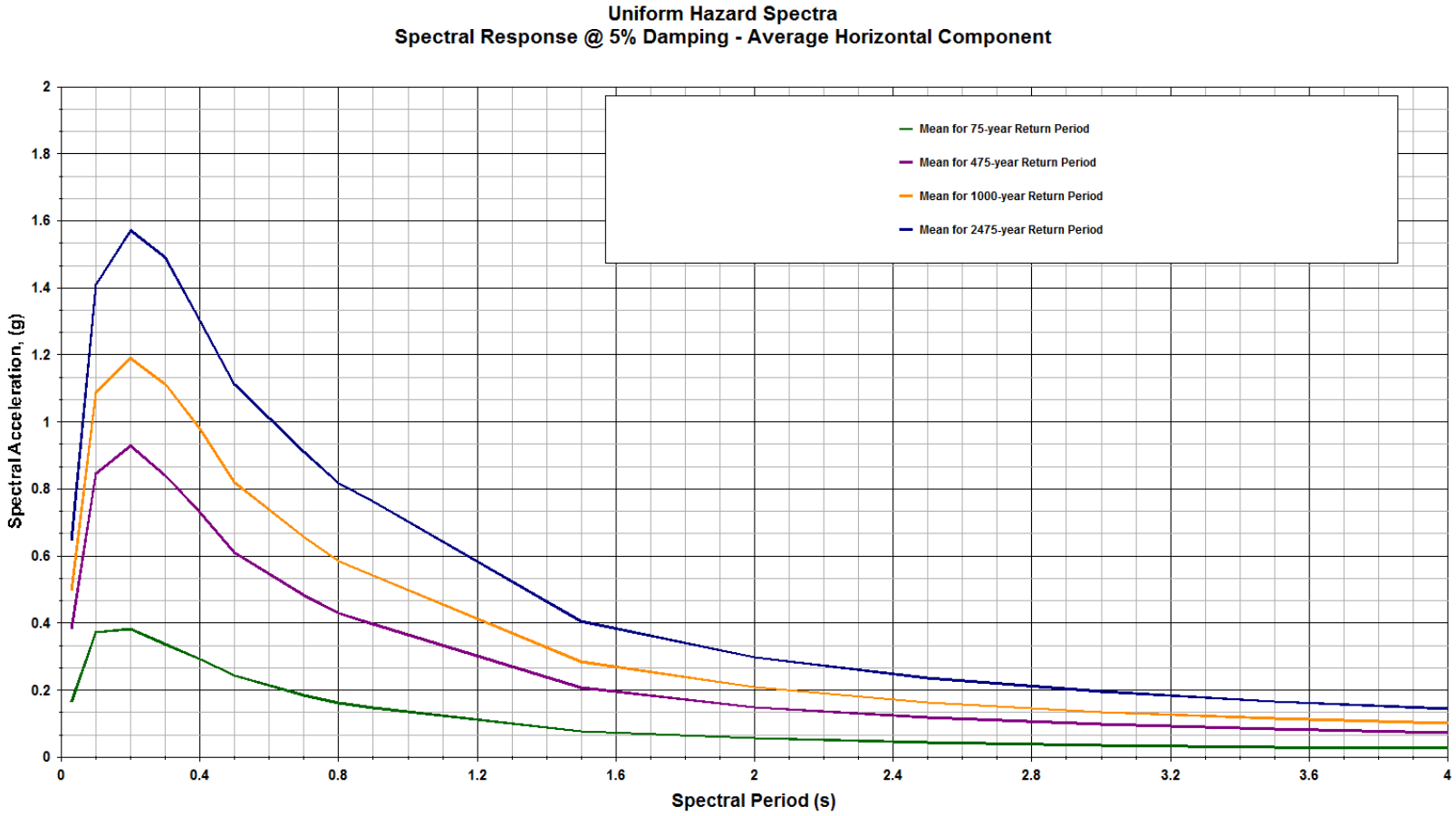

Figure B. 1 Average Probabilistic Spectra Graphs of Balıklı Bridge for Return Periods of 75, 475, 1000 and 2475 Years

Table B. 5 Probabilistic Spectra Results of Panayır Bridge for a Return Period of 75 Years (50% Probability of Exceedance in 50 years)

75 Years Return Period					
Spectral Period (sn)	**Average Spectral Acceleration(g)**	**Abrahamson-Silva (2008)**	**Boore et al. (1997)**	**Gulerce et al. (2015)**	**Gülkan-Kalkan (2004)**
PGA	0.1683	0.1692	0.1693	0.1074	0.2061
0.10	0.3752	0.3543	0.3064	0.2020	0.5258
0.20	0.3864	0.4072	0.3928	0.2558	0.4530
0.30	0.3410	0.3275	0.3512	0.2298	0.4284
0.40	0.2949	0.2616	0.2906	0.1955	0.3990
0.50	0.2465	0.2113	0.2389	0.1642	0.3408
0.60	0.2155	0.1733	0.1965	0.1393	0.3218
0.70	0.1867	0.1466	0.1655	0.1218	0.2863
0.80	0.1639	0.1271	0.1428	0.1076	0.2578
0.90	0.1494	0.1120	0.1259	0.0954	0.2456
1.00	0.1400	0.0995	0.1122	0.0856	0.2452
1.50	0.0785	0.0577	0.0782	0.0514	0.1188
2.00	0.0578	0.0377	0.0673	0.0340	0.0846
2.50	0.0451	0.0281	0.0538	0.0255	0.0679
3.00	0.0365	0.0220	0.0442	0.0202	0.0564
3.50	0.0307	0.0175	0.0375	0.0159	0.0484
4.00	0.0267	0.0143	0.0327	0.0132	0.0416

Table B. 6 Probabilistic Spectra Results of Panayır Bridge for a Return Period of 475 Years (10% Probability of Exceedance in 50 years)

475 Years Return Period					
Spectral Period (sn)	**Average Spectral Acceleration(g)**	**Abrahamson-Silva (2008)**	**Boore et al. (1997)**	**Gulerce et al. (2015)**	**Gülkan-Kalkan (2004)**
PGA	0.3856	0.3913	0.3602	0.3100	0.4582
0.10	0.8500	0.8250	0.7457	0.5882	1.0940
0.20	0.9284	0.9633	0.9206	0.7382	1.0440
0.30	0.8407	0.7660	0.8692	0.6361	1.0450
0.40	0.7309	0.6170	0.7599	0.5351	0.9350
0.50	0.6120	0.5059	0.6497	0.4503	0.7818
0.60	0.5504	0.4208	0.5460	0.3803	0.7666
0.70	0.4845	0.3589	0.4679	0.3288	0.6897
0.80	0.4307	0.3128	0.4050	0.2894	0.6256
0.90	0.3985	0.2752	0.3538	0.2541	0.5983
1.00	0.3827	0.2434	0.3145	0.2279	0.6125
1.50	0.2077	0.1411	0.2074	0.1331	0.3015
2.00	0.1489	0.0986	0.1637	0.0937	0.2176
2.50	0.1182	0.0731	0.1301	0.0699	0.1728
3.00	0.0988	0.0568	0.1095	0.0544	0.1432
3.50	0.0836	0.0456	0.0948	0.0432	0.1230
4.00	0.0728	0.0365	0.0827	0.0347	0.1084

Table B. 7 Probabilistic Spectra Results of Panayır Bridge for a Return Period of 1000 years (5% Probability of Exceedance in 50 years)

1000 Years Return Period					
Spectral Period (sn)	**Average Spectral Acceleration(g)**	**Abrahamson-Silva (2008)**	**Boore et al. (1997)**	**Gulerce et al. (2015)**	**Gülkan-Kalkan (2004)**
PGA	0.5003	0.4990	0.4639	0.4134	0.5970
0.10	1.0930	1.0610	0.9730	0.7891	1.3890
0.20	1.1910	1.2200	1.1550	1.0100	1.3560
0.30	1.1110	1.0040	1.1200	0.8616	1.3940
0.40	0.9781	0.8063	1.0200	0.7288	1.2340
0.50	0.8183	0.6651	0.8779	0.6086	1.0390
0.60	0.7445	0.5543	0.7498	0.5168	1.0330
0.70	0.6550	0.4782	0.6450	0.4476	0.9291
0.80	0.5831	0.4170	0.5587	0.3941	0.8447
0.90	0.5405	0.3677	0.4969	0.3467	0.8074
1.00	0.5257	0.3271	0.4399	0.3121	0.8325
1.50	0.2837	0.1947	0.2878	0.1849	0.4099
2.00	0.2075	0.1272	0.2234	0.1225	0.3001
2.50	0.1622	0.0989	0.1778	0.0945	0.2387
3.00	0.1339	0.0767	0.1461	0.0742	0.2000
3.50	0.1147	0.0619	0.1253	0.0595	0.1695
4.00	0.1009	0.0514	0.1108	0.0498	0.1476

Table B. 8 Probabilistic Spectra Results of Panayır Bridge for a Return Period of 2475 Years (2% Probability of Exceedance in 50 years)

2475 Years Return Period					
Spectral Period (sn)	**Average Spectral Acceleration(g)**	**Abrahamson-Silva (2008)**	**Boore et al. (1997)**	**Gulerce et al. (2015)**	**Gülkan-Kalkan (2004)**
PGA	0.6512	0.6345	0.5960	0.5373	0.7945
0.10	1.4160	1.3600	1.2040	1.0470	1.8580
0.20	1.5760	1.6060	1.4680	1.3120	1.8670
0.30	1.4830	1.2770	1.4350	1.1410	1.9790
0.40	1.2940	1.0600	1.2960	0.9840	1.7080
0.50	1.1050	0.8771	1.1510	0.8184	1.4030
0.60	1.0260	0.7388	1.0160	0.6986	1.4180
0.70	0.9055	0.6341	0.8750	0.5994	1.2800
0.80	0.8105	0.5534	0.7657	0.5282	1.1700
0.90	0.7547	0.4935	0.6822	0.4684	1.1190
1.00	0.7448	0.4380	0.6048	0.4202	1.1620
1.50	0.3993	0.2581	0.4013	0.2483	0.5742
2.00	0.2936	0.1725	0.3091	0.1655	0.4261
2.50	0.2326	0.1273	0.2451	0.1229	0.3404
3.00	0.1935	0.1031	0.2059	0.1005	0.2837
3.50	0.1636	0.0830	0.1737	0.0802	0.2424
4.00	0.1423	0.0693	0.1504	0.0670	0.2127

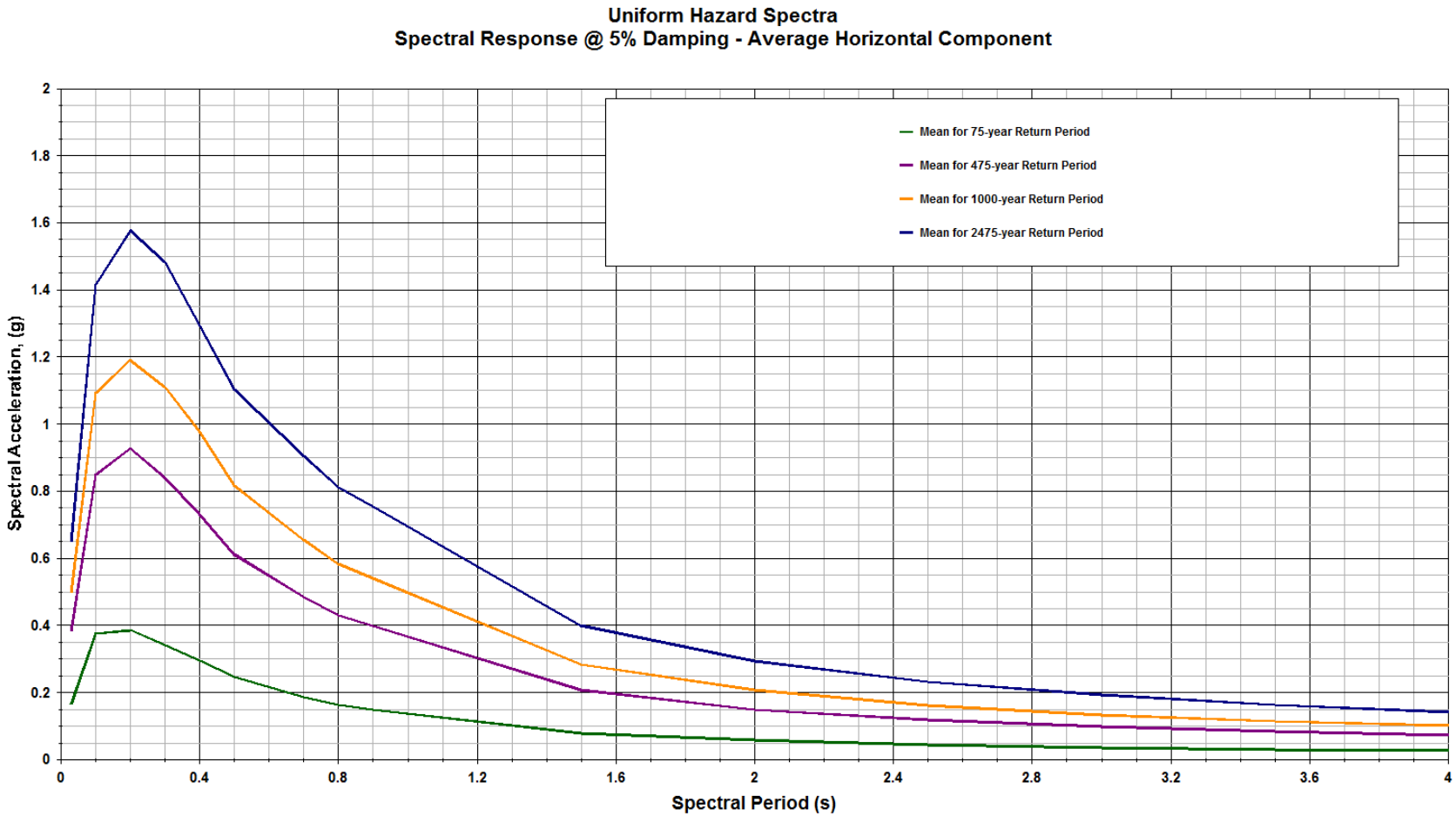

Figure B. 2 Average Probabilistic Spectra Graphs of Panayır Bridge for Return Periods of 75, 475, 1000 and 2475 Years

Table B. 9 Probabilistic Spectra Results of Demirtaş Viaduct for a Return Period of 75 Years (50% Probability of Exceedance in 50 years)

75 Years Return Period					
Spectral Period (sn)	**Average Spectral Acceleration(g)**	**Abrahamson-Silva (2008)**	**Boore et al. (1997)**	**Gulerce et al. (2015)**	**Gülkan-Kalkan (2004)**
PGA	0.1719	0.1719	0.1730	0.1132	0.2123
0.10	0.3829	0.3582	0.3210	0.2125	0.5389
0.20	0.3992	0.4152	0.4101	0.2691	0.4685
0.30	0.3526	0.3365	0.3665	0.2413	0.4436
0.40	0.3048	0.2702	0.3043	0.2064	0.4114
0.50	0.2541	0.2191	0.2490	0.1723	0.3504
0.60	0.2217	0.1804	0.2059	0.1453	0.3305
0.70	0.1923	0.1522	0.1721	0.1270	0.2947
0.80	0.1683	0.1319	0.1478	0.1126	0.2651
0.90	0.1534	0.1166	0.1305	0.1007	0.2528
1.00	0.1436	0.1041	0.1167	0.0901	0.2523
1.50	0.0810	0.0607	0.0816	0.0540	0.1220
2.00	0.0597	0.0395	0.0704	0.0352	0.0871
2.50	0.0467	0.0291	0.0561	0.0264	0.0701
3.00	0.0376	0.0230	0.0464	0.0211	0.0581
3.50	0.0316	0.0185	0.0390	0.0166	0.0501
4.00	0.0274	0.0150	0.0338	0.0137	0.0429

Table B. 10 Probabilistic Spectra Results of Demirtaş Viaduct for a Return Period of 475 Years (10% Probability of Exceedance in 50 years)

475 Years Return Period					
Spectral Period (sn)	**Average Spectral Acceleration(g)**	**Abrahamson-Silva (2008)**	**Boore et al. (1997)**	**Gulerce et al. (2015)**	**Gülkan-Kalkan (2004)**
PGA	0.3879	0.4016	0.3531	0.2996	0.4583
0.10	0.8668	0.8591	0.7240	0.5830	1.1010
0.20	0.9298	0.9899	0.8901	0.7239	1.0450
0.30	0.8416	0.7788	0.8368	0.6225	1.0500
0.40	0.7322	0.6249	0.7329	0.5231	0.9440
0.50	0.6141	0.5093	0.6291	0.4390	0.7896
0.60	0.5555	0.4231	0.5353	0.3701	0.7762
0.70	0.4902	0.3607	0.4622	0.3206	0.6996
0.80	0.4367	0.3136	0.4025	0.2812	0.6331
0.90	0.4052	0.2759	0.3546	0.2480	0.6047
1.00	0.3913	0.2442	0.3149	0.2224	0.6202
1.50	0.2089	0.1420	0.2047	0.1308	0.3045
2.00	0.1500	0.0972	0.1609	0.0903	0.2207
2.50	0.1190	0.0721	0.1283	0.0671	0.1754
3.00	0.0997	0.0560	0.1080	0.0525	0.1452
3.50	0.0843	0.0448	0.0932	0.0417	0.1247
4.00	0.0735	0.0363	0.0814	0.0339	0.1099

Table B. 11 Probabilistic Spectra Results of Demirtaş Viaduct for a Return Period of 1000 Years (5% Probability of Exceedance in 50 years)

1000 Years Return Period					
Spectral Period (sn)	**Average Spectral Acceleration(g)**	**Abrahamson-Silva (2008)**	**Boore et al. (1997)**	**Gulerce et al. (2015)**	**Gülkan-Kalkan (2004)**
PGA	0.5098	0.5272	0.4529	0.4250	0.5919
0.10	1.1190	1.1180	0.9477	0.8290	1.3880
0.20	1.2080	1.2870	1.1270	1.0280	1.3420
0.30	1.1180	1.0370	1.0920	0.8686	1.3870
0.40	0.9880	0.8327	1.0030	0.7271	1.2310
0.50	0.8285	0.6827	0.8783	0.6053	1.0400
0.60	0.7599	0.5659	0.7655	0.5114	1.0370
0.70	0.6732	0.4861	0.6745	0.4416	0.9346
0.80	0.5996	0.4222	0.5888	0.3871	0.8470
0.90	0.5557	0.3720	0.5223	0.3409	0.8078
1.00	0.5413	0.3299	0.4625	0.3065	0.8352
1.50	0.2859	0.1948	0.2838	0.1806	0.4100
2.00	0.2077	0.1276	0.2158	0.1201	0.3021
2.50	0.1623	0.0978	0.1710	0.0915	0.2404
3.00	0.1339	0.0759	0.1412	0.0720	0.2014
3.50	0.1148	0.0610	0.1213	0.0575	0.1707
4.00	0.1009	0.0506	0.1074	0.0476	0.1486

Table B. 12 Probabilistic Spectra Results of Demirtaş Viaduct for a Return Period of 2475 Years (2% Probability of Exceedance in 50 years)

2475 Years Return Period					
Spectral Period (sn)	**Average Spectral Acceleration(g)**	**Abrahamson-Silva (2008)**	**Boore et al. (1997)**	**Gulerce et al. (2015)**	**Gülkan-Kalkan (2004)**
PGA	0.6785	0.7024	0.5882	0.5900	0.7852
0.10	1.4630	1.4660	1.2090	1.1460	1.8390
0.20	1.6310	1.7660	1.4490	1.4280	1.8190
0.30	1.5140	1.3710	1.4260	1.1980	1.9470
0.40	1.3160	1.1190	1.3130	1.0200	1.6820
0.50	1.1290	0.9299	1.1930	0.8445	1.3920
0.60	1.0590	0.7738	1.0770	0.7137	1.4120
0.70	0.9450	0.6646	0.9725	0.6115	1.2770
0.80	0.8438	0.5756	0.8537	0.5355	1.1630
0.90	0.7822	0.5108	0.7591	0.4740	1.1080
1.00	0.7692	0.4528	0.6751	0.4237	1.1540
1.50	0.4025	0.2648	0.4017	0.2485	0.5682
2.00	0.2917	0.1766	0.2936	0.1651	0.4259
2.50	0.2309	0.1290	0.2332	0.1219	0.3402
3.00	0.1917	0.1036	0.1955	0.0990	0.2836
3.50	0.1621	0.0833	0.1646	0.0788	0.2423
4.00	0.1410	0.0693	0.1431	0.0655	0.2126

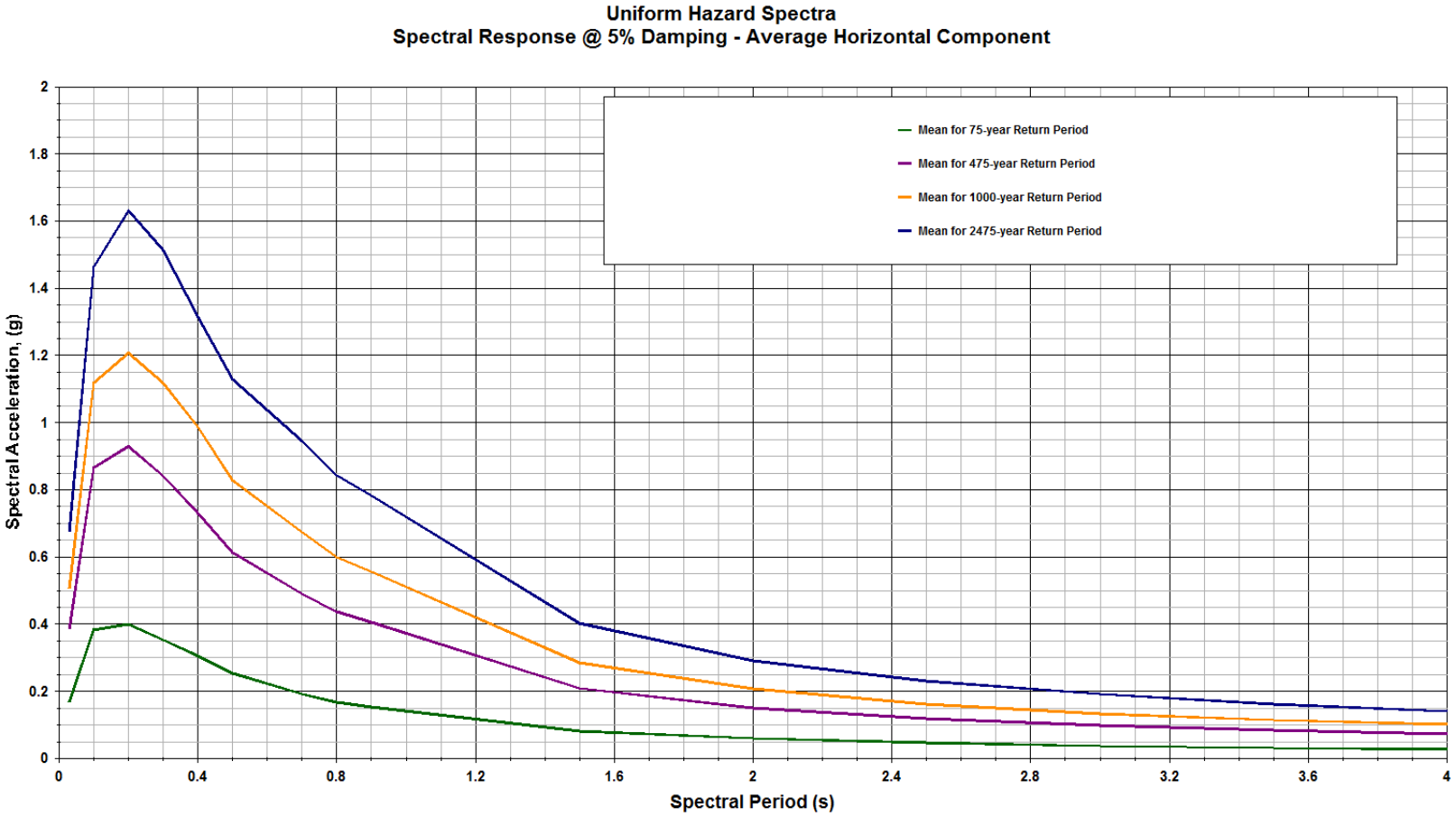

Figure B. 3 Average Probabilistic Spectra Graphs of Demirtaş Viaduct for Return Periods of 75, 475, 1000 and 2475 Years